UNIVERSITÀ DEGLI STUDI DI MESSINA

DIPARTIMENTO DI SCIENZE CHIMICHE, BIOLOGICHE,

FARMACEUTICHE ED AMBIENTALI

DOTTORATO DI RICERCA IN SCIENZE CHIMICHE

DOCTOR OF PHILOSOPHY IN CHEMICAL SCIENCES

ADVANCED CHROMATOGRAPHIC TECHNIQUES COUPLED TO MASS SPECTROMETRY FOR THE ANALYSIS OF MATRICES OF NUTRITIONAL AND NUTRACEUTICAL INTEREST

PhD Thesis of:
Paola Arena

Tutor:
Prof. Luigi Mondello

Coordinator:
Prof. Paola Dugo

XXXIV CICLO (2018-2021)

Preface

The research work described in this PhD thesis was mainly focused on the development of analytical methods based on chromatography coupled to mass spectrometry (MS), for the analysis of matrices containing molecules of nutritional and nutraceutical interest, with particular emphasis on lipids, peptides and polyphenols.

Most of the scientific efforts were put into developing multitechnique analytical approaches for the retrieval and valorization of the protein and lipid fractions from the wastes of the fishery industry. Specifically, this research allowed the identification of valuable molecules in tuna by-products, such as omega-3 polyunsaturated fatty acids (ω-3 PUFA), e.g., docosahexaenoic acid (C22:6) and eicosapentaenoic acid (C20:5) and short- and medium-size tryptic peptides with antimicrobial activity. The characterized components will be conveniently combined in nutraceutical formulations, beneficial for human health.

Additional research activities have been focused on the elucidation of the lipid profile of different plant oils and related products, with particular emphasis on glycerolipids in their native form. For such purposes, liquid chromatography (LC), comprehensive liquid chromatography (LCxLC) and subcritical solvent chromatography (subFC) approaches coupled to atmospherical pressure chemical ionization-MS (APCI-MS) have been exploited as powerful analytical strategies for the characterization of complex matrices. Furthermore, aiming at improving the identification process in LC, a recently introduced linear retention index (LRI) approach has been employed in combination to MS, to achieve a reliable identification of triacylglycerols (TAGs) components. The investigation of less conventional matrices allowed to improve the LRI laboratory-constructed database; in detail, a substantial contribution was provided by the analysis of marine organisms samples, i.e. tuna waste oil, highly rich in ω-3 PUFA-containing TAGs. Within the same study, matrices containing uncommon fatty acids and their positional isomers have been investigated, i.e. hemp seed oil, highly rich in ɣ- and α-linolenic acids. Finally, *Hibiscus sabdariffa* and *Zingiber officinale* extracts were characterized by LC coupled to photodiode array (PDA) and MS detection, and the availability of polyphenols at the colon level was evaluated for their potential applications in the treatment of intestinal ailments.

TABLE OF CONTENTS

1 Advanced chromatographic techniques in food analysis

1.1 The importance of analytical chemistry in food science

Analytical chemistry is often described as a branch of chemistry which deals with the characterization of the composition of a sample; more in detail this discipline is focused on the identification of components in a mixture and/or the determination of their amounts.

However, this definition cannot be considered fully exhaustive, since almost all researchers perform qualitative or quantitative measurements in their field of expertise. Therefore, the real objective of analytical chemistry is not the mere execution of a routine measurement, but rather the development of new analytical methods suitable for specific applications, the improvement of existing methods or the extension of already established methods to different kind of samples [1].

For such reasons, analytical chemistry is routinely employed in almost all scientific fields, ranging from engineering to medicine, physics to geology and so on. Moreover, its multidisciplinary nature makes it a "central science", able to serve as a bridge between industry and academic research [2].

Analytical chemistry has always had a fundamental role in food science, since foods represent intricate and heterogeneous mixtures of many biochemical components. For such a reason, the development of suitable analytical methods has a crucial role in defining the chemical, physical, biological and sensory properties of food products and the changes they can undergo during processing and storage.

As is well known, analytical methodologies have undergone through an enormous evolution over the years, from basic chemical assays to advanced instrumental platforms. The considerable progress in food analysis is definitely related to the technological development, which has led to the design of highly sophisticated analytical instrumentations and software, but also to the attempt to meet the growing needs of the consumers. As evidence of this, various analytical approaches are widely applied to study different food matrices, aiming to assess the nutritional value, quality, authenticity, safety and stability of each product. Finally, analytical chemistry substantially contributes to food-related information and to implementing the laws and regulations concerning in the food sector [3].

Analytical techniques have the arduous task of overcoming the challenges of a globalized world, which include, above all, the sustainability of food production and maximization of the resources. In fact, the latest trends in the field of food analysis pay considerable attention on the environmental impact, production costs and reduction of waste materials. Nowadays, combined analytical techniques are conveniently employed to study the chemical composition at molecular level of many foods, thus, obtaining information regarding the entire panel of components in foods. These approaches provide a useful fingerprint for each food matrix and represent valuable tools to assess food authenticity and quality [4].

1.2 Chromatography as a powerful and versatile analytical technique

The first scientist who performed a chromatographic separation was the Russian botanist Michail Tswett around 1903 [5]. In his experiments, a primitive chromatographic system consisting in a packed column with a calcium carbonate as stationary phase and ether and alcohol as mobile phase, was successfully employed to separate and isolate green leaf pigments. The colored bands formed along the adsorbent bed inspired the term "chromatography" (from the Greek, "chroma", colour and "grafos", writing) which is still used today to describe separation techniques that employ a mobile and a stationary phase. Since these early experiments, many scientists gave a substantial contribution to this analytical technique. Among them, A.J.P. Martin and R.L.M Synge were responsible of the invention of partition chromatography (for which they received the Nobel prize) [6], while the collaboration between A.T. James and A.J.P. Martin resulted in the discovery of gas-liquid chromatography (GLC) [7], which represented a huge step forward for the development of the technique. From the late '60 the term "modern chromatography" was introduced, to indicate the developments in equipment, columns, automation and detection systems [8].

It should be considered that, during the early years, the development of liquid chromatography (LC) was very slow and challenging although it was introduced half a century earlier than the gas chromatography (GC) counterpart. In contrast, the development of GC was substantially fast, as demonstrated by the fact that, in around ten years from its introduction, this innovative separation method became one of the most employed analytical technique for the separation of volatile compounds. Probably, the

most relevant obstacle to the development of LC, delayed with respect to GC, was the initial difficulty in making sensitive in-line detectors. The elution of each solute was originally monitored by collecting a high number of fractions of the column eluent and by analyzing those fraction by means of other techniques, such as colorimetric assays. For that reason, a big step forward for LC was represented by the development of the first form of refractive index (RI) detector and the first electrical conductivity detector (ECD) [9, 10]. Today, the performance of LC instrumentation is equivalent to that of GC and the technique seems to be even more versatile. However, much greater research and development efforts were required for LC with respect to GC in past years, until the achievement of this result.

Chromatography has been defined from the International Union of Pure and Applied Chemistry (IUPAC) as "A physical method of separation in which the components to be separated are distributed between two phases, one of which is stationary (stationary phase) while the other (the mobile phase) moves in a definite direction" [11].

The chromatographic process is the result of a repeated absorption/desorption acts of the sample components along the stationary bed, being the chromatographic separation made possible by the differences in the distribution constants of the different components. Such distribution constant K_C, describes the degree of interaction of the solute with the stationary phase and therefore the relative tendency of that solute to be distributed between stationary and mobile phases (K_C is equal to the ratio of the concentration of the analyte in the stationary phase by the concentration in the mobile phase at equilibrium).

The most common distinction of chromatographic methods can be made according to the physical nature of the mobile phase. In GC, the mobile phase is represented by an inert gas, in LC the mobile phase is represented by a liquid, while in supercritical fluid chromatography (SFC) and subcritical chromatography (subFC) separations are carried out using a substance above its critical temperature and pressure.

In a similar way, another classification depends on the physical nature of the stationary phase. In GLC and gas-solid chromatography (GSC) the mobile phase is represented by a gas, while the stationary phases are a liquid in the first case and a solid in the latter case. Conversely, when the mobile phase is a liquid it is possible to distinguish between two sub-classes, namely liquid-liquid chromatography (LLC) and liquid-solid chromatography (LSC), being the stationary phase a liquid and a solid, respectively.

Generally, the stationary phase consists of a porous, granular powder material which is uniformly packed into a tube (column). The most employed sorbents are represented by solids of high surface area, inert sorbents of controlled pore size, solids used as support for a thin film of liquid or alternatively solid materials modified by bonding ligands to their surface. In other cases, the stationary phase can be distributed as a thin layer or film on the wall of an open tube of capillary dimensions maintaining a central open passage way. Last, the sorbent can be distributed as a thin and homogenous layer on a flat glass or alternatively on a inert backing plate, as in the case of the thin-layer chromatography (TLC) in which the action of capillary forces determines the movement of the mobile phase through the layer of sorbent [12]. Although TLC performance is substantially much lower with respect to LC, the simplicity and the low cost of the equipment make it a very popular technique even today.

In the overwhelming majority of cases, chromatography is nowadays performed by the introduction of a small volume of sample into the flowing mobile phase (eluent), the passage through the column and the subsequently observation of the different constituents of the sample which are progressively eluted and leave the column in form of concentration bands separated in time. The samples, which can be gaseous, liquid or solid, may be of varying complexity, and therefore they may consist of a single substance or may be characterized by a large number of components, containing a wide range of different chemical species.

The final result of the chromatographic separation is the chromatogram, which represents a record of the concentration or the mass profile of the sample constituents. A lot of information can be extrapolated from the chromatogram, such as immediate evidence of the sample complexity, which is obviously related to the number of observed peaks, the peak position and retention time, which positively support the qualitative identification of the analytes, the relative concentration or amount of each peak, which are employed for the quantitative assessment and an indication of the column performances.

Nowadays, chromatography is considered as one of the most versatile and powerful analytical technique and for this reason it has acquired a role of primary importance in modern analyses [13]. As a result, considerable confidence has been placed in chromatographic techniques to overcome challenging analytical issues and among them,

the possibility of resolving very complex matrices represents the greatest advantage of chromatography.

For such a reason, separation techniques are routinely employed in most laboratories, being conveniently used in every branch of chemistry, biochemistry and especially in the rapidly evolving field of biotechnology, both at the academic and the industrial level. In this scenario, the fields of application of chromatography are directly related to the ever-advancing scientific sectors for which analytical protocols and methods are highly and continuously demanded. This is the case of food and environmental analysis, pharmaceutical, clinical and forensic fields.

The continuous development of chromatographic techniques reveals to be necessary since the new analytical procedures demand high-throughput separations, robustness, high resolution and an acceptable analysis time for the specific application; moreover, considerable attention is paid on column technology aiming at the development of highly performing stationary phases [14].

Although chromatography represents an indispensable tool for the analysis of most samples, the employment of such technique must be inserted in a wider context in which the coupling of diverse analytical techniques or separation dimensions may be indispensable to provide a comprehensive characterization of a complex matrix.

In this context, the hyphenation of chromatography to mass spectrometry (MS) represents the most convenient and widely used coupling, since this approach combines the high separation power of the first technique and the enormous potential in structural elucidation and components identification of the latter. In fact, MS deals with the study of analytes through the formation of gas-phase ions, with or without fragmentation, which are detected and characterized on the basis of their mass-to-charge ratios (*m/z*) and their relative abundance [15].

Another analytical strategy, widely employed for the resolution of complex mixtures of numerous components, consists in the coupling of two or more separation dimensions. On the other hand, multidimensional approaches aim at enhancing the resolving power, and therefore the peak capacity, of the chromatographic system. Analytes separation is obtained through the coupling of diverse mechanisms of retention; particularly, this is achieved by transferring selected fractions of eluate from the first separation system to the next separating system [16].

Finally, among the less conventional analytical techniques, SFC and subFc are progressively gaining considerable attention as a viable alternative to LC and GC. In fact, supercritical and subcritical fluid-based approaches show a reduced environmental impact ("green separations") and allow for minimizing organic solvent consumption. Moreover, the mobile phases employed in these techniques are characterized by low viscosities and high diffusion coefficients, thus, enabling fast and highly efficient separations with reduced pressure drop [17].

1.3 Hyphenated analytical techniques

Hyphenated analytical techniques are based on the coupling of two or more different techniques, in which the first generally deals with the separation of the mixture, while the subsequent/s are designated for identification and/or quantitation of the analytes. The term hyphenated analytical techniques was introduced by Hirschfeld in 1980, when describing GC-MS and LC-MS, he emphasized the importance of the "hyphen" as a symbol of their common principle, that is the "marriage" of separated analytical techniques by means of proper interfaces [18]. Such definition has been therefore used to refer to the online combination of a separation technique and one or more spectroscopic detection techniques (Figure 1.1).

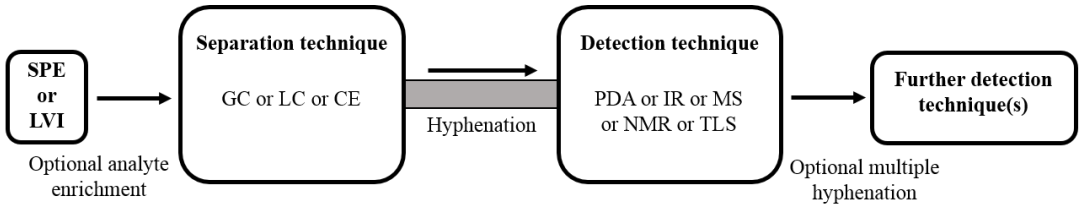

Figure 1.1 Schematic representation of the hyphenated analytical techniques.

The need of coupling diverse analytical techniques not only derives from the simple interest in analyzing real-world samples, but also from the attempt to characterize "all known compounds" or "all possible compounds" present in a highly complex matrix. In recent years, sciences as metabolomics, lipidomics, proteomics have gained increasing importance because modern analytical methods aim at the characterization of almost all the metabolites, lipid species or proteins of a certain sample. For such reasons, untargeted approaches are increasingly used and many reasearches are intended to obtain a

“fingerprint” of the sample, since the metabolite profile is unique for each investigated matrix. Despite many diverse hyphenated analytical techniques have been extensively exploited, chromatographic techniques online coupled to mass spectrometry detection have pride of place among the most used and useful approaches for the elucidation of real world-samples.

GC-MS represents the most powerful analytical tool available today for the analysis of volatile (VOCs) and semi-volatile (SVOCs) compounds in many different fields as food analysis, environmental and petrochemistry applications; for such a reason it has been considered “the gold standard” technique for VOCs and SVOCs characterization. In most cases a chemical modification of the analytes as silylation and methylation prior to the GC-MS analysis is required, to enable the analysis of non-volatile and highly polar compounds. In fact, the biggest limits of the technique concern the analysis of highly polar and high molecular weight components, and obviously thermally labile compounds; for the study of such kinds of analytes in pharmaceuticals and biological samples LC-MS is a more popular technique.

However, in more recent times, great efforts have been put in overcoming such limits, together with the attempts to reach a sufficient characterization of complex matrices with unkown constituents. As an example, to extend the applicability of the technique, some of the employed strategies involved the decrease of the residence time of analytes and the reduction of elution temperatures [19]. Conventional GC-MS approaches may require long sample preparation steps and long analysis time; moreover, the sample handling together with the use and mantainence of GC-MS instruments, the use of diverse software platforms and data elaboration require trained operators. Fast and ultra-fast GC-MS approaches have also been investigated, but these applications present in practice a very limited usage since they require specially designed and expensive instrumentation [20]. Miniaturized GC-MS was also exploited but at the price of reduced sample capacity, since miniaturized columns present loadability accordingly reduced. Nowadays, GC-MS applications in untargeted metabolomics are still limited for the poor availability of reference mass spectra in commercial libraries and for the reduced comparability between spectra obtained with different soft ionization techniques, highly dependent on ionization conditions [21]. Moreover, a huge demand of mass spectral databases has been registered, to fulfill the requests of the “omic” approaches, especially concerning the availability of

reference spectra obtained through soft ionization techniques, tandem MS and high-resolution MS. Powerful and sophisticated software reveals to be necessary to manage the results, allowing for the extrapolation of relevant data, elimination of noise, background and useless information, and lastly enabling the statistical processing of data. Regarding the ionization techniques, electron ionization (EI), performed at high energy (70 eV), is the most widely used in GC-MS [22]. Such hard ionization conditions result in the generation of stable, highly reproducible, mass spectra, enabling the comparison with the spectra recorded in reference libraries. Nevertheless, one of the most significant limits is represented by the identification of unknown compounds, not included in commercial libraries, which subjected to EI fragmentation leads to unspecific/difficult to attribute mass ions. For such reasons, in most recent years, different soft ionization approaches have been evaluated in GC-MS, to produce more informative mass spectra with reduced fragmentation.

Chemical ionization (CI) in positive ion mode has been traditionally used to obtain spectra with intense, clearly detectable, protonated analyte molecules and fewer fragment ions than EI. As an example, the complementary use of CI and EI has been evaluated for the elucidation of unknown components; particularly, the first ionization technique was convenient for molecular mass determination, while the structure information generated by the EI together with the accurate mass measurement provided by the TOF analyzer was undispensable for the proposal of an appropriate formula [23].

Soft-ionization techniques, as field ionization (FI) and single- or multi-photon photoionization (PI) and atmospheric pressure chemical ionization (APCI) have been also exploited in GC-MS. As an example, GC-APCI-MS has been conveniently employed in metabolomic analysis of fruits [24], steroid hormone analysis [25] and pesticide residue determination [26]. Recently, modified EI sources have also been introduced, allowing operating ionization at lower energy with a reduced loss of sensitivity [27]. The most significant limit of soft ionization is represented by a highly condition-dependent fragment production, thus making these techniques less usefl in untargeted approaches.

As far as MS instrumentation is concerned, the latest trends have focused on the design of sensitive, robust, faster and smaller devices. Among the different mass analyzers, the quadrupole analyzer (Q) represented the most employed for routine analysis since its introduction. The triple quadrupole (QqQ) is widely used in targeted approaches as it

allows to perform tandem MS analysis, thus, providing increased sensitivity and selectivity. Furthermore, the use of the *Multiple Reaction Monitoring* (MRM) mode (Figure 1.2) is highly recommended from European regulations for positive analyte confirmation in forensic, toxicological, environmental and food analysis [28].

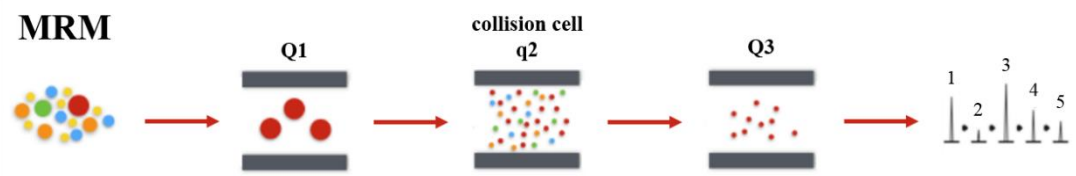

Figure 1.2 Schematic representation of the MRM mode.

Among the high-resolution mass analyzers, Orbitrap and TOF analyzers are the most employed for untargeted applications. The possibility to perform accurate mass measurement make them suitable analyzers for compound identification, allowing also for elemental composition and structure elucidation. Despite the numerous advantages of high-resolution mass analyzers, low-resolution analyzers are still today preferred for diverse applications. Such choice may result from the low regulatory limits required for the detection of trace compounds in high complex matrices, which make untargeted analysis almost impracticable and from the well-established use of low-resolution libraries in which reference mass spectra result to be slightly different from those acquired with high resolution spectra, thus reducing the quality match [29]. However, high-resolution GC-MS is widely used both for research purposes but also in many areas of application, like petrochemical, environmental and biochemistry [30]. Moreover, coupling the high separation power of multidimensional techniques, such as comprehensive two-dimensional GC (GC×GC), to the high acquisition speed of TOF analyzers reveals to be highly beneficial for untargeted analysis of complex matrices [31].
As for LC-MS, it represents an indispensable tool in modern analytical laboratories; in fact, the enormous improvements it has undergone over the last twenty years have made it the election technique for biochemical, clinical and pharmaceutical applications, for food analysis and in general for all the “omic” sciences.
Recent trends in LC-MS approaches regard system miniaturization, with a progressive reduction of column diameters from standard-/narrow- bore (3 - 4.6/ 1 - 3 mm) to capillary columns (< 1 mm), and the transition to chip-based separations that is gaining increasing

popularity [32]. The employment of operational flow rates in the range of nL/min make nanoelectrospray ionization (nanoESI) the most suitable approach for MS coupling. Additional analytical tasks to which much attention is being paid in recent years are high throughput analysis and system automation. Such technological improvements are highly requested to analyze many samples and manage enormous amounts of data, as in the case of clinical laboratories, for which non-supervised system operations are also highly convenient. As a result, sample preparation, analysis and data processing can be totally automated by using modern robotic platforms [33]. Furthermore, the potential of chemical derivatization, originally limited to GC, was also exploited in LC-MS for diverse purposes such as: increase of analytes stability, improvement of the retention behavior of problematic analytes, enhancement of analyte ionization efficiency in MS interfaces; improvement of MS selectivity; employment of isotope- and or fluorescent-labeling strategies [34].

Great efforts have been put in the improvement of packing materials and stationary phases based on totally porous particles, superficially porous particles and monoliths [35, 36]. Emerging trend in the field of packing materials and stationary phases regard the use of submicron colloidal particles, 3D-printed columns, diamond-based material and open tubular columns [37-40].

Nowadays, considerable importance has been put also in fast LC-MS techniques, aiming to achieve the highest analysis throughput without sacrificing separation efficiency. Ultra high-performance liquid chromatography (UHPLC) represents the most convenient and widespread technique to perform fast analysis, providing narrow chromatographic peaks. This approach is based on the use of columns packed with reduced size particles (usually sub-2-μm) and powerful chromatographic systems with an extended pressure range (up to 1200–1400 bar), allowing for ultra-fast and/or ultra-high-resolution separations [41]. From the other side, mass analyzers must meet the requirements dictated by the coupling to fast chromatographic separations, such as a high acquisition speed.

Concerning the ionization techniques, ESI is the most widely used for the analysis of polar, thermally labile and high molecular weight analytes, with particular emphasis on biomolecules; even APCI-MS is quite common in LC-MS, particulary employed for the analysis of medium polar to non-polar organic compounds [42]. In numerous applications, both polarity modes are conveniently used in a single run to gain

complementary information of the analytes; as a result, instruments with a fast polarity switching are highly required, even if this task is more challenging to achieve for the high-resolution mass analyzers, because of the relatively long time required by the electronics for the stabilization of high voltages. The use of multimode ionization sources has been also exploited, allowing the combination of ESI and APCI ionization techniques in a single run; qualitative performances of the combined sources have been compared to those of the single interfaces obtaining almost equivalent mass spectra in a reduced time [43]. The atmospheric pressure photoionization (APPI) is currently not so widely used as ESI and APCI, probably for its lower sensitivity at higher liquid solvent flow rates; in fact generally a dopant, such as toluene or acetone, is added to the mobile phase to enhance the ionization efficiency. However, further research and development in the design of APPI sources may extend the applicability of the technique in the near future [44]. Despite the common use in GC-MS, EI has been exploited also in LC-MS as an alternative to atmospheric pressure ionization techniques. Great scientific efforts have been put to enable the coupling between LC and EI-MS, both for the stringent requirements of EI, related to the use of high-vacuum and high-temperature conditions, but also for the need to remove the LC eluent before to enter the ion source; regarding the latter, common instrumental set-up based on low flow rate nano-LC system coupled to a high vacuum EI source.

Among the advantages of such coupling, the comparison of EI mass spectra to those recorded in commercial libraries, leading to fast and automatic identifications, should be mentioned. Moreover, in most cases, the typical fragmentation obtained through EI allows for the prediction of the structure of unknown analytes, even when they are not present in databases [45].

Even for LC-MS, the use of low-resolution mass analyzers, as Q analyzer, is fairly popular for routine use in common laboratories, due to the reduced costs and size of the spectrometers. Other simple and cheap instruments conveniently employed in routine applications are the spherical and linear ion traps (IT).

QqQ mass analyzers are commonly used in targeted and quantitative approaches; in fact the increased sensitivity, precision, robustness and selectivity obtained in selected and multiple reaction monitoring (SRM-MRM) modes make this analyzer the “gold standard” for LC-MS quantitative analysis [46].

In recent years, great scientific efforts have been put into the technological development of MS instruments, to promote a progressive transition to high-resolution and ultrahigh-resolution analyzers; in fact the potential of ultrahigh-resolution and ultrahigh mass accuracy may open new possibilities in both qualitative and quantitative approaches.

Among the high-resolution instruments, TOF analyzers are more widely used since they offer impressive features in term of acquisition speed and mass accuracy, theoretically unlimited mass range, with relatively lower costs. The ultrahigh-resolution Fourier-transform ion cyclotron resonance (FTICR) and Orbitrap analyzers, probably show the optimum operational parameters and result to be highly suited for proteomics, lipidomics and metabolomics applications. Such analyzers, providing resolution values in the range of 30,000-1,000,000 (FWHM) and mass accuracy < 5 ppm, allow for the resolution of ions showing the same nominal mass and therefore the accurate mass measurement of such analytes, usable to determine the ions formula or at least reducing the number of possible candidates, the latter resulting to be highly beneficial in the "omics" approaches [47]. Nevertheless, the high instrumental complexity of ultrahigh-resolution analyzers, together with the high costs, have partially limited their widespread use.

Hybrid instrumentations have gained considerable attention because they combine the features of different mass analyzers and allow for tandem MS applications. Among them, Q-TOF instruments are widely used for structure characterization since they provide high mass accuracy employing both full scan and MS/MS experiments [48].

The most common types of mass analyzers employed routinely are listed in Table 1.1 along with their features and specifications.

Considerable attention has been put also in the coupling between LC and ion mobility spectrometry (IMS), which was exploited over the past few decades for its great potential in proteome profiling, genomics and metabolomic applications. In IMS, gas phase ions are separated on the basis of their different mobilities in low or high electric fields; this technique allow for ions differentiation on the basis of mass, size, shape and charge, providing a variety of additional information. Such technique offers a great number of advantages, allowing for the separation of isomers, as in the case of carbohydrates and the separation of isobars; moreover ions showing similar characteristics, in terms of structure or charge state can be separated in unique mass-mobility correlation lines; as an example databases of collision cross-sections of peptides derived from proteases

Table 1.1 Features and specifications of the most common mass analyzers used in LC-MS.

Analyzer	**Accuracy (ppm)**	**Resolution**	***m/z* Range**	**Scan rate**	**Sensitivity**	**MS tandem capability**
TOF	5-50	10,000-20,000	No upper limit	Very fast	Femtomole	No
TOF-TOF	5-50	10,000-40,000	No upper limit	Very fast	Femtomole	MS/MS
Magnetic sector	1-5	1000-100,000	10,000	Slow	Picomole	No
Q	50-100	2000	50-4000	Fast	Femtomole	No
QqQ	50-100	2000	50-4000	Fast	Attomole	MS/MS
LIT	50-100	2000	50-2000; 200-4000	Fast	Femtomole	MS^n
QIT	50-100	2000	50-2000; 200-4000	Slow	Picomole	MS^n
Orbitrap	< 1	15,000-100,000	50-8000	Moderate	Femtomole	No
FTICR	< 1	500,000-1,000,000	10,000	Slow	Femtomole	MS^n
Hybrid Analyzer						
MS1	**MS2**					
Qq	TOF	5-50	10,000-40,000	10,000	Moderate-Fast	Attomole	MS/MS
Qq	LIT	100	2000	2000	Moderate-Fast	Attomole	MS^n, MS/MS
Qq	Orbitrap	< 5	17,500-240,000	50-8000	Moderate	Femtomole	MS^n, MS/MS
QIT	TOF	2-5	10,000	10,000	Moderate-Fast	Attomole	MS^n, MS/MS
LIT	Orbitrap	< 5	50,000-500,000	50-2000; 200-4000	Moderate	Femtomole	MS^n
Qq	FTICR	< 2	50,000-500,000	50-2000; 200-4000	Slow	Femtomole	MS/MS
LIT	FTICR	1-2	50,000-800,000	50-2000; 200-4000	Slow	Femtomole	MS^n

QqQ, Triple quadrupole, LIT, Linear ion trap.

digestion have been recently developed. IMS has been also used in the characterization of the charge-state conformations and folding of proteins. In the vast mayority of applications, IMS has been conveniently coupled to MS (LC-IMMS) by selecting analyzers as TOF, Q, IT and FT-ICR. Furthermore, an ion mobility cell may be coupled to other ion mobility cells or to hybrid mass spectrometers, allowing for MS/MS analysis [49, 50].

Concerning the fragmentation technique employed in LC-MS/MS approaches, collision induced dissociation (CID), which is mediated by a neutral gas as argon or nitrogen, is the most widely and traditionally used approach. In detail, in the proteomic field, CID represents a well established and robust fragmentation method for peptides obtained by protease digestion. Nevertheless, electron capture dissociation (ECD) and electron transfer dissociation (ETD) have emerged more recently as complementary electron-based dissociation techniques for protein characterization. In fact in CID approaches, the multiple collisions with the inert backgroung gas induce a vibrational activation of peptide ions, followed by a vibrational redistribution of the internal energy (equilibration); when the internal energy exceed the fragmentation threshold the weakest chemical bonds are preferentially cleaved. This process results in the predominant formation of y- and b-type fragment ions, obtained by the cleavage of amide bonds; the cleavage doesn't occure equally along the peptide backbone, in fact the fragmentation near the glutamic acid, aspartic acid and proline residues is preferred. For the same principle of the cleavage of the weakest bond, CID fragmentation may preclude the study of post-translational modifications (PTMs) by determining their loss from the amino acidic side chains [51]. From the other side, electron-based dissociation techniques provide alternative fragmentation patterns, with a predominant formation of c- and z-type ions (cleavage of the N-Cα bonds) while preserving more labile PTMs. In ECD, the exothermic capture of a thermal electron induces a nonergodic fragmentation of the peptide ion without a prior redistribution of the internal energy; therefore, the cleavage occurs where the radical has been originally formed. Similarly in ETD, a radical anion is used to transfer the electron to the peptide ion. Nevertheless, the existing search algorithms for analysis of ETD and ECD data are not as advanced as for CID, thus making the first approaches less employed. In more recent times, CID and electron-based dissociation techniques have been employed in combination to obtain orthogonal

datasets, of the same peptides, used for deducing their amino acid sequences and possible PTMs. The use of two different fragmentation strategies provides a more confident identification through the cross-validation of the results obtained by database searching [52].

In recent years, LC-MS-based untargeted approaches have gained considerable importance for the growing interest in "omic" applications, such as discovery proteomics and non-targeted metabolomics. In fact, recent trends aim at the comprehensive evaluation of all the measurable components of a certain sample, including both the known and unknown ones. In this context, the most common data acquisition techniques are data- dependent acquisition (DDA) and data-independent acquisition (DIA), sometimes referred as MS^E or SWATH (sequential window acquisition of all theoretical fragment-ion spectra) (Figure 1.3). In both techniques, a full MS1 scan acquisition is followed by one or multiple MS/MS (or MS2) acquisitions, performed by using different strategies. In detail, in DDA approach a defined number of precursor ions are selected from the full MS1 scan according to specific criteria, especially depending on ion abundance and intensity, so that only a particular subset of analytes will be subjected to the fragmentation steps. In DIA techniques, all the ions within an *m/z* window are fragmented without a previous selection; in this approach MS/MS scans are collected independently from precursor ion information.

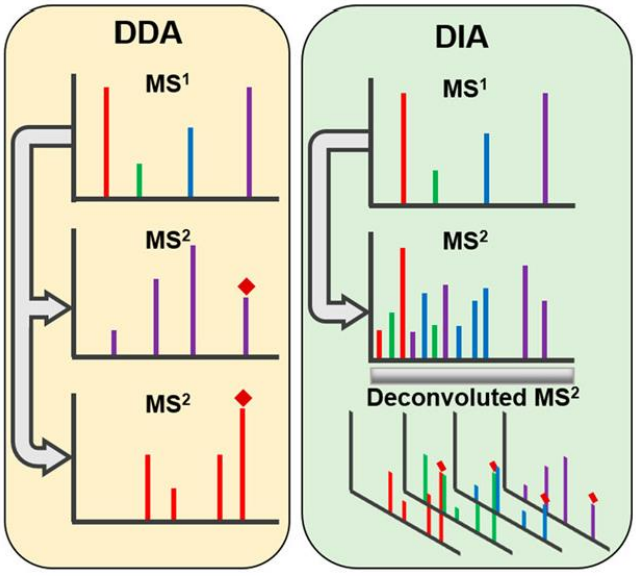

Figure 1.3 Schematic representation of DDA and DIA acquisition techniques.

DDA represents a powerful strategy and traditionally most used, however it shows some limitations, especially related to the limited number of components selectable as precursor ions, which is highly dependent from the mass analyzer MS/MS sampling speed. Such approach is based on a random sampling model biased toward high-abundance compounds; moreover, in a highly complex sample as a protein digest, a consistent percentage of analytes may remain unsampled, while relatively high variability of the sampled components may be registered between replicate analyses of the same samples. Conversely, data processing of the MS/MS spectra obtained by DIA approaches result to be complex and prone to misleading annotations. Shared fragments deriving from co-isolated precursor ions may coexist in a multiplexed MS2 spectra; thus making the conventional databases strategies for analyte identification less effective if compared to DDA [53,54].

1.4 Unconventional analytical techniques

1.4.1 Multidimensional Liquid Chromatography

Despite the great development of LC techniques, especially in terms of column technologies, instrumentation and dedicated software, one-dimensional LC (1D-LC) approaches are not always able to resolve real-world samples. These limitations may be due to the high complexity of the matrices under investigation, as in the case of biological samples consisting of hundreds of metabolites, exceeding the capacity of the system to separate the mixture into pure compounds. Furthermore, species which are difficult to separate may consist of closely related compounds, regardless the matrix complexity.

The separation capability of a chromatographic system is described by the *peak capacity* (n_C), which represents the number of peaks that can be separated within a retention window [55]. The "Statistical Theory of peak Overlap" proposed by Davis and Giddings has allowed an estimation of the constituents, belonging to a certain sample, which would be (on average) resolved as distinct chromatographic peaks, taking into account the combination of sample of various complexity and the peak capacities of the employed separation systems. Their findings have pointed out that the peak capacity value of a chromatographic system should be much higher than the number of the sample constituents. In detail, it has been demonstrated that, even for less complex samples, when the number of constituents to be separated exceeds 37% of the peak capacity of the

separation system, statistically the resolution of the peaks results to be compromised and, as a consequence, many peaks derive from the coelution of two or more compounds [56]. Multidimensional Liquid Chromatography (MDLC), which is based on the coupling of multiple separation dimensions differing in their retention mechanisms, may represent a viable solution to the limitations of 1D-LC; specifically, this approach allows for an increase of the peak capacity of the chromatographic system and therefore, it determines a potential improvement of compounds separation with decreased number of coelutions.

The operating principle of two-dimensional LC (2D-LC) consists in the transfer of one or more fractions of the effluent from the first dimension (^{1}D) column to a second dimension (^{2}D) column, so that, ideally, the ^{2}D is able to resolve all the analytes contained in the effluent fractions deriving from the ^{1}D on the basis of the different selectivity of the two separation dimensions.

Depending on the fractionation strategy of the effluent from ^{1}D column, 2D-LC techniques can be classified in [57] *Heart Cutting LC* (LC-LC) and *Comprehensive LC* (LC×LC).

In LC-LC only few selected fractions, containing the target analytes, are conveyed into the ^{2}D. The ^{1}D column is used to extract (detection in absence of interfering compounds) and enrich (preconcentration) analytes, while the ^{2}D is employed to separate the molecules of interest. Historically, LC-LC has been widely employed for the quantitation of a reduced number of target compounds in diverce matrices [58].

In LC×LC the whole effluent from the ^{1}D column is subjected to the ^{2}D separation. This approach is able to provide information on a largest number of analytes, ideally by fractionating and therefore separating all the components of the mixture. LC×LC is conveniently employed for applications of metabolomics and proteomics, by using MS for compounds detection [59, 60].

In more recent times, different intermediate and hybrid approaches between LC-LC and LC×LC, have been investigated. Among them, it is important to mention, *multiple heart cutting* (mLC-LC) and *selective comprehensive* 2D-LC (sLC × LC). mLC-LC can be viewed as an extension and improvement of the single heart-cut approach, since it allows that single fractions from several ^{1}D peaks (multiple regions of the ^{1}D effluent) are subjected to separation in the second dimension. In such cases the traditional LC-LC approach should require multiple sample injections in the ^{1}D to allow multiple fractions

to be analyzed in the ^{2}D column, thus, increasing the analysis times or requiring offline fractions collection. mLC-LC usually involves the use of sampling interfaces, allowing for the simultaneous collection of a fraction from the ^{1}D while separating the constituents of another fraction in the ^{2}D. In detail, the employed instrumentation enables the parallel execution of these processes (sampling of the ^{1}D/transfer to the ^{2}D) so that multiple peaks can be trapped and analyzed separately in ^{2}D [61, 62].

Concerning sLC×LC, it can be considered as a "selective" approach because only selected regions of the ^{1}D effluent are subject to further separation in a comprehensive manner, so that the resolution of the separation of the ^{1}D separation is preserved and improved in the ^{2}D. The cut fractions from the ^{1}D separation are temporarily stored to permit the sampling time to be different from the analysis time in ^{2}D. Each obtained fraction is transferred in the second dimension when the ^{2}D separation of the previous fraction is completed [63]. The sLC×LC approach requires very sophisticated instrumentation, both for the collection/storage of the fractions obtained from each ^{1}D peak and for the subsequent serial injections of those fractions into the ^{2}D column.

Furthermore, 2D-LC can be performed in *offline* or *online* mode. In the first case, one or more fractions collected from the ^{1}D (manually or by means of a fraction collector) are separated from the solvent by evaporation, dissolved again and injected into the second dimension. The *offline* 2D-LC approaches result to be easier to develop since they don't require sophisticated devices or transfer valves; such techniques are exempt from solvent and flow rate incompatibility issues between the two dimensions and the optimization of the separation of ^{1}D and ^{2}D can be carried out independently of each other. Nevertheless, the *offline* mode shows limits as time consumption, reduced reproducibility and impossible automation, together with potential susceptibility to sample loss, degradation or contamination.

In *online* 2D-LC the solute transfer into the ^{2}D column is totally automatized, without requiring any interruption of the flow. The two separation dimensions are connected by means of an interface or modulator, such as a switching valve. Compared to the *offline* mode, this approach provides higher resolving power, reduction of the analysis times, improved reproducibility, higher information obtainable from a single analysis, reduced sample handling and therefore contamination. The limitations of *online* 2D-LC are the need of sophisticated instrumentation, the high demand in interfaces/transfer devices and

software specifically designed for this kind of approach, the possible incompatibility of the mobile phases of the two dimensions and the potential difficulties in coupling the different separation methods. Despite such limitations, the vast majority of 2D-LC more recent works are focused on *online* approaches, probably thanks to the considerable improvements in LC technologies, which allow for highly automation by employing robust and precise commercial instruments [64]. The comparison between the offline and online 2D-LC approaches is reported Table 1.2.

Table 1.2 Comparison between offline and online 2D-LC

	Offline 2D-LC	**Online 2D-LC**
Advantages	Simpler instrumentation	Automation
	Independent optimization of the separation dimensions	Reduced analysis time
		Higher resolving power
	Exempt from solvent and flow rate incompatibility	Higher reproducibility
		Reduced sample handling
Disadvantages	Time consumption	Higher costs
	Reduced reproducibility	Sophisticated interfaces/modulators
	Potential sample loss and contamination	Difficulties in coupling diverse separation mechanisms

Among the separation mechanisms used in 2D-LC, reversed phase (RP-LC) has been extensively employed as first dimension separation technique; in some cases, it is even used in both ^{1}D and ^{2}D, by selecting totally different mobile phases or diverse stationary phases. Other separation mechanisms conventionally employed for the ^{1}D are hydrophilic interaction chromatography (HILIC), ion-exchange chromatography techniques (IEX) and size exclusion chromatography (SEC). Concerning the ^{2}D, RP-LC is the most widely used separation mechanism, due to the fast equilibration times, easy coupling to MS and the employment of gradients going from high to low percentages of water allowing the elution under optimal conditions of components with a wide range of polarity. SEC is

also quite used as ^{2}D, offering the employment of simple instrumentation and the possibility possibility of coupling to many detectors [65].

Regarding the detection systems conventionally employed in 2D-LC approaches, UV-Vis spectrophotometers are routinely used in the vast majority of quantitative applications; particularly, the reduced costs of such devices have encouraged their use. The combination of two-dimensional techniques and MS instruments has been widely exploited for a great number of applications; in detail, both single (e.g. Q, ToF, Orbitrap) and hybrid mass analyzers (e.g. Q-TOF) have been used. On the other hand, fluorescence, light scattering and refractive-index detection techniques are less commonly employed in 2D-LC setups.

Concerning the fields of applications, 2D-LC analytical approaches have been extensively employed in food analysis, since food products generally represent highly complex and heterogeneous mixtures. Furthermore, the recent trends in modern food analysis deal with the characterization of the maximum possible number of components of the investigated matrices, therefore an increased resolving power of the separation techniques employed for such approaches is highly desirable [66].

In detail, 2D-LC setups have been used in food safety for the determination of environmental pollutants [67], pesticides [68], and antibiotics [69]. Different 2D-LC approaches have been used for food quality evaluation, as in the case of the changes occuring in the metabolites profile during red wine aging [70] and authenticity assessment, especially for protected designation of origin (PDO) [71] and protected geographical indication products (PGI).

2D-LC systems are increasingly used in lipidomics, aiming at the whole characterization of lipid species in the samples of interest. Considering that such components show a large diversity in polarity and chemical structure, multidimensional techniques may be highly useful for the separation of specific lipid classes, as in the case of glycerophospholipids (e.g. phosphatidylcholines PC, phosphatidylserines PS and phosphatidylethanolamine PE). As an example, a HILIC×RPLC-ESI-MS set-up was employed for the analysis of phospholipids in cow's milk and plasma sample, allowing for the identification of components belonging to six different classes (of which PC resulted to be the most complex in the investigated samples) [72].

Furthermore, 2D-LC reveals to be a powerful strategy even in the evaluation of the whole lipidome of the investigated sample. For such purpose, a HILIC×RPLC-MS/MS approach was exploited to quickly fingerprint lipids in the Mediterranean mussel (*Mytilus galloprovincialis*), allowing the identification of more than 200 neutral and polar lipids [73]. The convenience in such coupling, results from the ^{1}D HILIC capability of separating lipid classes and the ^{2}D RP-LC ability to separate the lipid species inside each class, according to their increasing hydrophobicity. Triacylglycerols (TAGs) have been also investigated by means of 2D-LC, but due to the more hydrophobic nature of these lipid species, TAGs are not usually analysed by HILIC and normal-phase LC (NP-LC) approaches. More convenient couplings for TAG analysis are represented by silver ion LC (Ag^{+}-LC), in which the separation is ruled by the lipid unsaturation degree and position of DBs, and RP-LC. This approach was successfully demonstrated by Holčapek's group for TAG analysis in complex mixtures of plant and animal origin; an off-line setup consisting of non-aqueous reversed phase LC (NARP-LC) as ^{1}D and Ag^{+}-LC as ^{2}D, with APCI-MS detection was investigated for this purpose [74].

Over the last twenty years 2D-LC has been extensively employed in proteomics, especially in *peptide fingerprinting*. LCxLC approaches are commonly selected for these kinds of applications, even if the *Multidimensional Protein Identification Technology* (MudPIT) based on the use of a biphasic microcapillary column packed with strong cation exchange (SCX) and RP packing material and direct coupling to ESI-MS, specific for peptide analysis, has been largely employed [75]. In such context, 2D-LC usually is used as investigative tool for the untargeted analysis, while MS is employed for the identification. Thus, the optimization of the separation dimensions is some cases may be less important. Nevertheless, the recent development of the biopharmaceutical sector, highlighted the need of 2D-LC analytical methods with a sufficient peak capacity, quantitatively more precise and coupled to cheaper spectrophotometers (e.g. UV-Vis) for the quantitation of enzymatic digests of monoclonal antibodies, or mixture of biotherapeutic large proteins [76, 77].

1.4.2 Supercritical and subcritical fluid chromatography

Since its introduction in 1962 [78] supercritical fluid chromatography (SFC) has represented a valuable environmentally friendly analytical techniques, which combine the

avantages of GC and HPLC. In fact, SFC has an extended range of accessible analytes compared to the other techniques, since GC is restricted to volatile, thermally stable and usually non-polar compounds, while HPLC, despite covering the widest analyte polarity range, requires the employment of distinct elution modes for the analysis of non-polar and polar components (e.g., NP, RP, HILIC, IEC). Conversely, SFC allows for the separation of the most lipophilic and hydrophilic of analytes within a single chromatographic run on the basis of their different partition coeffient (log P), enabling for the easy switching between nonpolar and polar elution modes.

However, only in the last decade SFC has reached its industrial age, leading to the development of sophisticated instrumentation for managing supercritical fluids (SFs), designed to allow precise and reliable control of both temperature and pressure at the column inlet and outlet. Such technological improvements have contributed to make SFC the election technique for a wide range of applications, such as for chiral and semi-preparative analysis of food, cosmetic and pharmaceutical products [79].

An SF is any substance at a temperature and pressure above its critical point (Pc). The latter concept was introduced by Andrews in 1869 [80] to define the end point of a liquid–vapor equilibrium curve, above which liquid and gas co-exist as a unique phase (Figure 1.4). As a result, SFs show peculiar physical properties, as compressibility and solvating power which are similar to those of gases and liquids, respectively.

SF diffusion coefficients are similar to those of gas and the viscosities are 10-100 times lower than liquids, thus providing faster separation kinetics and limited pressure drop at increased flow rates. Furthermore, SF polarity increases with density, thus enabling the separation of a wide range of analytes [81]. Different gases may be used as SFs, as water, ammonia and hydrogen; however, CO_2 presents the most suitable features since it reaches the supercritical state above the critical temperature of 31 °C, close to the ambient temperature and the critical pressure of 73,8 bar, accessible for the analysis of biological components. Further, CO_2 is a nontoxic, non flammable inert and cheap solvent and its separation properties may be widely manipulated by changing the pressure and temperature [82]. For such reasons, in recent years SFC has decisively shifted its focus on the use of carbon dioxide as mobile phase, mixed with other co-solvents [83].

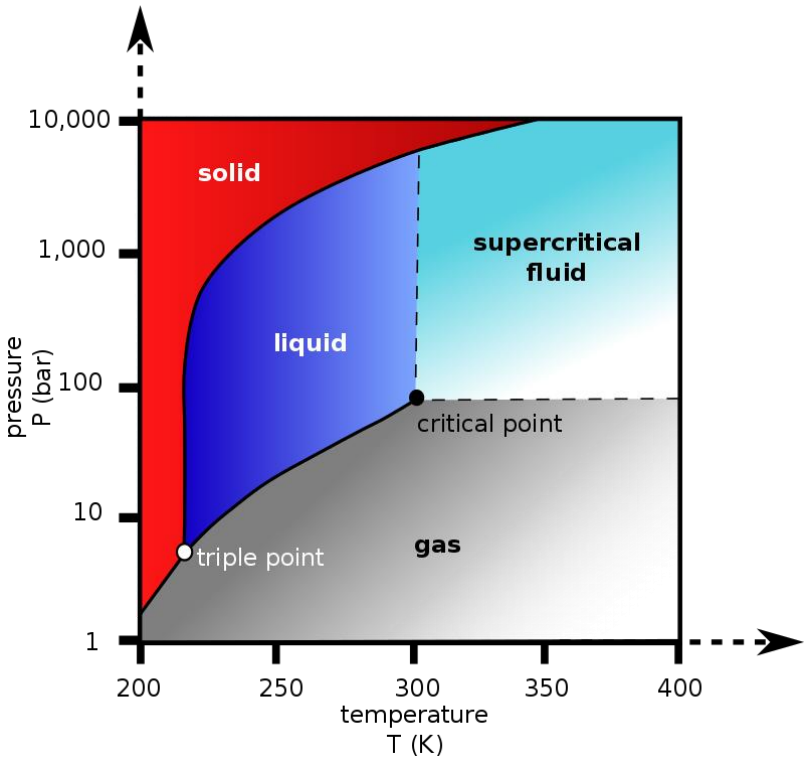

Figure 1.4 Phase diagram of carbon dioxide

In fact, pure CO_2 presents an excellent solvating power for non-polar analytes, enabling the analysis of hydrophobic molecules; conversely, carbon dioxide turns out not to be suitable for the analysis of polar compounds. To overcome such limitations, co-solvent, also defined as modifiers are tipically added in small amounts (comprised in the 2-40% range) to extend the range of SFC-amenable analytes. The most employed modifiers are organic solvents as acetonitrile, 2-propanol, and methanol and their employment allows for the solubilization of more polar components by introducing specific additional interactions such as hydrogen bonds or dipole-dipole to tune selectivity factors; this results in the increase of the mobile phase elution strength and therefore, in a shorter retention.

Nevertheless, it should be considered that the addition of an organic co-solvent determines a shift of the critical temperature and pressure to higher values and for that reason, reach the critical state in some cases may be detrimental both for the system and for the analysis of thermolabile compounds. The practical consequence is that most of SFC separations are not performed using supercritical conditions, but rather “subcritical” ones and hence the term “subFC” [84]. In detail, the subcritical condition may be reached

by maintaining the pressure above the critical value while keeping the temperature below the critical value. Furthermore, subcritical fluids show physical properties closer to those of liquids both in terms of eluting strength and diffusion coefficients; the latter without determining a reduction of the chromatographic efficiency [85]. In sub-critical conditions, when a polar co-solvent (e.g., acetonitrile) and hydrophobic stationary phases (e.g. octadecylsilica) are used, analytes retention behaviour generally follow the rules of RP-LC.

More recently, the novel backpressure regulator design, the reduced void volumes and the higher upper pressure limits have made SFC instruments fully compatible with sub-2-μm and superficially porous particles stationary phases; thus, enabling a progressive transition to ultra-high-performance SFC (UHPSFC), characterized by improved chromatographic resolution and reduced analysis time, without the limitations deriving from liquid viscosity traditionally encountered in UHPLC [86].

Concerning the detection systems, carbon dioxide allows for the coupling to the most widespread detectors such as UV, MS and evaporative light scattering (ELSD). In detail, the weak absorbance of CO_2 at low wavelengths is highly beneficial for UV detection, allowing for monitoring wavelengths closer to 200 nm. The UV detector is placed between the column and the backpressure regulator to keep the mobile phase in a condensed state, for that reason a pressure resistant flow cell is required. Conversely, the ELSD and MS detectors are located after the backpressure regulator, enabling the depressurization of the mobile phase and the easier transition of CO_2 to the gaseous state. It is noteworthy that the increased accessibility to mass spectrometers in the supercritical fluids instruments technology, has led to an extension of the SFC applications for which less informative detection systems are not sufficient. As a consequence, the hyphenation to MS (SFC-MS) is used in the vast majority of the most recent applications.

Traditionally, supercritical fluids have been extensively employed also in the extraction (SFE) of natural products, being GC and LC the most employed analytical techniques for the analysis of such extracts [87]. Nowadays, SFC is widely applied for the separation of compounds in natural and food matrices and as a result, recent approaches have dealt with the on-line coupling between SFE and SFC, being SFs suitable for both extraction and analysis of target analytes [88]. Among foods and natural products constituents, lipids and carotenoids have represented the main target of SFC applications, due to the high

solubility of such components in pressurized carbon dioxide mobile phases [89]. Nevertheless, different metabolites have also been investigated by using SFC techniques, as coumarins, flavonoids and carbohydrates [90-92]. Furthermore, SFC has gained increasing importance in the field of bioanalysis, being the most relevant research focused on pharmacokinetic studies, forensic applications (regarding drugs of abuse and doping agents) and lipidomics [93].

Concerning the analysis of contaminants, most applications are focused on the determination of pesticides in different matrices as wastewater and soil [94], while an emerging environmental application regards the analysis of halogenated pollutants [95]. Petrochemical analysis represents another traditional field of research of SFC approaches, due to the limited polarity of petroleum components which make carbon dioxide highly suitable as mobile phase [96]. Most recent applications in this field have involved the analysis of biomass-related products, such as the biodiesel, a diesel fuel deriving from renewable sources, which is gaining considerable attention [97].

1.5 Nutritional and nutraceutical properties of food products

The importance of food and food-related products and their influence on human health has ancient origins. As confirmation of this, Hippocrates of Kos, considered one of the most outstanding figures in the history of medicine, had highlighted that medical art would have no reason to exist if human beings had not adopted a balanced diet, considering the latter a necessary condition to preserve health. The development of an awareness of the importance of food and nutrition has been a gradual and continuous process which continues even today.

In recent times, the development of advanced analytical techniques and highly sophisticated instrumentation have allowed not only the in-depth characterization of foods composition, but also the detection of potential harmful contaminants and the evaluation of micro costituents presenting nutraceutical and nutritional interests. Relating to this, modern scientific research must necessarily have a multidisciplinary nature to achieve increasingly ambitious results and to allow the resolution of challenging and multifactorial problems. Nowadays, food science and nutrition are highly related to disciplines as biotechnology, pharmacology and medicine, opening new scenarios and providing impressive opportunities [98]. In this context, concepts as nutritional genomics,

functional foods, nutraceuticals, foodomics, and nutrimetabolomics have been introduced and gained considerable importance as an attempt to describe those applications at the boundary between two or more scientific disciplines (Figure 1.5).

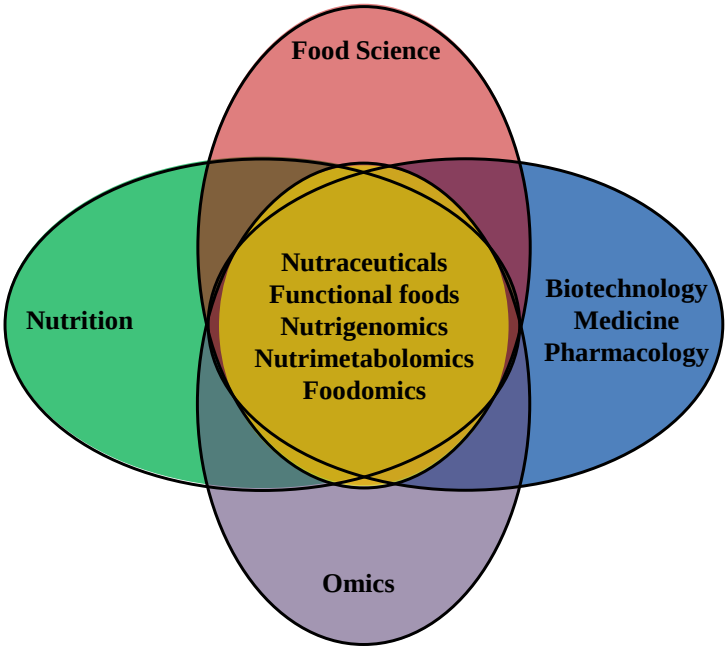

Figure 1.5 Multidisciplinary approaches in modern sciences.

Food and food-derived products are considered as primary sources of macronutrients and micronutrients, indispensable for the human nutrition, but also as sources of components that although not having a caloric and nutritional value, exert beneficial effects on human health. Such components are defined as “nutraceuticals”, term which has been coined to describe any non-pharmaceutical substance that may provide health benefits, including the prevention of certain diseases [99]. The term results from the combination of “nutri”, related to the nutrition concept and “-ceutical”, which emphasizes the potential similarity to the pharmaceutical compounds.

Foods may naturally contain nutraceutical components, or such valuable components may be eventually added to the foods which don’t contain them. Furthermore, components exerting nutritive, nutraceutical, or physiological effects may be formulated in food supplements, which represent concentrated sources of nutrients, normally administered in form of capsules, tablets, liquids contained in vials, powders and so on. In Figure 1.6 are reported some nutraceutical components naturally contained in food products.

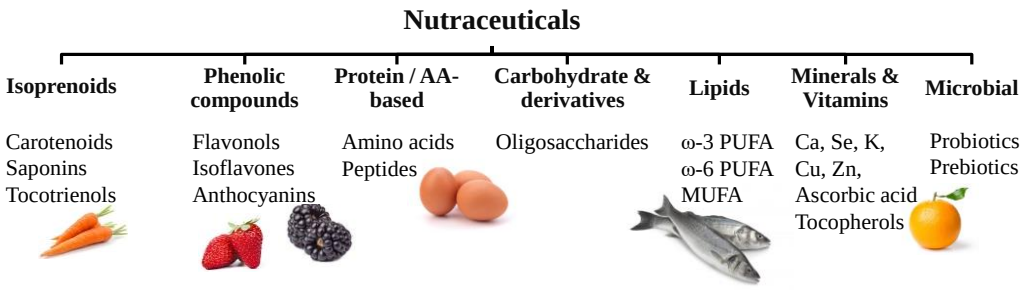

Figure 1.6 Nutraceuticals from food and food-derived products.

Furthermore, in more recent times considerable attention has been put also in the evaluation of new and unconventional sources of functional ingredients; as a result, a number of applications have dealt with the retrieval of valuable food ingredients from industrial by-products [100, 101].

While food supplements have been clearly framed to a normative level, the concept of nutraceuticals results to be less defined from this point of view. In general, legislative authorities such as EFSA (European Food Safety Authority), pay considerable attention to the health claims which may be approved for food supplements in order to protect the consumers from misleading indications [102]. In this light, it is highly important that any additional benefits beyond those defined by the national and international legislation are proven by scientific evidence.

In view of the well-established correlation between nutrition and human health, many valuable components, deriving from various natural sources, have been considered for the introduction in the human diet, as food ingredients or dietary supplements, for their potential health benefits. In detail, the consumption of micronutrients, such as vitamins and minerals and macronutrients such as lipids, proteins and carbohydrates may be promoted to prevent or alleviate nutritional deficiencies. As an example, fortified foods enriched with vitamins and minerals and dietary supplements containing essential fatty acids and aminoacids are conventionally used for such purposes. Alternatively, the consumption of specific components may be recommended for their novel actions and health benefits which totally differ from the traditional nutritional purposes, as in the case of polyphenols, showing antioxidant properties [103] and peptides, presenting antihypertensive, antimicrobial, antioxidant activities together with chemical and

physical functional properties as solubilizing, foaming agents and emulsifying properties [104, 105].

As a result, modern analytical techniques, which are capable of “resolving” the complexity of foods, have a key role in ensuring an extensive and accurate knowledge of food structure and composition, bearing in mind the potential implications on human health. Thus, new analytical methods allowing for the whole characterization of food matrices and the identification of potential valuable components are highly requested.

1.6 References

1. Harvey D. Modern Analytical Chemistry. Boston, McGraw-Hill, 2000.
2. Skoog D.A., West D.M., Holler F.J., Crouch S.R. Fundamentals of Analytical Chemistry, Belmont, CA: Brooks/Cole, Cengage Learning, 2014.
3. Gallo M., Ferranti P., The evolution of analytical chemistry methods in foodomics, J. Chromatogr. A 2016, 1428, 3-15.
4. Nielsen S.S. Introduction to Food Analysis. In: Nielsen S.S. (Eds.) Food Analysis. Food Science Text Series. Springer, Cham. 2017, pp 3-14
5. Tswett M., “Physikalisch-chemische Studien über das Chlorophyll. Die Adsorption.” Ber. dtsch. botan. Ges. 1906, 24, 316–323.
6. Martin A.J.P., SyngeR.L.M., A new form of chromatogram employing two liquid phases. Biochem. J. 1941, 35, 1358-1368.
7. James A.T., Martin A.J.P. Gas-liquid partition chromatography: the separation and microestimation of volatile fatty acids from formic acid tododecanoic acid. Biochem. J. 1952, 50, 679-690.
8. Snyder L.R., Kirkland J.J., Dolan J.W. Introduction to Modern Liquid Chromatography 3rd Edition, John Wiley and Sons, Inc, New York, 2011.
9. Tiselius A., ClaessonS., Arkiv. Kemi Mineral. Geol., 1942, 15B, 18.
10. James A.T., Martin A.J.P., Randall S.S., Automatic fraction collectors and a conductivity recorder, Biochem. J., 1951, 49, 293-299.
11. IUPAC. Compendium of Chemical Terminology, 2nd ed. (the "Gold Book"). Compiled by McNaught A.D., Wilkinson A.. Blackwell Scientific Publications, Oxford, 1997. Online version, 2019- created by S. J. Chalk.
12. Poole C.F., Poole S.K., Fundamental relationships of chromatography, in Chromatography Today (Fifth Edition), Poole C.F., Poole S.K. (Eds.) Elsevier, 1991, pp 1-103.
13. Scott R.P.W. The Chromatographic Separation in Techniques and Practice of Chromatography, CRC Press Taylor & Francis Group 6000 Broken Sound Parkway NW, Suite 300 Boca Raton, FL, 2019, pp. 33487-2742.

14. Núñez O., Gallart-Ayala H., Martins C.P., Lucci P. New trends in fast liquid chromatography for food and environmental analysis. J Chromatogr A. 2012, 9, 1228, 298-323.
15. Murray K.K., Boyd R.K., Eberlin M.N., Langley G.J., Li L., Naito Y. Definitions of terms relating to mass spectrometry (IUPAC Recommendations 2013). Pure Appl. Chem. 2013, 85, 1515-1609.
16. Giddings J.C., Use of Multiple Dimensions in Analytical Separations, in Multidimensional Chromatography Techniques and Applications, Cortes H.J (Ed.) Marcel Dekker, Inc, New York, 1990.
17. Li F., Hsieh Y., Supercritical fluid chromatography-mass spectrometry for chemical analysis, J. Sep. Sci. 2008, 31, 1231-1237.
18. Hirschfeld T., The Hy-phen-ated Methods. Anal. Chem. 1980, 52, 297A–312A.
19. Leppert J., Härtel M., Klapötke T.M., Boeker P., Hyperfast flow-field thermal gradient GC/MS of explosives with reduced elution temperatures, Anal. Chem. 2018, 90, 8404-8411.
20. Mastovská K., Lehotay S.J. Practical approaches to fast gas chromatography-mass spectrometry. J Chromatogr A. 2003, 1000, 153-180.
21. Vinaixa M., Schymanski E.L., Neumann S., Navarro M., Salek R.M., Yanes O. Mass spectral databases for LC/MS- and GC/MS-based metabolomics: state of the field and future prospects, TrAC Trends Anal. Chem. 2016, 78, 23-35.
22. Tranchida P.Q., Aloisi I., Giocastro B., Mondello L., Current state of comprehensive two-dimensional gas chromatography-mass spectrometry with focus on processes of ionization, TrAC Trends Anal. Chem. 2018, 105, 360-366.
23. Portolés T., Pitarch E., López F.J., Hernández F., Niessen W.M.A., Use of soft and hard ionization techniques for elucidation of unknown compounds by gas chromatography/time-of-flight mass spectrometry, Rapid Commun. Mass Spectrom. 2011, 25, 1589-1599.
24. Hurtado-Fernández E., Pacchiarotta T., Mayboroda O.A., Fernández-Gutiérrez A., Carrasco-Pancorbo A. Metabolomic analysis of avocado fruits by GC-APCI-TOF MS: effects of ripening degrees and fruit varieties. Anal Bioanal Chem 2015, 407, 547–555.
25. Hennig K., Antignac J.P., Bichon E., Morvan M., Miran I., Delaloge S., Feunteun J., Le Bizec B. Steroid hormone profiling in human breast adipose tissue using semi-automated purification and highly sensitive determination of estrogens by GC-APCI-MS/MS. Anal Bioanal Chem 2018, 410, 259–275.
26. Gómez-Pérez M., Plaza-Bolaños P., Romero-González R., Martínez Vidal J., Garrido Frenich A. Evaluation of the Potential of GC-APCI-MS for the Analysis of Pesticide Residues in Fatty Matrices, J. Am. Soc. Mass Spectrom. 2014, 25, 5, 899-902.
27. Alam M.S., Stark C., Harrison R.M., Using Variable Ionization Energy Time-of-Flight Mass Spectrometry with Comprehensive GC×GC To Identify Isomeric Species, Anal. Chem. 2016, 88, 4211–4220.

28. European Commission, 2002/657/EC, Commission Decision of 12 August 2002 implementing Council Directive 96/23/EC concerning the performance of analytical methods and the interpretation of results, Off. J. Eur. Commun. L 221, 2002, 8-36.
29. Gruber B., David F., Sandra P. Capillary gas chromatography-mass spectrometry: Current trends and perspectives. Trends Anal. Chem. 2020, 124, 115475.
30. Špánik I., Machyňáková A., Recent applications of gas chromatography with high-resolution mass spectrometry, J. Sep. Sci. 2018, 41, 163-179.
31. Marriott P.J., Chin S., Nolvachai Y., Techniques and application in comprehensive multidimensional gas chromatography – mass spectrometry, J. Chromatogr. A, 2021, 1636, 461788.
32. Lavrik N.V., Taylor L.T., Sepaniak M.J. Nanotechnology and chip level systems for pressure driven liquid chromatography and emerging analytical separation techniques: a review. Anal Chim Acta. 2011, 694, 6-20.
33. Kertesz V., Van Berkel G.J. Fully automated liquid extraction-based surface sampling and ionization using a chip-based robotic nanoelectrospray platform. J Mass Spectrom. 2010, 45, 252-260.
34. Xu F.G., Zou L., Liu Y., Zhang Z.J., Ong C.N., Enhancement of the capabilities of liquid chromatography–mass spectrometry with derivatization: General principles and applications. Mass Spectrom. Rev. 2011, 30, 1143-1172.
35. Svec F., Lv Y., Advances and recent trends in the field of monolithic columns for chromatography. Anal. Chem. 2015, 87, 250-273.
36. Broeckhoven K., Desmet G., The future of UHPLC: towards higher pressure and/or smaller particles? TrAC Trends Anal. Chem. 2014, 63, 65-75.
37. Rogers B.A., Wu Z., Wei B., Zhang X., Cao X., Alabi O., Wirth M.J., Submicrometer particles and slip flow in liquid chromatography, Anal. Chem. 2015, 87, 2520-2526.
38. Nawada S., Dimartino S., Fee C., Dispersion behavior of 3D-printed columns with homogeneous microstructures comprising differing element shapes, Chem. Eng. Sci. 2017, 164, 90-98.
39. Xue Z., Vinci J.C., Colón L.A., Nanodiamond-decorated silica spheres as a chromatographic material, ACS. Appl. Mater. Interfaces 2016, 8, 4149-4157.
40. Chung Lama S., Sanz Rodriguez E., Haddad P.R., Paull B., Recent advances in open tubular capillary liquid chromatography, Analyst 2019, 144, 3464-3482.
41. Fekete S., Schappler J., Veuthey J., Guillarme D., Current and future trends in UHPLC, Trends Anal. Chem. 2014, 63, 2-13.
42. Lísa M, Holčapek M. Triacylglycerols profiling in plant oils important in food industry, dietetics and cosmetics using high-performance liquid chromatography-atmospheric pressure chemical ionization mass spectrometry. J Chromatogr A. 2008, 1198, 115-130.
43. Gallagher R.T., Balogh M.P., Davey P., Jackson M.R., Sinclair I., Southern L.J. Combined Electrospray Ionization−Atmospheric Pressure Chemical Ionization

Source for Use in High-Throughput LC−MS Applications. Anal. Chem. 2003, 75, 973–977.
44. Robb D.B., Blades M.W., State-of-the-art in atmospheric pressure photoionization for LC/MS, Anal. Chim. Acta 2008, 627, 34-49.
45. Famiglini G., Palma P., Termopoli V., Cappiello A. The history of electron ionization in LC-MS, from the early days to modern technologies: A review. Anal. Chim. Acta 2021, 1167, 338350.
46. Rolando C., Sablier M. Multiquadrupoles. In The Encyclopedia of Mass Spectrometry: Theory and Ion Chemistry. Armentrout P.B. (ed.), Elsevier, Oxford, 2003.
47. Griffiths W.J., Wang Y. Mass spectrometry: from proteomics to metabolomics and lipidomics. Chem. Soc. Rev. 2009, 38, 1882-96.
48. Holčapek M., Jirásko R., Lísa M., Recent developments in liquid chromatography–mass spectrometry and related techniques. J. Chromatogr. A, 2012, 1259, 3-15.
49. Dodds J.N., Baker E.S., Ion Mobility Spectrometry: Fundamental Concepts, Instrumentation, Applications, and the Road Ahead. J. Am. Soc. Mass Spectrom. 2019, 30, 2185–2195.
50. Kanu A.B., Dwivedi P., Tam M., Matz L., Hill Jr H.H. Ion mobility–mass spectrometry. J. Mass Spectrom. 2008, 43, 1–22.
51. Sobott F., Watt S.J., Smith J., Edelmann M.J., Kramer H.B., Kessler B.M. Comparison of CID versus ETD based MS/MS fragmentation for the analysis of protein ubiquitination. J. Am. Soc. Mass Spectrom. 2009, 20, 1652–1659.
52. Kim M., Pandey A., Electron transfer dissociation mass spectrometry in proteomics. Proteomics 2012, 12, 530–542.
53. Fernández-Costa C., Martínez-Bartolomé S., McClatchy D.B., Saviola A.J., Yu N., Yates J.R. Impact of the Identification Strategy on the Reproducibility of the DDA and DIA Results. J. Proteome Res. 2020, 19, 3153–3161.
54. Egertson, J., Kuehn, A., Merrihew, G., Bateman N.W, MacLean B.X., Ting YS, Canterbury J.D., Marsh D.M., Kellmann M., Zabrouskov V., Wu C.C., MacCoss M.J. Multiplexed MS/MS for improved data-independent acquisition. Nat Methods 2013, 10, 744–746.
55. Giddings, J.C. Maximum number of components resolvable by gel filtration and other elution chromatographic methods. Anal. Chem. 1967, 39, 1027−1028.
56. Davis J.M., Giddings J.C. Statistical theory of component overlap in multicomponent chromatograms. Anal. Chem. 1983, 55, 3, 418–424.
57. Mondello L., Lewis C., Bartle K.D. Multidimensional Chromatography, John Wiley and Sons, Chichester, 2001
58. Apffel J.A., Alfredson T.V., Majors R.E. Automated on-line multi-dimensional high performance liquid chromatographic techniques for the clean-up and analysis of water-soluble samples, J. Chromatogr. A, 1981, 206, 43-57.

59. Kuehnbaum N.L., Britz-McKibbin P. New advances in separation science for metabolomics: resolving chemical diversity in a post-genomic era. Chem. Rev. 2013, 113, 2437-68.
60. Wu Q., Yuan H., Zhang L., Zhang Y. Recent advances on multidimensional liquid chromatography–mass spectrometry for proteomics: From qualitative to quantitative analysis—A review. Anal. Chim. Acta 2012, 731, 1-10.
61. Pursch M., Buckenmaier S. Loop-Based Multiple Heart-Cutting Two-Dimensional Liquid Chromatography for Target Analysis in Complex Matrices. Anal. Chem. 2015, 87, 5310−5317.
62. Zhang K., Li Y., Tsang M.; Chetwyn N.P. Analysis of pharmaceutical impurities using multi-heartcutting 2D LC coupled with UV-charged aerosol MS detection.J. Sep. Sci. 2013, 36, 2986-2992.
63. Groskreutz S.R., Swenson M.M., Secor L.B., Stoll D.R. Selective comprehensive multi-dimensional separation for resolution enhancement in high performance liquid chromatography. Part I: principles and instrumentation. Journal of chromatography. A. 2012, 1228, 31-40.
64. Pirok B.W.J., Gargano A.F.G., Schoenmakers P.J. Optimizing separations in online comprehensive two-dimensional liquid chromatography. J Sep Sci. 2018, 41, 68–98.
65. Pirok B.W.J., Stoll D.R., Schoenmakers P.J., Recent Developments in Two-Dimensional Liquid Chromatography: Fundamental Improvements for Practical Applications. Anal. Chem. 2019, 91, 240-263.
66. Montero L., Herrero M., Two-dimensional liquid chromatography approaches in Foodomics – A review. Anal. Chim. Acta, 2019, 1083, 1-18.
67. Nestola M., Friedrich R., Bluhme P., Schmidt T.C. Universal Route to Polycyclic Aromatic Hydrocarbon Analysis in Foodstuff: Two-Dimensional Heart-Cut Liquid Chromatography-Gas Chromatography-Mass Spectrometry. Anal Chem. 2015, 12, 6195-6203.
68. Kittlaus S., Schimanke J., Kempe G., Speer K., Development and validation of an efficient automated method for the analysis of 300 pesticides in foods using two-dimensional liquid chromatography–tandem mass spectrometry. J. Chromatogr. A, 2013, 1283, 98-109.
69. Wang L., Yang B., Zhang X., Zheng H. Novel Two-Dimensional Liquid Chromatography–Tandem Mass Spectrometry for the Analysis of Twenty Antibiotics Residues in Dairy Products. Food Anal. Methods 2017,10, 2001–2010.
70. Willemse C.M., Stander M.A., Vestner J., Tredoux A.G. J., de Villiers A. Comprehensive Two-Dimensional Hydrophilic Interaction Chromatography (HILIC) × Reversed-Phase Liquid Chromatography Coupled to High-Resolution Mass Spectrometry (RP-LC-UV-MS) Analysis of Anthocyanins and Derived Pigments in Red Wine. Anal. Chem. 2015, 87, 12006–12015.

71. Montero L., Ibáñez E., Russo M., di Sanzo R., Rastrelli L., Piccinelli L.A., Celano R., Cifuentes A., Herrero M. Metabolite profiling of licorice (Glycyrrhiza glabra) from different locations using comprehensive two-dimensional liquid chromatography coupled to diode array and tandem mass spectrometry detection, Anal. Chim. Acta, 2016, 913, 145-159.
72. Dugo P., Fawzy N., Cichello F., Cacciola F., Donato P., Mondello L. Stop-flow comprehensive two-dimensional liquid chromatography combined with mass spectrometric detection for phospholipid analysis. J. Chromatogr. A 2013, 1278, 46-53.
73. Donato P., Micalizzi G., Oteri M., Rigano F., Sciarrone D., Dugo P., Mondello L. Comprehensive lipid profiling in the Mediterranean mussel (Mytilus galloprovincialis) using hyphenated and multidimensional chromatography techniques coupled to mass spectrometry detection. Anal. Bioanal. Chem. 2018, 410, 3297-3313.
74. Holčapek, M., Velínská, H., Lísa, M., Cesla, P. Orthogonality of silver-ion and non-aqueous reversed-phase HPLC/MS in the analysis of complex natural mixtures of triacylglycerols. J. Sep. Sci. 2009, 32, 3672–3680.
75. Wolters D.A., Washburn M.P., Yates J.R. An automated multidimensional protein identification technology for shotgun proteomics. Anal Chem. 2001, 73, 5683-5690.
76. Stoll D.R., Carr P.W. Two-Dimensional Liquid Chromatography: A State of the Art Tutorial. Anal. Chem. 2017, 89, 1, 519–531.
77. Vanhoenacker G., Vandenheede I., David F., Sandra P., Sandra K. Comprehensive two-dimensional liquid chromatography of therapeutic monoclonal antibody digests. Anal. Bioanal. Chem. 2015, 407, 355-366.
78. Klesper K., Corwin A.H., Turner D. A. High pressure gas chromatography above critical temperatures, J. Org. Chem. 1962, 27, 700-701.
79. Hofstetter R.K., Hasan M., Eckert C., Link A. Supercritical fluid chromatography. ChemTexts 2019, 5, 13.
80. Thomas A. The Bakerian lecture: on the continuity of the gaseous and liquid states of matter. Philos. Trans. R. Soc. 1869, 159, 575–590.
81. Saito M. History of Supercritical fluid chromatography: Instrumental development. J. Biosci. Bioeng. 2013, 115, 590-599.
82. Taylor, L. T., Supercritical fluid chromatography. Anal. Chem. 2010, 82, 4925-4935.
83. Tarafder A. Metamorphosis of supercritical fuid chromatography to SFC: an overview. Trends Anal. Chem. 2016, 81, 3-10.
84. Lesellier E. Overview of the retention in subcritical fluid chromatography with varied polarity stationary phases. J Sep Sci. 2008, 31, 1238-1251.
85. Ashraf-Khorassani M., Shah S., Taylor L.T., Column efficiency comparison with supercritical fluid carbon dioxide versus methanol-modified carbon dioxide as the mobile phase. Anal. Chem. 1990, 62, 1173-1176.

86. Nováková L., Grand-Guillaume Perrenoud A., Francois I., West C., Lesellier E, Guillarme D. Modern analytical supercritical fluid chromatography using columns packed with sub-2 μm particles: a tutorial. Anal. Chim. Acta. 2014, 824,18–35.
87. Herrero M., Cifuentes A., Ibañez E. Sub- and supercritical fluid extraction of functional ingredients from different natural sources: plants, food-by-products, algae and microalgae: a review. Food Chem. 2006, 98, 136-48.
88. Zoccali M., Giuffrida D., Dugo P., Mondello L. Direct online extraction and determination by supercritical fluid extraction with chromatography and mass spectrometry of targeted carotenoids from red habanero peppers (Capsicum chinense Jacq.). J. Sep. Sci. 2017, 40, 3905–3913.
89. Donato P., Sciarrone D., Dugo P., Mondello L. Applications of supercritical fluid chromatography in the field of edible lipids, in Supercritical Fluid Chromatography, Rosse G. (ed.), Berlin, Boston: De Gruyter, 2018, pp. 189-192.
90. Winderl B., Schwaiger S., Ganzera M. Fast and improved separation of major coumarins in Ammi visnaga (L.) Lam. by supercritical fluid chromatography J. Sep Sci. 2016, 39, 4042–4048.
91. Huang Y., Feng Y., Tang G., Li M., Zhang T., Fillet M. Development and validation of a fast SFC method for the analysis of flavonoids in plant extracts. J. Pharm. Biomed. Anal. 2017, 140, 384–391.
92. Pauk V., Pluháček T., Havlíček V., Lemr K. Ultra-high performance supercritical fluid chromatography-mass spectrometry procedure for analysis of monosaccharides from plant gum binders. Anal. Chim. Acta. 2017, 989, 112-120.
93. West C., Current trends in supercritical fluid chromatography, Anal. Bioanal. Chem. 2018, 410, 6441–6457.
94. Cheng Y., Zheng Y., Dong F., Li J., Zhang Y., Sun S. Stereoselective analysis and dissipation of propiconazole in wheat, grapes, and soil by supercritical fluid chromatography-tandem mass spectrometry. J. Agric. Food Chem. 2017, 65, 234-243.
95. Riddell N., van Bavel B., Ericson Jogsten I., McCrindle R., McAlees A., Chittim B. Coupling supercritical fluid chromatography to positive ion atmospheric pressure ionization mass spectrometry: ionization optimization of halogenated environmental contaminants. Int. J. Mass Spectrom. 2017, 421,156-163.
96. Thiébaut D. Separations of petroleum products involving supercritical fluid chromatography. J. Chromatogr. A. 2012, 1252, 177-188.
97. Ashraf-Khorassani M., Yang J., Rainville P., Jones M.D., Fountain K.J., Isaac G., Taylor L.T. Ultrahigh performance supercritical fluid chromatography of lipophilic compounds with application to synthetic and commercial biodiesel. J. Chromatogr. B. 2015, 983-984,94–100.
98. Herrero M., Simó C., García-Cañas V., Ibáñez E., Cifuentes A. Foodomics: MS-based strategies in modern food science and nutrition. Mass Spectrom. Rev. 2012, 31, 49–69.

99. De Felice S.T. The nutraceutical revolution: its impact on food industry R&D. Trends Food Sci. Technol. 1995, 6, 59–61.
100. Espro C., Paone E., Mauriello F., Gotti R., Uliassi E., Bolognesi M.L., Rodríguez-Padrón D., Luque R. Sustainable production of pharmaceutical, nutraceutical and bioactive compounds from biomass and waste. Chem. Soc. Rev., 2021, 50, 11191-11207.
101. Rigano F., Arena P., Mangraviti D., Donnarumma D., Dugo P., Donato P., Mondello L., Micalizzi G. Identification of high value generating molecules from the wastes of tuna fishery industry by liquid chromatography and gas chromatography hyphenated techniques with automated sample preparation. J. Sep. Sci. 2021, 44, 1571-1580.
102. Regulation (EC) No 1924/2006 of the European Parliament and of the Council on nutrition and health claims made on foods. Official Journal of the European Union
103. Luca S.V., Macovei I., Bujor A., Miron A., Skalicka-Woźniak K., Aprotosoaie A.C., Trifan A. Bioactivity of dietary polyphenols: The role of metabolites. Crit. Rev. Food. Sci. Nutr. 2020, 60, 626-659.
104. Karami Z., Akbari-adergani B. Bioactive food derived peptides: a review on correlation between structure of bioactive peptides and their functional properties. J. Food Sci. Technol. 2019, 56, 535–547.
105. Fernandes S.S., Silveira Coelho M., de las Mercedes Salas-Mellado M., Bioactive Compounds as Ingredients of Functional Foods: Polyphenols, Carotenoids, Peptides From Animal and Plant Sources, in Health Benefits and Potential Applications Segura Campos M.R., Bioactive Compounds, Woodhead Publishing, 2019, 129-142.

2 Retrieval and characterization of valuable compounds from the wastes of tuna fishery industry by employing hyphenated analytical techniques

2.1 Introduction

In recent years, the growing awareness of the negative effects inevitably related to industrial progress, such as the steady increase of environmental pollution, the limitation of biological resources and the massive production of wastes, has promoted the progressive transition from the current linear economic model to a circular economic model. Circular economy is a system in which all the activities, from the extraction to the production and consumption, are planned to minimize wastes and to maximize the use of resources, therefore, such economic model is substantially based on the re-use of industrial by-products, deriving from different manufacturing processes, as the starting material for obtaining other products of economic interest [1].

The use of waste products as a starting material for different production cycles can also be extended to the *Blue Economy*, which is focused on human activities involving the sea, the coast and the seabed as resources for industrial processes and economic purposes. The growing interest in the blue economy derives from the enormous potential of seas and oceans for many activities, such as aquaculture, fisheries, marine biotechnology, maritime tourism, maritime transport and renewable marine energy [2]. In this context, a responsible use of sea resources, ensuring respect for the ecosystem and biodiversity, should be promoted. Regarding this concept, the Food and Agriculture Organization of the United Nations (FAO) championed the creation of the *Code of Conduct for Responsible Fisheries*, containing a series of principles and standard of behavior promoting best practices for conducting fishing and aquaculture in a responsible and sustainable way [3]. In this regard, one of the most common examples related to the incorrect use of marine resources is centred on the tuna fishing industry, which represents a significant portion of the global fish trade. In fact, processing of raw fish into food products generates a large amount of wastes, which can be as high as 70% of the original material [4]. Tuna by-products usually comprise meat, scales, head and viscera and most of them are discarded because they are regarded as low-value resources. For this reason, a better use of the wastes within a circular economy system could maximize the profit from fish resources while reducing the environmental impact.

Due to the significant content in ω-3 and ω-6 fatty acids (FAs), vitamins, minerals, amino acids, peptide and proteins, tuna by-products may be considered as valuable sources of bioactive molecules, thus a promising re-use of tuna wastes may concern their employment as functional food ingredients in the production of dietary formulations and nutraceuticals [5]. Omega-3 and omega-6 polyunsaturated fatty acids (PUFA) are commonly used as dietary supplements because they exert beneficial effects on the cardiovascular and nervous systems and contribute to maintain normal triacyglycerol and cholesterol levels in the blood. These compounds also exert a structural role, by increasing cellular membranes fluidity, play an important role in the production of high-density lipoproteins and represent essential precursors of anti-inflammatory and pro-inflammatory molecules, the latter acting predominantly as signal transmitters [6]. Nevertheless, the classical formulations of dietary supplements usually show reduced patients' compliance, especially when formulated in capsules containing fish oil, notoriously characterized by unpleasant taste and smell. Another issue for the formulation of nutraceuticals is represented by the reduced bioavailability of bioactive molecules that must be delivered to the target sites. In addition to the lipid fraction, extensively investigated in terms of antioxidant and anti-inflammatory properties, even the protein fraction deserves an equal attention, since the tuna processing industry causes an incredible waste of noble proteins. In detail, fish protein hydrolysates (FPH), potentially obtainable by enzymatic digestion of proteins derived from tuna by-products may be conveniently added to nutraceutical formulations increasing the functional, biological and nutritional properties of the final product. As a result, the design of nutraceuticals in which lipid components are associated with peptides could improve the physical and chemical properties of formulations in terms of solubility, emulsifying properties and stability [7], leading to the creation of systems capable of conveying the lipid fraction at the sites of action thanks to improved bioavailability. The protein counterpart could also exert additional antimicrobial, antioxidant and antihypertensive activities characteristics of the peptides eventually contained in the formulation. Ultimately, the combination of ω-3/ω-6- containing lipids and peptides in micro-nanoformulations, could provide an improvement of the physico-chemical properties of the preparations, potential increase of the formulation bioavailability, additional biological activities related to the peptide

amino acidic sequences, increased patient compliance compared to traditional formulations.

Most recent works were focused on the retrieval of molecules of nutraceutical interest from tuna industrial by-products [8–10]; the majority of them aimed at the exclusive investigation of the protein [11–13], or the lipid fraction [14], especially regarding the FA and PUFA content [15, 16]. Despite the total FA composition of different Thunnus species was extensively elucidated in previous studies [17–19], few studies dealt with the evaluation of the fish native lipid composition [20, 14].

Concerning the lipid fraction, FAs are generally investigated in forms of fatty acid methyl esters (FAMEs) derivatives, obtained through a transesterification procedure, and subsequently analyzed by gas chromatography-flame ionization detection or gas chromatography-mass spectrometry (GC-FID or GC-MS) [21], while the most suitable approach for intact lipid analysis is represented by RP-LC [22, 23] followed by MS and tandem MS. In RP-LC, lipid species elute according to the increasing partition number (PN), defined as the total carbon number (CN) minus twice the number of DBs (PN = CN-2DBs) [24, 25]. On the other side, LC-MS/MS represents the election technique for protein and peptides analysis, both for top down and bottom-up approaches [26, 27].

Concerning peptide separation, RP-LC is the most employed separation mode, being the reduced amount of organic solvents required and the ease of hyphenation to MS highly beneficial for such applications; peptide partition coefficients are very sensitive to organic modifier concentration in the mobile phase, and the resolution will increase upon increasing the column length [28, 29].

The aim of the present work was the retrieval and identification of high value generating molecules from tuna by-products by employing a multi-technique analytical approach. *Thunnus albacares* was selected as model organism for fish processing by-products and as the starting material for extraction and analysis.

For such a purpose, lipid characterization was performed by using two fully automated preparative stations, on-line coupled to GC-MS/FID for FAME analysis [30] and to UHPLC-MS/MS for intact lipid analysis. The latter automated platform was employed for the first time, allowing for fast, sensitive and selective monitoring of different lipid classes. For intact lipid extraction, miniaturization of Folch [31] and Bligh&Dyer procedures [32] was mandatory to achieve compatibility with automation. As for

peptides, extraction by isoelectric solubilization/precipitation was performed [33, 34], followed by enzymatic digestion and UHPLC-MS/MS analysis. Furthermore, the use of bioinformatics tools highlighted the presence of potential antimicrobial peptides in tuna by-products. In this respect, the novelty of this study consists of a comprehensive evaluation of both the peptide and the lipid tuna fractions, also in terms of fish native lipid composition, for which scant literature data are available.

Furthermore, as part of this project, a recently introduced linear retention index (LRI) approach in LC [35] was employed for a reliable identification of TAG species in oils derived from tuna by-products. A mixture of odd carbon number TAGs was used as reference homologue series for the calculation of the LC retention indices. In this case, the identification was based on a *dual filter approach*, considering the information obtained from mass spectra and the retention behaviour of analytes (LRI tolerance window of ± 15). The predominance of TAG containing PUFA, characteristic of tuna waste oil, was highly useful for the implementation of the laboratory constructed LRI database.

2.2 Material and Methods

2.2.1 Reagents

For lipids and peptides analysis the following solvents were employed: LC-MS grade 2-propanol, acetonitrile (ACN), water, ammonium formate ($HCOONH_4$), formic and trifluoroacetic acids (FA and TFA). For lipid extraction, reagent grade methanol (CH_3OH), chloroform ($CHCl_3$), sodium chloride (NaCl) and distilled water were used. For protein extraction and enzymatic digestion distilled water, hydrochloric acid (HCl), sodium hydroxide (NaOH), trypsin, $HCOONH_4$ and TFA were employed. For lipid derivatization into fatty acid methyl esters (FAMEs) methanolic solutions of sodium methoxide (CH_3ONa 0.5% *w/v*) and boron trifluoride (BF_3 14% *w/v*), HPLC grade *n*-heptane and a saturated NaCl solution were used. For UHPLC-MS/MS method optimization a HPLC peptide standard mixture (H2016) consisting of glycine-tyrosine, valine-tyrosine-valine, methionine enkephalin acetate, leucine enkephalin and Angiotensin II Acetate was employed. For optimization of the phospholipids (PLs) MS/MS transitions were employed: 1,2-dioleoyl-sn-glycero-3-phosphocholine, 1-stearoyl-2-hydroxy-sn-glycero-3-phospho-(1′-rac-glycerol), 1,2-dipalmitoyl-sn-glycero-

3-phospho-L-serine sodium salt, L-α-phosphatidylethanolaminedioleoyl and phosphatidylinositol sodium salt.

A standard mixture of trinonanoin (C9C9C9), triundecanoin, (C11C11C11), tritridecanoin (C13C13C13), tripentadecanoin (C15C15C15), triheptadecanoin (C17C17C17) and trinonadecanoin (C19C19C19) in 2-propanol was employed for LRI calculation. All the reagents, solvent and standard materials employed in this research were purchased from Merck Life Science (Darmstadt, Germany).

2.2.2 Sample preparation

Yellowfin tuna (*Thunnus albacares*) wastes and edible parts (muscle) were obtained from fresh samples purchased in a local fish market in Messina, Italy. Tuna waste oil was obtained by wastes grinding and decantation.

Concerning the lipid fraction, two robotic preparative stations, AOC-6000 and CLAM-2030 (Shimadzu Europa, Duisburg, Germany), coupled to GC-FID/MS and UHPLC-MS/MS systems, respectively, were used to fully automate the extraction procedures.

A direct derivatization procedure was employed to obtain FAMEs from intact lipids. Briefly, 500µL of CH_3ONa methanolic solution were added to 20 mg of tuna tissue (muscle or wastes as a mixture of skin, heart and head) into a magnetic cap vial. After agitation, 100 s at 2000 rpm, the reaction mixture was heated at 95 °C for 15 min. Afterwards, 500 µL of BF_3 solution were added and the mixture was vortexed for 100 s at 2000 rpm and subsequently heated at 95 °C for 15 min. For FAME extraction, 350 µL of *n*-heptane and 250 µL of a saturated NaCl solution were added to the mixture. After agitation for 100 s at 2000 rpm, the mixture was incubated at room temperature, allowing for phase separation. Finally, the *n*-heptane upper layer was subjected to GC-FID/MS analysis.

For intact lipids extraction, the miniaturization of Folch and Bligh&Dyer methods was necessary to achieve compatibility with the CLAM-2030 robotic preparative unit, since the maximum working volume allowed by the instrument was equal to 350 µL. Briefly, in accordance with the Folch procedure, 200 µL of $CHCl_3$ and 100 µL of CH_3OH were added to 80 mg of tuna tissue (muscle and waste); conversely, according to the Bligh&Dyer method, the ratio of $CHCl_3$:CH_3OH was reversed (1:2), therefore, 100 µL of $CHCl_3$ and 200 µL of CH_3OH were added to the sample. After the addition of the

reagents, the mixture was shaken for 100 s at 2000 rpm and then, 30 µL of a saturated NaCl solution were added and the mixture was shaken again for 60 s at 1500 rpm, allowing for phase separation between organic and aqueous layer. Afterwards, the mixture was filtered under vacuum and the collection vial was directly transferred to the autosampler of the UHPLC-MS/MS system for the injection of the lower organic phase. Tuna waste oil was diluted in 2-propanol (1000 ppm) and injected into the UHPLC-MS system for TAG analysis.

Concerning the protein fraction, the extraction was based on an isoelectric solubilization-precipitation (ISP) procedure, also referred as pH shift process. In detail, 20 g of tuna wastes were homogenized in 9 volumes (180 mL) of ice-cold distilled water. The proteins in the suspension were solubilized under acidic or alkaline conditions in different collection tubes, by adding 1N NaOH to reach pH values of 10.5, 11.0 and 11.5 and 1N HCl to reach pH values of 3.5, 3.0 and 2.5. The obtained suspensions were centrifugated for 25 min at 8000 g and the supernatants were separated from the deposits. Afterwards, the solubilized proteins were precipitated by adding alternatively, 1N NaOH or 1N HCl to each collection tube until pH 5.5 was reached (isoelectric point of the muscle proteins). Another centrifugation step, for 25 min at 8000 g, allowed the collection of the precipitated proteins. For the enzymatic digestion, 100 mg of each protein fraction obtained by ISP were pooled together and dissolved in 10 mL of 0.01 M $HCOONH_4$ in water. Then, 1 N NaOH was added to reach a pH value of 8.0 and the solution was heated in a boiling water bath for 6 minutes. After cooling, trypsin was added to the solution in the substrate:enzyme ratio of 50:1 and the mixture was allowed to react at 37 °C for 4 h. The reaction was quenched by adding 0.1% TFA, to pH 2.0. The digest was filtered through a 0.45 µm nylon membrane (Whatman). For the optimization of the UHPLC-MS/MS method, aqueous solutions of the peptide standard mixture (500 ppm) were injected into the system.

2.2.3 Instruments and analytical conditions

As far as the total FA analysis is concerned, direct derivatization procedure, FAME extraction and the following GC-FID/MS analysis were fully automatized by employing the AOC-6000 robotic workstation installed on a Nexis GC-2030 equipped with a FID detector and coupled to a TQ8050 mass spectrometer (Shimadzu Europa, Duisburg,

Germany) by means of a Y splitting unit placed at the column outlet. In detail, 1 m × 0.1 mm id, and 0.35 m × 0.1 mm id fused silica capillaries, connected to the splitting unit, were directed to the MS and FID, respectively. Thus, the flow was diverted (6.6:3.4 ratio) allowing for the simultaneous acquisition of FID and MS data in a single run. The injection of 0.4 µL of the *n*-heptane FAME solution was performed in split mode, employing a 1:10 ratio. The GC separations were carried out on a medium-polarity ionic liquid (IL) capillary column, SLB-IL60 30 m × 0.25 mm id, 0.20 µm *d.f.* (Merck Life Science, Darmstadt, Germany). The temperature program was set as follows: 70 °C to 180 °C (held for 10 min) at 3.0 °C/min, and then to 280 °C at 3.0 °C/min. Helium was used as carrier gas, with an average linear velocity of 30 cm s^{-1} and initial pressure of 147.1 kPa. The FID parameters were set as follows: temperature, 280 °C; sampling rate, 40 ms; H_2 flow rate, 40 mL min^{-1}; make-up gas (N_2) flow rate, 30 mL min^{-1}; air flow rate, 400 mL min^{-1}. The MS parameters were: mass range, 40-650 amu; event time, 0.20 s; ion source temperature, 220 °C; interface temperature, 250 °C.

GCMSsolution ver. 4.50 software (Shimadzu Europa, Duisburg, Germany) was employed for MS data acquisition and processing, while LabSolution ver. 5.92 software (Shimadzu Europa, Duisburg, Germany) was used for FID data handling. The LIPIDS Mass Spectral Library ver. 1.0 (Shimadzu Europa, Duisburg, Germany) and a lab-constructed Linear Retention Indices (LRI) database were employed for FAs identification. A double filter approach was used for the spectral library search, consisting of LRI tolerance window of ±10 and minimum MS spectral similarity of 85%.

Regarding the analysis of intact lipids, the extraction procedure and the following subsequent UHPLC-MS/MS analysis were fully automatized by using the CLAM-2030 robotic workstation installed on a Nexera LC system coupled to LCMS-8060 QqQ MS detector through an ESI source (Shimadzu Europa, Duisburg, Germany). The LC system consisted of two LC-30AD dual-plunger parallel-flow pumps, a DGU-20A5R degasser, a SIL-30AC autosampler, a CTO-20AC column oven and a CBM controller. The UHPLC separations were carried out on an Ascentis Express C18, 100 x 2.1 mm, 2.7 µm *d.p.* column (Merck Life Science, Darmstadt, Germany), employing as mobile phases 20 mM $HCOONH_4$ in water (A) and 2-propanol/ACN/H_2O (60:36:4 *v/v/v*) with 0.1% formic acid (B). The gradient program was set as follows: 0-6 min, 80-100% B (held for 16 min). The flow rate was 0.4 mL/min; the injection volume was 1 µL and the column oven was set

at 40 °C. Regarding the MS parameters, the acquisitions were performed using an ESI interface operating in positive (+) and negative ionization modes (-), under the following conditions: interface temperature, 450 °C; CDL temperature, 250 °C; heat block temperature, 200 °C; nebulizing gas flow (N_2), 3 L/min; drying gas flow (N_2), 5 L/min; acquisition range, 350-1250 *m/z* (+) and 150-1250 *m/z* (-). Additional MS/MS experiments were optimized through the injection of single PLs standards and the selected events, including MS/MS event, polarity, diagnostic fragment and collision energy are repored below: galactocerebroside (CerGal), neutral loss (+), 162 Da, -35 V; lysophosphatidic acid (LPA), phosphatidic acid (PA), neutral loss (+), 115 Da, -25 V; lysophosphatidylcholine (LPC), phosphatidylcholine (PC), sphingomyelin (SM), precursor ion scan (+), 184 *m/z*, -25 V; lysophosphatidylethanolamine (LPE), phosphatidylethanolamine (PE), neutral loss (+), 141 Da, -30 V; lysophosphatidylglycerol (LPG), phosphatidylglycerol (PG), neutral loss (+), 153 Da, +35 V; lysophophatidylinositol (LPI), phosphatidylinositol (PI), precursor ion scan (-), 241 *m/z*, + 50 V; lysophosphatidylserine (LPS), phosphatidylserine (PS), neutral loss (+), 185 Da, -28 V.

LabSolution ver. 5.95 software (Shimadzu Europa, Duisburg, Germany) was employed for data acquisition and processing, while the LIPID MAPS Structure Database (LMSD, https://www.lipidmaps.org/data/structure/) was used for lipids assignment, by searching $[M+H]^+$ for LPC/PC/SM, $[M-H]^-$ for LPI/PI, and $[M+NH4]^+$ for TAG [36].

The analyses of tuna waste oil were performed both with the above reported analytical conditions and with another LC-MS set-up suitable for the separation and analysis of non-polar compounds. For the latter approach analyses were carried out on a Nexera UHPLC system coupled to a LCMS-2020 spectrometer through an APCI ionization source (Shimadzu Europa, Duisburg, Germany). UHPLC separations were performed on two serially coupled Ascentis Express C18 10 cm x 2.1 mm, 2.7 µm *d.p.* columns (Merck Life Science, Darmstadt, Germany). Mobile phases were acetonitrile (A) and 2-propanol (B) and the gradient program was: 0-105 min, 0-50% B, held for 5 min. The flow rate was 0.5 mL/min, the injection volume was 10 µL and the oven temperature was 35 °C. Concerning the MS parameters, the acquisition were performed using an APCI interface in both positive (+) and negative (-) ionization modes, with the following conditions: interface temperature, 450 °C; DL temperature, 250 °C; heat block temperature, 300 °C;

nebulizing gas flow (N_2), 1.5 L/min; drying Gas, 5 L/min; acquisition range, 250-1200 *m/z* (+) and 100-1200 *m/z* (-). Data acquisition and processing was handled by the LabSolution ver. 5.95 software (Shimadzu Europa, Duisburg, Germany).

LRI were calculated by employing the mixture of odd carbon number TAGs as references homologue series, according to the following equation [35]:

$$LRI = 100\,[z + 6\frac{t_{Ri} - t_{Rz}}{t_{R(z+6)} - t_{Rz}}]$$

Equation 2.1

where z represents a value equal to the PN of the standard TAG eluting immediately before the analyte; t_{Ri} is the analyte retention time, t_{Rz} and $t_{R(z+6)}$ are the retention times of the reference compound eluting immediately before and after the analyte, respectively; 6 represents the distance in terms of PN units between two consecutively eluted standards of the homologue series. A previous laboratory-made LRI database was used to identify TAGs, selecting an LRI tolerance window of ±15.

Concerning peptide analysis, an Acquity UPLC system coupled to Synapt G2-Si Q-ToF mass spectrometer through an ESI interface (Waters Corporation, Milford, USA) was employed. Separations were performed on one or two (serially coupled) Ascentis Express Peptide ES-C18, 150 × 2.1 mm, 2.7 µm *d.p.* columns (Merck Life Science, Darmstadt, Germany). Zero dead volume stainless steel tubing (5 cm L and 0.07 I.D.) was used as column connector. Mobile phases were: 0.1% F.A. in water (A) and 0.1% F.A. in ACN (B). The gradient program was: 0-15 min, 0-50% B and it was proportionally expanded, 0-30 min, 0-50% B, to keep the same retention factors for the separation on the two coupled columns. The flow rate was 0.3 mL/min, column oven was set at 35 °C and the injection volumes were 2 µL and 4 µL for one and two column setups, respectively. Concerning the MS and MS/MS parameters, an ESI source was used in positive ionization mode, employing the following parameters: source temperature, 90° C; desolvation temperature, 250 °C; desolvation gas (N_2) flow, 650 L/h; nebulizer gas flow, 6.5 bar, sampling cone voltage, 40 V; capillary voltage, 2.5 kV.

A FastDDA acquisition mode was used for precursor ions selection, employing the following conditions: MS Survey range, 100-1800 *m/z*; MS/MS range, 50-1800 *m/z*; MS scan time, 0.2 s; maximum number of ions selected for MS/MS from a single MS Survey

scan, 5; Stop MS/MS criteria, TIC $10e^5$ or 0.6 s; collision energy (TRAP CE), *m/z* dependent ramp applied for low (100 *m/z*, 15-25 V) and high mass (1800 *m/z*, 55-65 V). The Q-ToF spectrometer was calibrated, prior to use, upon infusion of a sodium formate 2-propanol/water solution, while Leucine enkephalin (*m/z* 556.2771, positive ionization mode) was used as LockSpray reference compound, for internal lock-mass correction. MassLynx ver. 4.1 and ProteinLynx Global SERVER (PLGS) ver. 3.0.3 software (Waters Corporation, Milford, USA) were employed for data acquisition and processing. The MS/MS datasets as .pkl file were subjected to MASCOT MS/MS ion search (https://www.matrixscience.com), selecting the SwissProt database and restricting the search to *Actinopterygii* class (ray-finned fishes); trypsin was selected as enzyme (MC 2), oxidation (M) and deamidation (N, Q) were selected as variable modifications. A precursor mass tolerance of 3 ppm and a fragment mass tolerance of 0.6 Da was selected. Results were validated trough MS/MS spectra manual checking. Peptides sequences were investigated by ClassAMP [37] (http://www.bicnirrh.res.in/classamp/) for antimicrobial activity prediction.

2.3 Results and Discussion

2.3.1 Fatty Acids

The total fatty acid composition of tuna muscle and waste was investigated through a fully automated method, from sample preparation to FAMEs analysis and identification [30]. The use of a direct derivatization procedure in which the derivatization regents were added directly on the tissue, without requiring any preliminary liquid-liquid extraction of lipids, allowed to speed up the analytical workflow and to reduce the solvent consumption. The basic reagent (CH_3ONa) induced transesterification of sterol and glycerol esters (viz. CEs, MAGs, DAGs, TAGs, PLs and LPLs), while the acidic reagent (BF_3) promoted esterification of the free FAs. The GC-FID profiles obtained for tuna edible parts and waste tissues are reported in Figure 2.1 (compound identification by triple quadrupole MS). From a visual inspection, it can be easily appreciated that both samples show identical qualitative FA profile, being the main differences related to the PUFA content. In detail, peaks at t_R 51.7 and 57.6 min, later identified by GC-MS as eicosapentaenoic acid (C20:5n3, Ep) and docosahexaenoic acid (C22:6n3, Dh), respectively, showed much higher intensity in the waste tissues (panel B), with respect to

the edible part (panel A). Such components, representing the main omega-3 FAs, account for the nutritional value of functional food ingredients [6].

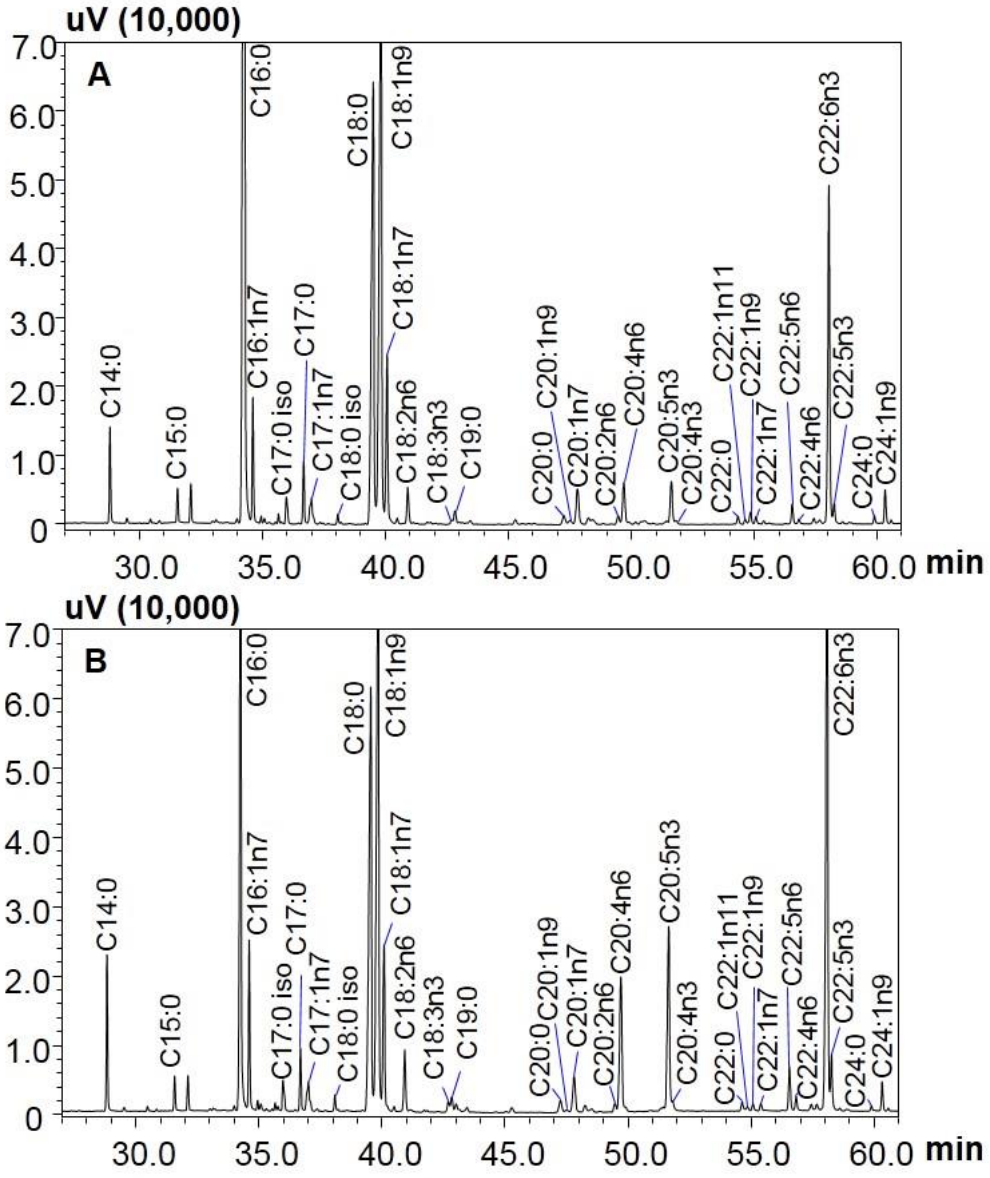

Figure 2.1 GC-FID profiles of FAMEs in tuna edible part (A) and tuna wastes (B) (peak identification was performed by QqQ MS).

Furthermore, it should be noted that the compound eluted at t_R 49.7 min, identified by GC-MS as arachidonic acid (C20:4n6, Ar) also eluted as a much more intense peak in

tuna wastes compared to the edible part. The latter finding is noteworthy since Ar represents the precursor of numerous lipid mediators, thus its dietary intake should be carefully monitored to ensure an optimal ω-6/ω-3 ratio [6].

In Table 2.1 the qualitative and quantitative results obtained for tuna muscle and wastes are showed. Identification was based on minimum MS spectral similarity (85%) and the comparison between the experimental and tabulated LRI values. In detail, a satisfactory match between the experimental MS spectra and the library was achieved for all the compounds, with similarity values >90%; while only few exceptions were obtained for the low abundant FAMEs (<0.3%), for which 85%-89% similarity scores were considered acceptable. The employment of a second filter for library search, consisting of a tolerance window of ±10 units between the experimental and reference LRI values, allowed to confirm the results.

Considering the quantitative point of view, as shown in Table 2.1, Dh and Ep amounts resulted to be approximately double and triple (viz. 16.4% vs. 8.5% and 4.8% vs. 1.3%, respectively) in wastes compared to the edible part, thus highlighting the higher content of ω-3 FAs in tuna by-products. Tuna wastes showed also a higher content of ω-6 FAs compared to the muscle counterpart. Specifically, Ar resulted to be the most abundant component of the class, with relative amounts determined as equal to 3.8% and 1.4% in the two investigated samples. Overall, the ω-6/ω-3 ratio resulted to be perfectly comparable in tuna muscle and wastes (3.3 and 3.4%, respectively). Also, the relative MUFA content was found consistent in both samples, as well as those of most SFAs, with the sole exception of P (palmitic acid, C16:0) which accounted for around 15% lower amount of total SFAs in wastes, compared to the muscle.

As a result, the lower SFAs/PUFAs ratio in tuna by-products would make the retrieval of ω-3 FAs as valuable ingredients for nutraceutical formulations easier compared to the edible part.

Table 2.1 FAMEs identified in tuna muscle and wastes by AOC6000-GC-FID/MS. For each compound are reported MS similarity (%), experimental and tabulated LRI value and the relative content (%).

Compound	MS (%)	LRI_{exp}	LRI_{tab}	Muscle (%)	Waste (%)
C14:0	95	1400	1400	1.67	2.34
C15:0	94	1502	1500	0.61	0.52
C16:0	96	1604	1600	37.85	24.10
C16:1n7	94	1616	1616	2.30	2.72
C17:0 iso	95	1657	1660	0.19	0.47
C17:0	95	1696	1700	1.19	1.03
C17:1n7	94	1710	1719	0.72	0.65
C18:0 iso	87	1749	1759	0.23	0.30
C18:0	96	1802	1800	14.74	12.16
C18:1n9	97	1810	1810	18.34	18.89
C18:1n7	97	1816	1820	4.19	3.66
C18:2n6	96	1840	1848	0.93	1.35
C18:3n3	93	1886	1900	0.13	0.28
C19:0	94	1887	1900	0.41	0.41
C20:0	93	1999	2000	0.36	0.41
C20:1n9	90	2006	2008	0.18	0.08
C20:1n7	96	2015	2015	1.33	1.13
C20:2n6	93	2059	2055	0.27	0.22
C20:4n6	94	2065	2063	1.39	3.83
C20:3n6	87	2070	2065	0.06	0.13
C20:5n3	95	2118	2122	1.30	4.83
C20:4n3	90	2123	2123	0.12	0.28
C22:0	89	2000	2000	0.22	0.23
C22:1n11	90	2208	2207	0.15	0.12
C22:1n9	90	2217	2217	0.34	0.17
C22:1n7	85	2228	2229	0.21	0.16
C22:5n6	92	2272	2274	0.47	0.95
C22:4n6	88	2283	2286	0.11	0.29
C22:6n3	96	2328	2335	8.49	16.37
C22:5n3	90	2337	2338	0.57	1.28
C24:0	90	2399	2400	0.19	0.10
C24:1n9	90	2416	2420	0.77	0.55

Total muscle FA content was determined as: 57.65% SFAs, 28.52% MUFAs, and 13.84% PUFAs (3.22% omega-6 and 10.62% omega-3). Total wastes FA content was determined as: 42.06% SFAs, 28.13% MUFAs, 29.80% PUFAs (6.76% omega-6 and 23.04% omega-3).

2.3.2 Intact Lipids

One of the main goals of the present work was the detailed elucidation of tuna tissues native lipid composition, both in terms of lipid class distribution and identification of the individual species within a class. Miniaturization of the extraction protocols revealed to be mandatory to achieve compatibility with automation, prior to UHPLC-MS analysis. In accordance with the recommendations from Organization for the Economic and Cooperation Development (OECD) [38], Folch and Bligh&Dyer procedures were applied in this research and the UHPLC-MS profiles of lipid extracts obtained from tuna wastes are reported in Figure 2.2 (panel A and B).

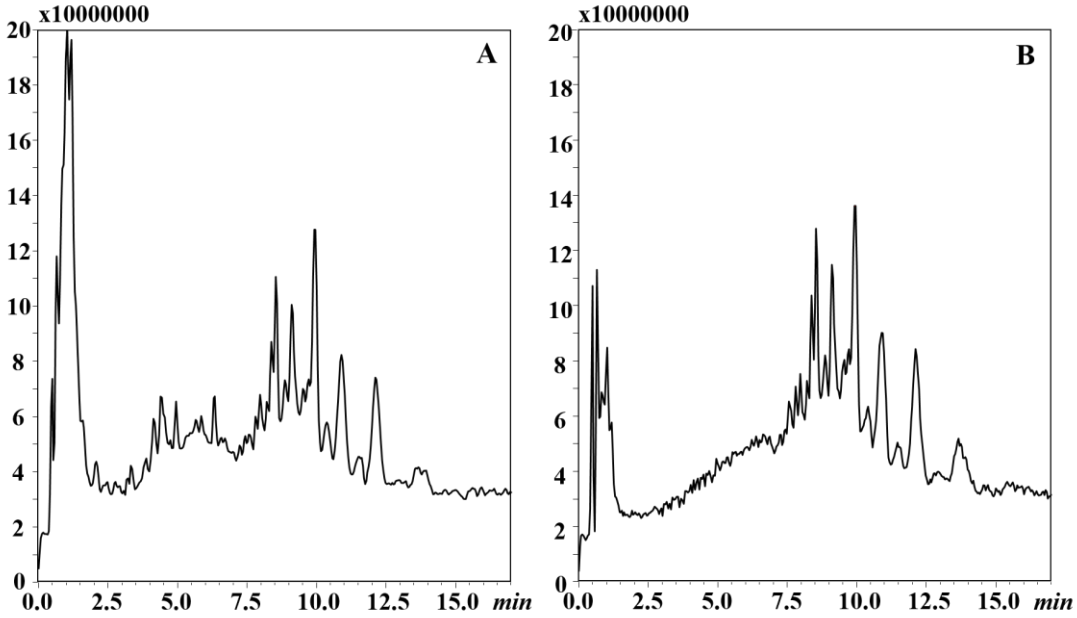

Figure 2.2 UHPLC-MS profile of tuna waste lipid extracts obtained through CLAM-2030 workstation, according to Bligh&Dyer A) and Folch B) extraction procedures.

As it can be easily observed, the UHPLC-MS profiles of the more hydrophobic lipids eluting between 7.5-15 min, which consisted predominantly of TAGs, resulted to be quite similar in the two extracts. Conversely, the Bligh&Dyer procedure (panel A) resulted to be more effective for the recovery of highly polar and polar lipids (LPLs, PLs), which eluted in the first portion of the chromatogram. Therefore, the Bligh&Dyer method was selected for the subsequent analyses, followed by an UHPLC-MS method [39] enabling

for fast lipid separation according to class polarity (e.g. LPLs, PLs and TAGs), and PN value of the species within each class.

In Figure 2.3 is showed the multiclass lipid distribution observed for tuna edible part and wastes. Three main regions could be clearly defined: highly polar lipids (LPLs), polar and medium-polar lipids (PLs and free cholesterol, Ch) and non polar lipids (TAGs), which elute depending on the increasing hydrophobicity (with PN values comprised between 30-50) [40].

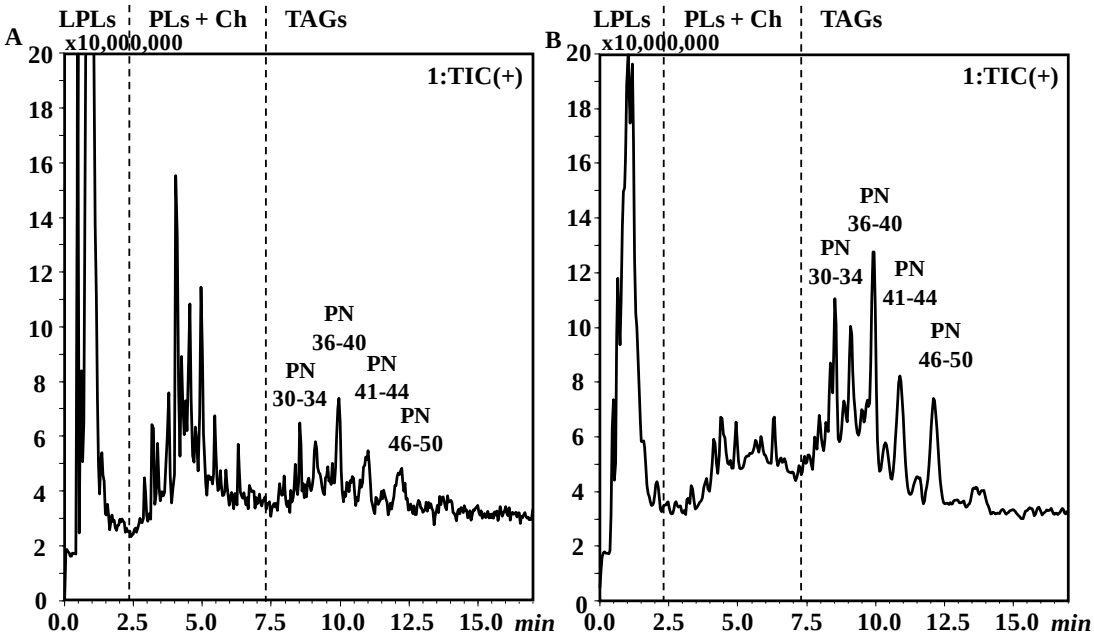

Figure 2.3 Multiclass lipid distribution observed in UHPLC-MS profiles of tuna muscle (A) and wastes (B).

From a visual inspection of the UHPLC-MS profiles, the higher signal intensities in the TAG region revealed the predominance of nonpolar lipids in tuna wastes (panel B) compared to the muscle counterpart; conversely, the muscle profile showed higher peak signals related to the more polar lipids (LPLs and PLs).

In Table 2.2 are listed the identified lipids in the investigated samples by using ESI QqQ MS in positive and negative ion modes. Retention time (t_R) detected ions and diagnostic fragments are reported for each lipid species, as well as PN, CN and DB values (e.g., PC 36:2 means a PC where CN is 36 and DB is 2). Under the experimental conditions

employed, ammonium and sodium adducts were generated from TAGs, while the more polar choline-containing lipids (lysophosphatidylcholines, LPCs, phosphatodylcholines, PCs, and sphyngomyelins, SMs) were mainly observed as protonated species ($[M+H]^+$), as well as sodium and potassium adducts of lower intensity. Lysophophatidylinositols and phosphatidylinositols were detected in negative ion mode, as deprotonated species ($[M-H]^-$), while Ch observed under positive polarity as dehydrated ion. The employment of the QqQ analyzer, capable of performing tandem MS, allowed for analytes fragmentation and selective monitoring of diagnostic fragments for each lipid class. In detail, it was possible to monitor the loss of the polar head of phospholipids in the form of neutral species (*neutral loss scan*) and to detect charged fragments for which the *m/z* difference coincided with the loss of that specific neutral; by this way, only the precursor ions resulting in that neutral loss were monitored. Moreover, it was possible to monitor all the ions ions which, subjected to fragmentation, originated a specific fragment (charged) with a given *m/z* (*precursor ion scan*); in this case, the first analyzer was set to perform a complete scan, while the second one was set to specific *m/z* values. As an example, Figure 2.4 (panel A) reported the proposed mechanism of the collision-induced decomposition of a generic protonated phosphatidylethanolamine which lead to the formation of an abundant ion that corresponded to the neutral loss of phosphoethanolamine (141 Da); while, panel B reported the mechanism for the formation of the phosphocholine ion at *m/z* 184, which resulted from the collision-induced decomposition of the phosphatidylcholine positive protonated molecule ion $[M+H]^+$. The MS/MS experiments optimized for PLs, which allowed the identification of such lipid components, are reported in Table 2.3. The precursor ion scan chromatogram of the fragment at *m/z* 184 obtained for choline-containing lipids is reported, by way of illustration, in Figure 2.5.

Table 2.2 Lipids identified in tuna muscle and wastes by CLAM2030-UHPLC-MS; PN, retention times (t_R) and detected ions are also reported.

	Compound		PN	t_R	$[M-H]^-$	$[M+H-H_2O]^+$	$[M+H]^+$	$[M+NH_4]^+$	$[M+Na]^+$	$[M+K]^+$	Fragments	Muscle	Wastes
1	LPC	20:5	10	0.71	-	-	542.3	-	564.3	-		x	x
2	LPI	22:6	10	0.72	643.3	-	-	-	-	-		x	
3	LPI	20:4	12		619.3	-	-	-	-	-		x	
4	LPC	22:6	10	0.77	-	-	568.2	-	590.2	606.2		x	x
5	LPC	16:1	14		-	-	494.2	-	516.2	-			x
6	LPC	20:4	12	0.81	-	-	544.2	-	566.2	582.2		x	x
7	LPC	O-18:1	16	0.89	-	-	508.2	-	530.2	-		x	x
8	LPC	22:5	12	0.96	-	-	570.3	-	592.3	-		x	x
9	LPC	16:0	16		-	-	496.2	-	518.2	534.2		x	x
10	LPC	18:1	16	1.01	-	-	522.2	-	544.2	560.2		x	x
11	LPI	18:0	18	1.06	599.3	-	-	-	-	-		x	x
12	LPC	18:0	18	1.32	-	-	524.3	-	546.3	-		x	x
13	LPC	20:0	20	1.82	-	-	552.3	-	574.3	-			x
14	PC	40:10	20	2.61	-	-	826.5	-	848.5	864.5		x	
15	PC	42:11	20	2.9	-	-	852.5	-	874.5	890.5		x	x
16	PC	40:9	22	3.06	-	-	828.5	-	850.5	866.5		x	
17	PC	36:6	24		-	-	778.5	-	800.5	816.5		x	
18	PC	44:12	20	3.22	-	-	878.4	-	900.4	916.4		x	x
19	PI	38:6	26	3.25	881.4	-	-	-	-	-		x	
20	PC	42:10	22		-	-	854.5	-	876.5	892.5		x	x
21	PC	38:7	24	3.39	-	-	804.5	-	826.5	-		x	x
22	SM	32:1;O2	30		-	-	675.5	-	697.5	-		x	x
23	PC	44:11	22	3.67	-	-	880.5	-	902.5	918.5		x	
24	PC	37:6	25		-	-	792.5	-	814.5	830.5		x	
25	SM	33:1;O2	31		-	-	689.5	-	711.5	-			x
26	PC	O-36:6	24	3.8	-	-	764.5	-	786.5	802.5		x	x
27	PC	36:5	26		-	-	780.5	-	802.5	818.5		x	x
28	PC	O-40:7/39:7	26/25		-	-	818.5	-	840.5	-		x	
29	PC	42:9	24	3.88	-	-	856.6	-	878.6	-		x	
30	PI	40:6	28	3.96	909.3	-	-	-	-	-		x	x
31	PC	38:6	26	4.06	-	-	806.5	-	828.5	-		x	x

32	PC	40:7	26		-	-	832.5	-	-	-	x	x
33	PI	38:4	30	4.13	885.3	-	-	-	-	-	x	x
34	PC	36:4	28		-	-	782.4	-	804.4	-	x	x
35	PC	32:1	30	4.28	-	-	732.5	-	-	-	x	x
36	SM	34:1;O2	32		-	-	703.5	-	725.5	-	x	x
37	Ch	-	-	4.38	-	369.2	-	-	-	-	x	x
38	PC	34:2	30	4.4	-	-	758.5	-	780.5	-	x	x
39	PC	O-38:6/37:6	26/25		-	-	792.5	-	814.5	830.5	x	x
40	PC	38:5	28	4.55	-	-	808.5	-	830.5	-	x	x
41	SM	37:3;O2	31				741.5	-	763.5	-	x	x
42	PC	O-36:4/35:4	28/27		-	-	768.5	-	790.5	806.5	x	x
43	PC	O-38:5/37:5	28/27		-	-	794.6	-	816.6	-	x	x
44	PC	40:6	28	4.76	-	-	834.6	-	856.6	-	x	x
45	PC	O-30:0/29:0	30/29		-	-	692.5		714.5			x
46	PC	O-32:1/31:1	30/29		-		718.5	-	740.5	-	x	x
47	PC	38:4	30		-	-	810.6	-	-	-	x	
48	PC	32:0	32	5.01	-	-	734.5	-	-	-	x	x
49	PC	34:1	32		-	-	760.5	-	782.5	-	x	x
50	PC	O-34:2/33:2	30/29	5.38	-	-	744.5	-	766.5	782.5	x	x
51	PC	O-36:1/35:1	34/33		-	-	774.5	-	796.5	-	x	x
52	PC	O-32:0/31:0	32/31	5.5	-	-	720.5	-	-	-		x
53	PC	O-34:1/33:1	32/31		-	-	746.6	-	768.6	-	x	x
54	PC	34:0	34		-	-	762.6	-	784.6	800.6	x	x
55	SM	40:2;O2	36	5.72	-	-	785.6	-	807.6	-	x	x
56	PC	36:1	34		-	-	788.6	-	810.6	-	x	x
57	SM	41:2;O2	37	6.05	-	-	799.6	-	821.6	-	x	x
58	SM	42:2;O2	38	6.38	-	-	813.6	-	835.6	-	x	x
59	SM	40:1;O2	38	6.41	-	-	787.7		809.7			x
60	SM	41:1;O2	39	6.86	-	-	801.6	-	823.6	-		x
61	SM	44:2;O2	40	7.07	-	-	841.7	-	863.7	-	x	
62	SM	42:1;O2	40	7.17	-	-	815.7	-	837.7	-	x	x
63	TAG	62:16	30	7.23	-	-	-	988.5	993.5	-		x
64	TAG	64:17	30	7.43	-	-	-	1014.7	1019.7	-		x
65	TAG	66:18	30	7.59	-	-	-	1040.7	1045.7	-		x

66	TAG	64:16	32	7.8	-	-	-	1016.6	1021.6	-			x
67	TAG	56:11	34		-	-	-	914.6	919.6	-			x
68	TAG	58:12	34	7.96	-	-	-	940.7	945.7	-			x
69	TAG	60:13	34		-	-	-	966.7	971.7	-		x	x
70	TAG	56:10	36	8.2	-	-	-	916.7	921.7	-		x	x
71	TAG	58:11	36	8.37	-	-	-	942.7	947.7	-	597.4	x	x
72	TAG	60:12	36	8.53	-	-	-	968.7	973.7	-	623.5, 649.3	x	x
73	TAG	62:13	36		-	-	-	994.7	999.7	-		x	x
74	TAG	58:10	38	8.86	-	-	-	944.8	949.8	-		x	x
75	TAG	60:11	38		-	-	-	970.7	975.7	-		x	x
76	TAG	52:6	40		-	-	-	868.8	873.8	-	523.3, 549.5, 575.5, 601.4	x	x
77	TAG	54:7	40	9.1	-	-	-	894.6	899.6	-		x	x
78	TAG	56:8	40		-	-	-	920.6	925.6	-		x	x
79	TAG	55:7	41		-	-	-	908.6	913.6	-			x
80	TAG	57:8	41	9.51	-	-	-	934.6	939.6	-			x
81	TAG	52:5	42		-	-	-	870.8	875.8	-			x
82	TAG	54:6	42	9.71	-	-	-	896.6	901.6	-		x	x
83	TAG	56:7	42	9.93	-	-	-	922.6	927.6	-	577.4, 649.4	x	x
84	TAG	58:8	42		-	-	-	948.6	953.6	-		x	x
85	TAG	56:6	44		-	-	-	924.7	929.7	-	523.3, 549.5, 575.5, 605.4	x	x
86	TAG	58:7	44		-	-	-	950.7	955.7	-		x	x
87	TAG	60:8	44	10.89	-	-	-	976.7	981.7	-		x	x
88	TAG	48:1	46		-	-	-	822.7	827.7	-		x	x
89	TAG	50:2	46		-	-	-	848.6	853.6	-		x	x
90	TAG	52:3	46		-	-	-	874.7	879.7	-			x
91	TAG	60:7	46		-	-	-	978.8	983.8	-	551.5, 577.5, 603.5		x
92	TAG	62:8	46		-	-	-	1004.7	1009.7	-			x
93	TAG	50:1	48	12.13	-	-	-	850.7	855.7	-		x	x
94	TAG	52:2	48		-	-	-	876.7	881.7	-		x	x
95	TAG	54:3	48		-	-	-	902.7	907.7	-			x
96	TAG	62:7	48		-	-	-	1006.7	1011.7	-	605.5		x
97	TAG	52:1	50	13.74	-	-	-	878.7	883.7	-			x
98	TAG	54:2	50		-	-	-	904.8	909.8	-			x

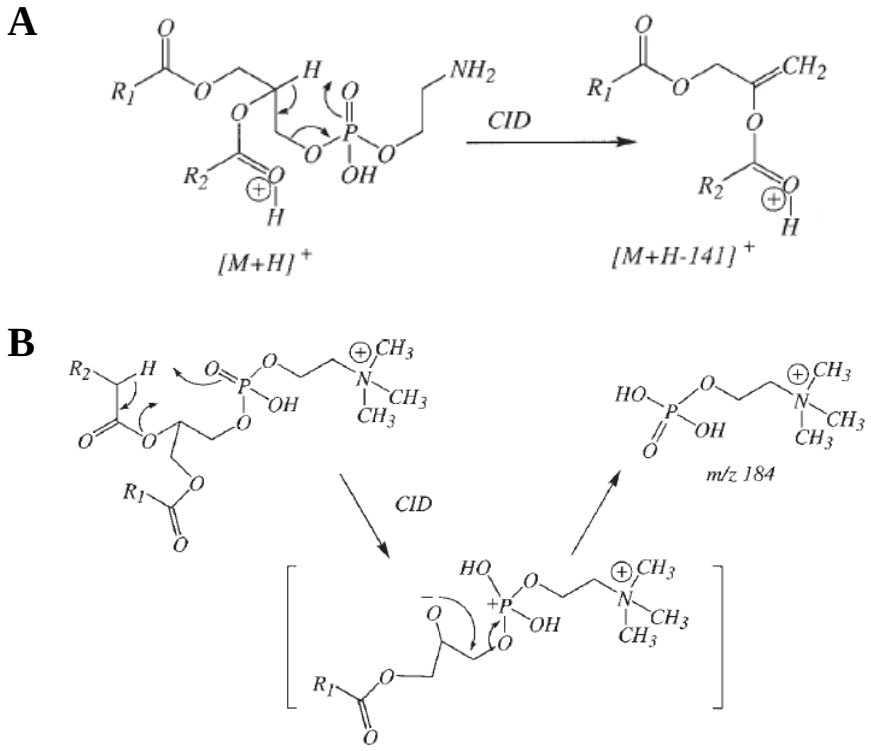

Figure 2.4 Collision-induced decomposition of phosphatidylethanolamine leading to the loss of phosphoethanolamine (panel A) and of phosphatidylcholine leading to the formation of the phosphocholine ion (panel B).

Table 2.3 MS/MS events optimized for each lipid class.

Lipid Class	MS/MS event	Polarity	Diagnostic Fragment	Energy (V)
CerGal	Neutral loss	+	162 Da	-35
LPA/PA	Neutral loss	+	115 Da	-25
LPC/PC/SM	Precursor ion	+	184 m/z	-25
LPE/PE	Neutral loss	+	141 Da	-30
LPG/PG	Neutral loss	-	153 Da	+35
LPI/PI	Precursor ion	-	241 *m/z*	+50
LPS/PS	Neutral loss	+	185 Da	-28

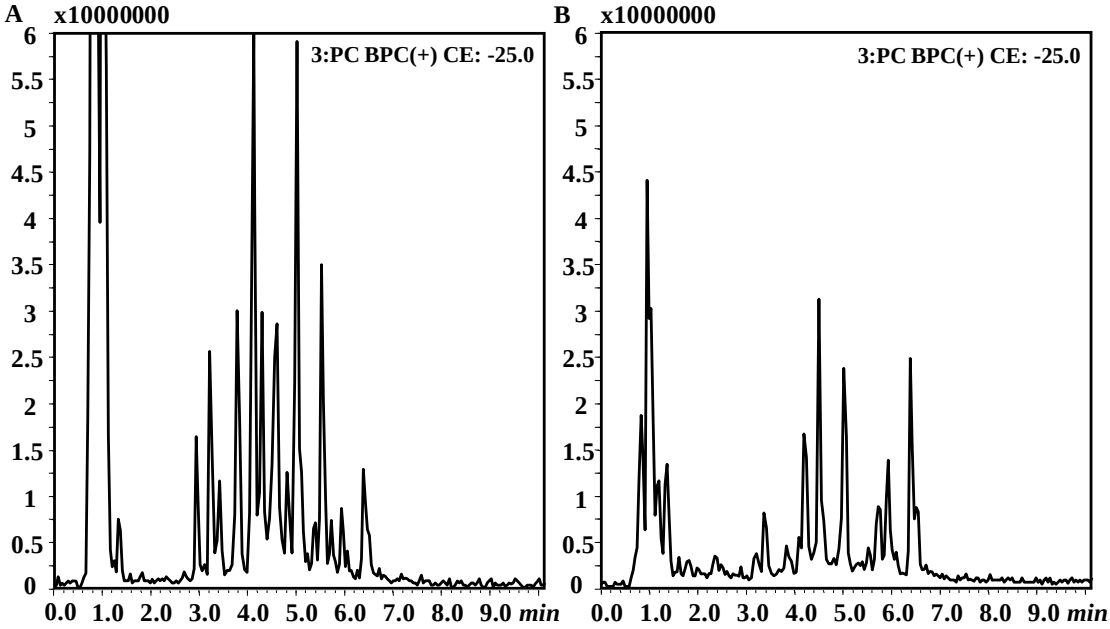

Figure 2.5 UHPLC-ESI MS/MS precursor ion scan chromatograms of choline-containing lipids (monitored fragment at m/z 184, +) of tuna edible part (A) and wastes (B).

For the most abundant TAGs, ions resulting from in-source molecule fragmentation were also detected, corresponding to the loss of a single FA $[M+H-FA]^+$ from the lipid species. In detail, in Figure 2.6 are reported the proposed mechanisms for the formation of the diacylglycerol-like fragment ions (DG^+), resulting from the loss of the FA esterified to the positions sn-3, sn2 and sn-1 of the glycerol backbone. The detection of the DG^+ ions allowed for inferring the FA composition of each TAG. For istance, the lipid species eluted at t_R 8.53 min and identified as TAG (60:12) by the LIPID MAPS database, may result from the combination of Dh, Ep and oleic acid (C18:1), due to the presence of fragments ions at *m/z* 649.3 and 623.5, deriving from the loss of Ep and Dh, respectively. In the identification process, the fatty acid GC-FID/MS profile assisted and positively supported the elucidation of intact lipid composition, since the most probable combination of FAs within each species is directly related to their relative abundance in the sample. As an example, for the PC (40:10) eluted at t_R 8.53 min, the presence of two Ep moieties is highly probable (since each Ep consists of a 20 carbon atoms chain and presents 5 double bounds, 20:5), while for PC (42:11) a contribution from Dh and Ep could be assumed (22:6 and 20:5, respectively).

In a similar way, for the highly unsaturated TAG (62:16), TAG (64:17) and TAG (66:18), eluted in the first part of the TAG region, the only possible candidates result from

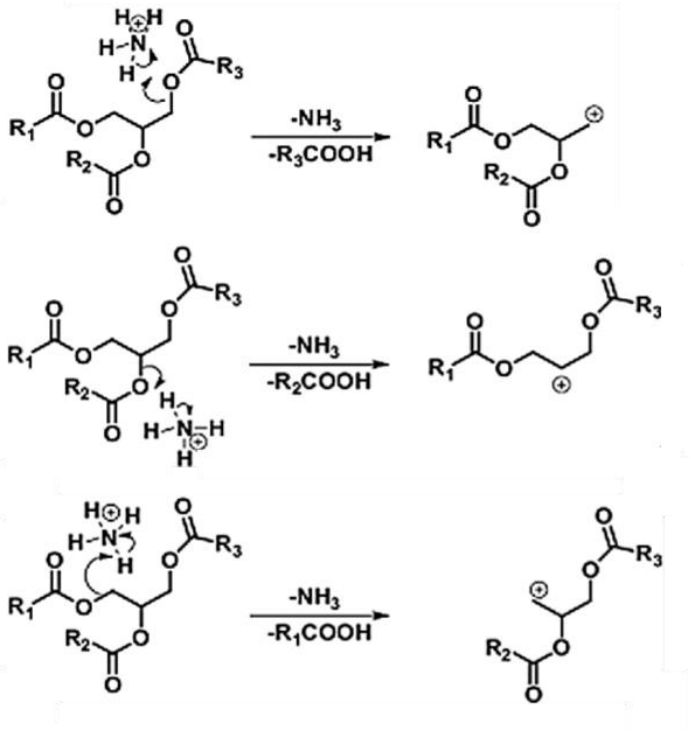

Figure 2.6 Proposed scheme of triacylglycerol fragmentation pathway.

different combination of Ep and Dh, as DhEpEp, DhDhEp and DhDhDh. Such low PN TAGs were identified exclusively in tuna wastes, whose UHPLC-MS profiles showed a higher abundance of non-polar lipid signals compared to the edible part (Figure 2.3); such findings were in perfect agreement with the quantitative GC-FID results, which revealed an approximately double and triple relative content of Dh and Ep in tuna by-products compared to the muscle (Table 2.1). As a result, 16 more TAGs were identified in tuna wastes with respect to the edible part (36 vs 20). Concerning the more polar lipids (LPLs and PLs), 61 species were identified and most of them were choline-containing lipids; in detail 10 LPCs, 34 PCs and 11 SMs. Plasmanyl PCs, in which one of the acyl chains is replaced by an alkyl group (O-PC), were also tentatively identified in the investigated samples; the latter finding was in agreement with previous literature, reporting a significant content of O-PC in marine organisms [20, 41]. According to the GC-FID/MS data, also the presence of PC and SM containing odd chain FAs may be hypothesized, thus resulting in choline-containing lipids characterized by odd CN (and PN values). As an example, PC(37:6) may result from the combinations of C20:5/C17:1 and C22:6/C15:0 FAs.

Among non-polar lipids, only two odd PN TAGs were detected, thus, in accordance with the limited occurrence of odd chain FAs in nature. However, a great interest in odd and branched chain FAs has been registered in the last decades, for their potential use as as potential anti-cancer agents since they are able to inhibit the FA biosynthesis in tumor cells [42, 43].

Ultimately, considerable differences were observed in TAG composition of tuna edible part and waste, being a high number of non-polar species detected only in the latter. Conversely, the qualitative polar lipid profiles resulted to be quite similar in tuna samples; in fact as can be observed in Table 2.2, the same number of LPLs was identified in waste and muscle (only a difference in two LPIs was observed between the samples), while few PLs were identified exclusively in one of the tuna tissues. From the other side, the comparison of the total ion chromatograms and precursor ion scan traces (Figures 2.3 and 2.5, respectively) highlighted higher signal intensities related to choline-containing lipids in tuna muscle.

The investigation of the intact lipid composition of tuna tissues provided highly useful and detailed information on the native lipid structures, defining the specific way in which FAs are arranged into the lipid species. As a result, it could be assumed that the higher amount of ω-3 PUFA in tuna wastes, assessed by GC-FID analysis, is mainly related to the higher concentration of TAGs containing Dh and Ep FAs.

These findings positively supported further investigation on the tuna oil, produced by decantation of the liquid coming from the cooking process of wastes, as a concentrated source of ω-3 PUFA containing TAGs. In detail, tuna waste oil was investigated by employing the fast UHPLC-MS method used for multiclass lipid separation of tuna tissues. Such approach may be conveniently used for fast screening applications, enabling rapid discrimination between oil samples showing different TAG UHPLC-MS profiles. However, as it is well-known, oil samples contain more than 90% of non-polar lipids and for such a reason, a different chromatographic method, providing increased efficiency for the separation of hydrophobic compounds, was successfully employed.

The comparison between the two chromatographic methods is reported in Figure 2.7 (panel A and B); as it can be easily observed from the reported chromatograms, the TAG profile of fish oil samples results to be much more complex than vegetable oils. The latter method, based on the serial coupling of two identical C18 columns and a slower gradient,

due to the improvement of the chromatographic resolution, enabled the separation of a large number of TAGs within the same PN regions. In this case, a recently introduced linear retention index (LRI) approach in LC-MS [35] was employed, allowing for a reliable elucidation of TAG species.

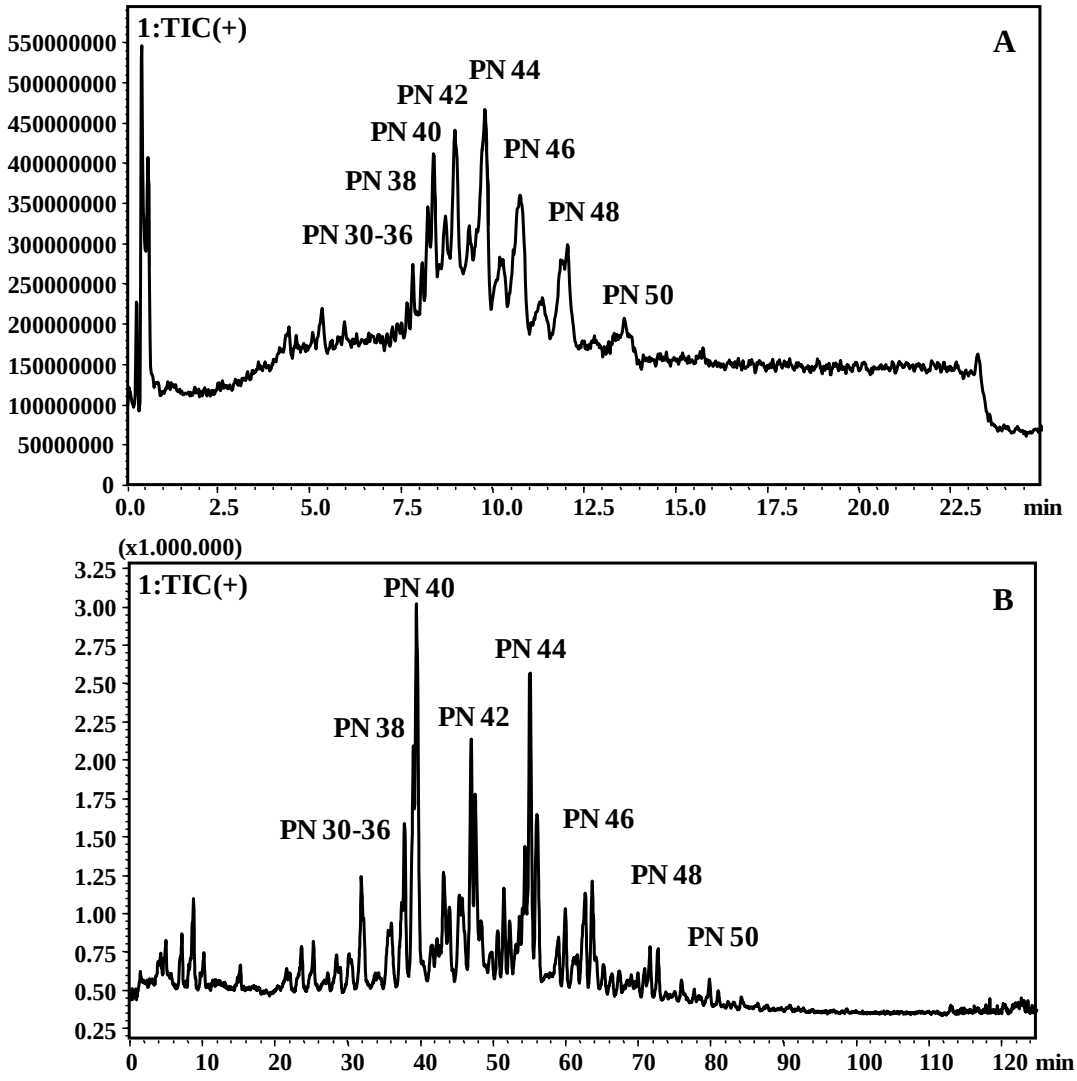

Figure 2.7 UHPLC-MS profiles of tuna waste oil by different chromatographic methods. Panel A) Column: Ascentis Express C18, 10 cm x 2.1 mm. 2.7 µm d.p.; Mobile phases: $HCOONH_4$ 20 mM in water (A) and 2-propanol/ACN/$HCOONH_4$ 20 mM 60/36/4 with 0.1% FA (B); Flow rate: 0.4 mL/min; Oven: 40 °C; Gradient: 0-6 min. 80-100%B; 6-22 min 100% B; ESI-MS (+). Panel B) Columns: 2 serially coupled Ascentis Express C18, 10 cm x 2.1 mm. 2.7 µm d.p.; Mobile phases: ACN (A) and 2-propanol (B); Flow rate: 0.5 mL/min; Oven: 35 °C; Gradient: 0-105 min. 0-50% B. held for 5 min; APCI-MS (+).

The identification process relied on a "dual-filter approach", which combine analytes retention behaviour (LRI) and APCI-MS spectra information; in detail, LRI were calculated employing the odd carbon number TAGs mixture as references homologue series according to Equation 2.1. The experimental LRI were compared to the reference LRI values from a previous lab-constructed database, selecting a tolerance window of ±15 units (Δ LRI). In Figure 2.8 are reported the UHPLC-MS TAG profiles of tuna waste oil and the reference homologue series, obtained under the same analytical conditions; PN values of eluted TAGs are also highlighted.

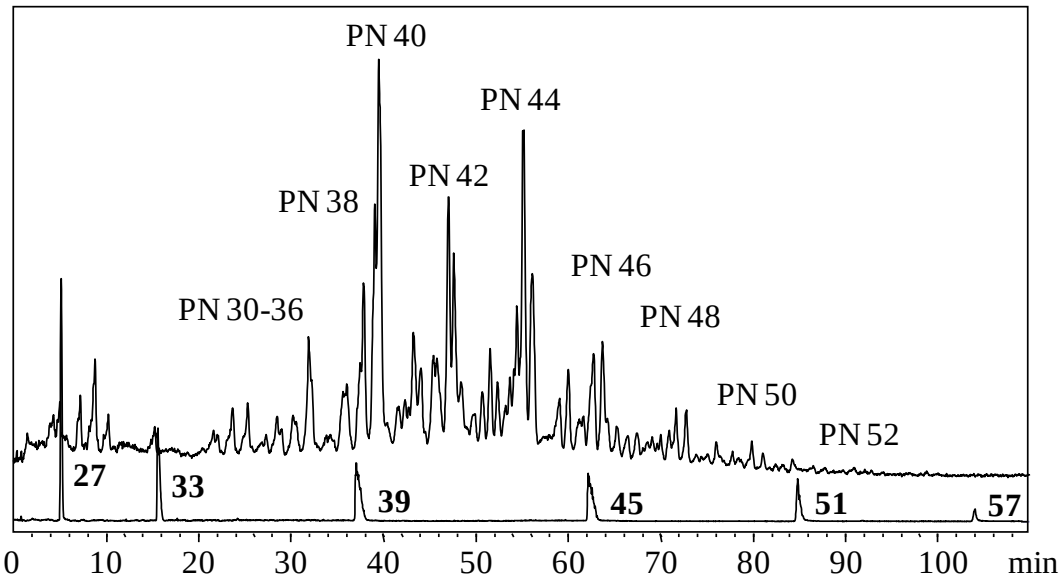

Figure 2.8 UHPLC-MS profiles of tuna waste oil and the odd carbon number TAGs reference homologue series (PN values were also reported).

Concerning the MS information, TAGs were mainly observed as protonated species ($[M+H]^+$), used for molecular mass determination, while the diacylglycerol-like fragment ions, resulting from the loss of a single FA $[M+H-FA]^+$, were employed for the determination of the FAs composition of each species.

Table 2.4 shows the identified TAGs along with their PN, theoretical and experimental LRI values (with their ΔLRI) and the relative weight concentrations (%) of each species. The high amount of Dh in tuna waste oil is clearly evident since such ω-3 PUFA is contained in almost all the identified species. The Table also highlights the usefulness and effectiveness of the LRI approach for reliable lipids identification; in particular, on 57 TAGs identified by APCI-MS spectra, 23 species were positively confirmed by the

comparison between their experimental LRI and the theoretical values. Given the limited knowledge on the lipid profiles of marine organisms and the high difficulty in creating an LRI database for LC deriving from the great number of FAs possible combinations in the constitution of each TAG, the LC-MS analysis of tuna waste oil resulted to be highly beneficial for the implementation of the lab-constructed LRI database. Such findings may contribute to the improvement of the identification process in LC-MS, making it more similar to a GC-MS one.

Table 2.4 TAGs identified in tuna waste oil, together with their PN, theoretical and experimental LRI values and relative content (%).

PN	TAG	LRI_{theor}	LRI_{exp}	ΔLRI	Relative content (%) (n=3)
30	DhEpEp	3475	3484	9	0.30 ± 0.08
30	DhDhEp	3521	3531	10	1.30 ± 0.19
30	DhDhDh	3571	3576	5	1.29 ± 0.22
32	DhEpAr-DhDpEp	-	3633	-	0.32 ± 0.04
32	DhDhDp	-	3666	-	0.76 ± 0.09
32	DhDhAr	-	3680	-	0.43 ± 0.09
34	DhEpPo	3711	3715	4	1.05 ± 0.12
34	DhEpM	-	3724	-	0.55 ± 0.07
34	DhDhPo	-	3762	-	2.53 ± 0.55
34	DhStL	-	3771	-	1.01 ± 0.03
35	DhDhC17:1-DhEpC17:1	-	3867	-	1.58 ± 0.45
36	EpEpP	-	3879	-	1.70 ± 0.32
36	DhEpO	3909	3916	7	1.88 ± 0.68
36	DhEpP	3921	3925	4	3.97 ± 0.43
36	DhDhO	3942	3954	12	5.49 ± 0.42
36	DhDhP	3958	3964	6	8.44 ± 1.93
38	DpEpP	-	4013	-	0.80 ± 0.11
38	DhArO	-	4016	-	0.66 ± 0.16
38	DhOLn	-	4032	-	1.14 ± 0.14
38	DpDhO	-	4041	-	0.57 ± 0.25
38	DpDhP	-	4053	-	3.19 ± 0.23
38	DhArP	-	4073	-	1.94 ± 0.32
38	DhEpS	4105	4105	0	2.41 ± 0.26
40	DhStG-EpOM	-	4115	-	2.46 ± 0.19
40	DhDhS- DhOPo- DhOL	4135	4144	9	5.84 ± 0.23
40	DhPPo	4148	4158	10	4.55 ± 0.12
40	DhPM	-	4176	-	1.79 ± 0.24
40	DhDpS	-	4231	-	1.46 ± 0.30
40	DhArS	-	4252	-	2.26 ± 0.25
41	DhC17:1P-EpC17:1P	-	4271	-	1.74 ± 0.45

42	EpOO	4289	4292	3	1.16 ± 0.32
42	EpOP	4308	4303	-5	1.51 ± 0.30
42	DhOO	4326	4321	-5	2.62 ± 0.22
42	DhOP	4340	4339	-1	8.14 ± 0.32
42	DhPP	4357	4361	4	5.17 ± 0.15
43	DhC17:1S	-	4431	-	1.88 ± 0.47
44	ArOP	-	4453	-	2.11 ± 0.21
44	DhOS	-	4521	-	3.73 ±0.31
44	DhSP	4546	4547	1	3.02 ± 0.29
46	OPPo	-	4564	-	0.69 ± 0.13
46	OPM	4584	4588	4	0.89 ± 0.15
46	DhSS	-	4741	-	0.84 ± 0.17
48	OOP	4756	4761	5	1.30 ± 0.17
48	OPP	4776	4791	15	1.34 ± 0.16
48	C24:1DhP	4876	4876	0	0.66 ± 0.07
48	C22:0DhP	-	4924	-	0.28 ± 0.04
50	GOP	4945	4949	4	0.14 ± 0.02
50	SOP	4973	4980	7	0.56 ± 0.06
50	C24:1DhS	-	5048	-	0.21 ± 0.05
52	AOP	-	5170	-	0.19 ± 0.06
54	C24:1OP	-	5310	-	0.16 ± 0.05

2.3.3 Peptides

In the last decades, fish protein hydrolysates (FPH) have gained increasing importance in the formulation of ω-3/ω-6 dietary supplements, due to their favourable physical and chemical properties and their potential antioxidant, antimicrobial and antihypertensive activities; these valuable properties substantially contribute to enhancing the stability, technological features and nutraceutical value of the formulations [7]. Therefore, part of the present research was focused on the retrieval and characterization of potential bioactive peptides in tuna wastes and for such purpose, many efforts were put on the development of a suitable analytical method for the analysis of complex mixtures of peptides.

In detail, a RP-UHPLC-MS/MS method was employed in this work, using an octadecylsilica stationary phase, consisting of fused-core particles (*d.p.* 2.7 μm) designed for ultrafast and ultrahigh resolution separation of peptides. Given the high complexity of the tuna waste samples, two identical C18 columns have been serially coupled, in an attempt to resolve the numerous coelutions observed for the one column-separation. In fact, being the plate number (N) equal to L/2*d.p.* (with L the column length and *d.p.* the

particle diameter), the coupling of two columns of the same dimensions (30 cm in total) produced an increase in the efficiency of the chromatographic system. For the two-column setup, the gradient was proportionally expanded to keep the same retention factors (xL factor) and the injection volume was doubled. Figure 2.9 shows the comparison between the UHPLC-MS profiles of the tuna tryptic digest obtained by one (panel A) and two-column setups (panel B); a visual inspection of the chromatograms immediately highlight the improvement in peptide separation obtained by the latter approach. The performances of the chromatographic systems were evaluated in terms of N and peak capacity (n_c), which were found to be proportional to the length of the stationary phase, as reported in Table 2.5.

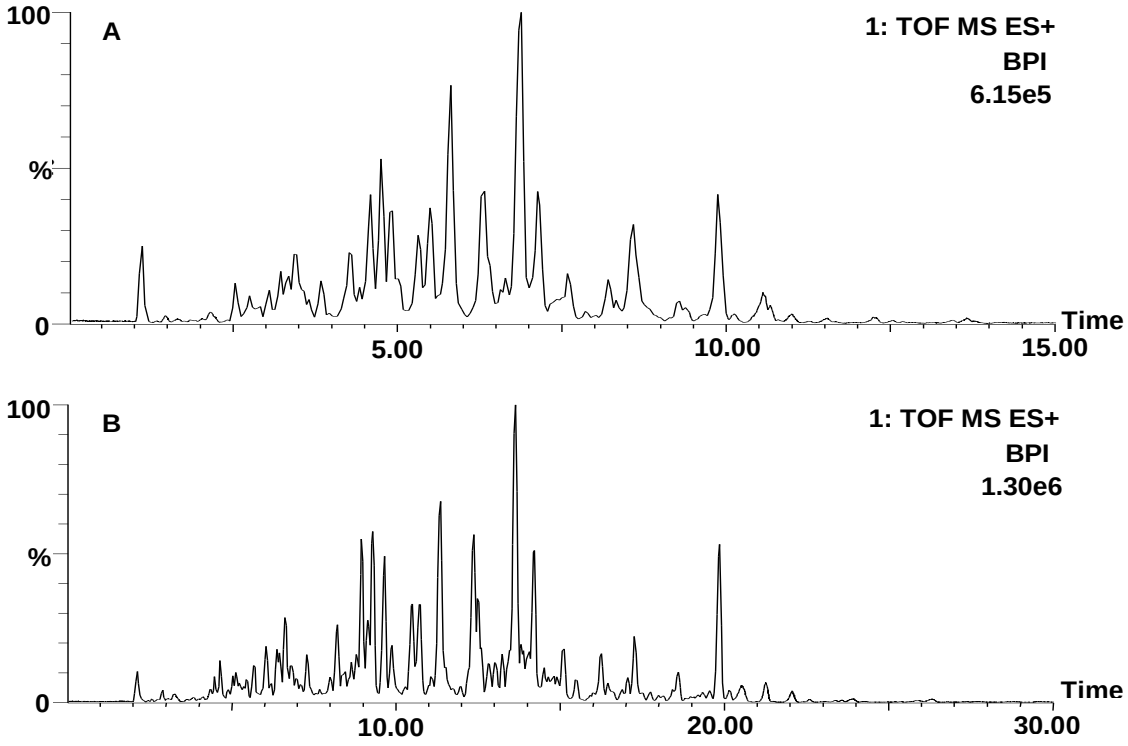

Figure 2.9 RP-LC separation of tuna tryptic digest (ESI-Q-ToF MS). Column: Ascentis Express Peptide ES-C18 150 × 2.1 mm. 2.7 µm d.p. at 35 °C. Mobile phases: 0.1% F.A. in water (A) and 0.1% F.A. in ACN (B). Flow rate: 0.3 mL/min. Gradient: 0-15 min, 0-50% B. Inj. vol.: 2 µL. B) Analysis on 2x columns. Gradient: adapted by the xL factor. Inj. vol.: 4 µL.

Table 2.5 Chromatographic parameters for the UHPLC-RP separation on one column (15 cm) and 2 serially coupled columns (30 cm). Method as in Figure 2.7.

	1 column setup	**2 column setup**
Backpressure (bar)	243	478
RunTime (min)	15	30
Efficiency N	≈ 26475	≈ 52640
Average peak width (min)	0.18	0.13
Peak capacity (n_C)	168	232

Despite tuna and tuna-like species represent significant sources of food and thus have a role of primary importance in the economy of many countries, there is a surprising lack of genomic information for *Thunnus* genus. Concerning *Thunnus albacares* species, the number of proteins annotated in common databases is even smaller, resulting in reduced indexed sequences and thus, making harder a confident peptide identification. The identification strategies when dealing with non model organism, as for yellowfin tuna, is usually based on the similarity to the proteins reported for close organisms, to sequences obtained by translating transcriptomic data or alternatively by de novo approaches, which do not rely on databases. However, the latter is certainly much more complex, long and laborious compared to the database identification strategies [44]. Peptide properties are closely related to the AA composition, being the molecular weight (MW) and the sequence length, the most important factors determining their activity. In detail, short peptides (<7 AA or MW <700−800 Da) are generally the most active, even if their identification by conventional proteomic approaches is hampered by the greater probability of being shared by several proteins. Conversely, long-size peptides (>25 AAs or MW >3000 Da) usually do not show biological activities, with few exceptions and are difficult to analyze. Therefore, medium-size peptides, with a chain length of 7-25 AA and a MW in the range of 800-3000 Da, represent the most common target of proteomic analysis for bioactivity screening. Such peptides are usually obtained by trypsin digestion, which is the most commonly used protease in proteomics [45]. Hereby, the study was focused on the characterization of short and medium-sized peptides in the tryptic digest obtained from the tuna myofibrillar fraction.

The workflow employed for peptide identification was based on the creation of an MS/MS dataset by using the PLGS software, containing information on precursor ions,

derived fragments, charge status and intensity. Such datasets, in the form of .pkl files, were submitted to MASCOT MS/MS ion search, by selecting Swissprot as reference database, *Actinopterygii* as taxonomy and trypsin as the enzyme. The results were manually validated by searching for fragment ions in the MS/MS spectra with particular reference to "b" and "y" (N-terminal and C-terminal, respectively) fragment ions, commonly obtained by the CID technique.

Afterwards, the potential antimicrobial activity of the identified peptides was investigated by ClassAMP [37], an open-access resource using machine learning-based predictive models. Although less studied, antimicrobial peptides (AMPs), obtained by the enzymatic hydrolysis of fish muscle, are gaining increasing importance as a natural alternative to antibiotics, since they are unaffected by antibiotic-resistance mechanisms [46]. For the investigated peptides, the AA composition, as well as the hydrophobicity, charge and structure, were used to describe the propensity of AA sequences to have antibacterial, antifungal or antiviral activity. The prediction was based on the use of support vector machines, i.e. learning models associated with regression and classification algorithms, by comparing peptide structural features to those of the sequences with well-known bioactivity, previously reported in the database.

The prediction results of the identified peptides, reported in Table 2.6, are ordered by the probability score (0-1), which describes the strenght of prediction; in detail, the higher the probability score, the greater is the possibility for a prediction being correct. The main action mechanisms of antimicrobial peptides are related to changes in the physiological function of membranes and alterations in cytoplasmic components, determining impairment of microorganisms cellular functions, which in turn leads to cellular death or metabolism depletion. The vast majority of AMP present a non-receptor-mediated mechanism of action, since such peptides do not have specific receptors but interact with more general targets such as cell membranes. For the latter, hydrophobicity, amphipathicity and electric charges of the different peptide regions, have a fundamental role. In fact, the AA composition of AMPs determines hydrophobic/hydrophilic and electrostatic affinities responsible for the correct binding to the target membranes, as well as the insertion into lipid bilayers, consequent pore formation and cellular extravasation. Antibacterial peptides are usually more positively charged, while antifungal peptides

have shown greater hydrophobicity [47]. The antimicrobial activity predicted for selected peptides identified in tuna by-products will be the subject of future biological assays.

Table 2.6 Results from ClassAMP for tryptic peptides obtained from tuna by-products.

	AA sequence	Probability	Prediction
1	YETDAIQR	0.999988389	Antibacterial
2	VGPPGPAGASGPPGPLGPMGKDGAR	0.999954345	Antibacterial
3	YEEGQSELEGAQK	0.998094964	Antibacterial
4	IPINNFK	0.997511534	Antibacterial
5	AVFPSIVGRPR	0.997510709	Antibacterial
6	TKYETDAIQR	0.994399291	Antibacterial
7	MEMQDVQLK	0.989512662	Antibacterial
8	ELGTVMR	0.988162831	Antibacterial
9	QKYEEGQSELEGAQK	0.978903822	Antibacterial
10	LLGMPSAEDMTNK	0.9752159	Antibacterial
11	AGLDAGGQTALR	0.97379213	Antibacterial
12	VAYNQIADIMR	0.953146439	Antifungal
13	AISEELDHALNDMTSI	0.949585941	Antifungal
14	LAEKDEEMEQIK	0.942206558	Antibacterial
15	SISEELDHALNDMTSI	0.940332207	Antifungal
16	VGLLHSQNTSLINTK	0.940317278	Antiviral
17	NVMGIIIADLEANYK	0.915025912	Antifungal
18	LISEVLVK	0.908723036	Antiviral
19	SYELPDGQVITIGNER	0.903795892	Antifungal
20	SLSTELFK	0.895998545	Antibacterial
21	LAEKDEEMEQIKR	0.890283294	Antibacterial
22	HKIPINNFK	0.889919042	Antifungal
23	NLQQEISDLTEQIGETGKSIHELEK	0.887272564	Antifungal
24	NMWAAFPPDVAGNVDYK	0.881257103	Antifungal
25	VLDPDATGTIK	0.880586208	Antibacterial
26	EAFTIIDQNRDGIISK	0.878250784	Antifungal
27	LQGEVEDLMIDVER	0.859827345	Antifungal
28	DAQLHLDDAVR	0.852042686	Antifungal
29	DLTDYLMK	0.847625444	Antifungal
30	EAFTIIDQNR	0.847344574	Antifungal
31	ILGNPTADDMANK	0.838632458	Antibacterial
32	KYEEVAR	0.832358844	Antibacterial
33	VLADWK	0.821418764	Antifungal
34	LQDAEESIEAVNSK	0.815814485	Antiviral
35	RGADAIK	0.81357129	Antifungal
36	TEELEEAK	0.808159562	Antibacterial
37	ILGNPTADDMANKR	0.804578919	Antibacterial
38	TVTNNLK	0.800426251	Antibacterial
39	GTEDELDKYSEALK	0.79438261	Antiviral
40	MEIDDLSSNMEAVAK	0.794356762	Antiviral
41	AGYEDYVEGLR	0.789317582	Antifungal
42	AEQSESDKK	0.788605428	Antifungal
43	NLQQEISDLTEQIGETGK	0.785030811	Antiviral
44	QGPAGLVGER	0.770218328	Antiviral

45	VLTDK	0.768253019	Antifungal
46	QADSVAELGEQIDNLQR	0.766348711	Antiviral
47	LQTENGEFSR	0.763197413	Antiviral
48	AADESER	0.762437989	Antifungal
49	LQDLVDKLQLK	0.75962173	Antiviral
50	TKLEQQVDDLEGSLEQEKK	0.754396496	Antiviral
51	ELESEVDAESR	0.754181418	Antifungal
52	IQLVEEELDRAQER	0.751841737	Antiviral
53	IEELEEEIEAER	0.75090114	Antifungal
54	KVQHEMEEAQER	0.750839132	Antiviral
55	KLEGDLK	0.75064252	Antifungal
56	ELEEISER	0.748972623	Antifungal
57	LEVAEK	0.747768177	Antifungal
58	TKLEQQVDDLEGSLEQEK	0.747374456	Antiviral
59	GEAGEAGER	0.744906609	Antifungal
60	NVQGQLKDAQLHLDDAVR	0.741856143	Antifungal
61	AALEQTER	0.74023153	Antiviral
62	VAEQELVDASER	0.735326198	Antiviral
63	GTYDDYVEGLR	0.734972134	Antibacterial
64	NVQGQLK	0.734427124	Antiviral
65	AELSESK	0.731174171	Antifungal
66	TEIQTALEEAEGTLEHEEAK	0.730936551	Antiviral
67	IEEELGAK	0.730841364	Antifungal
68	LEEAEK	0.729263088	Antifungal
69	LDLAGR	0.72833666	Antiviral
70	EAFGLFDR	0.727995459	Antifungal
71	EQYEEEQEAK	0.727837004	Antifungal
72	ILGNPSAEDMANKR	0.727711729	Antifungal
73	VQHEMEEAQER	0.727531975	Antiviral
74	LEQQVDDLEGSLEQEK	0.727314993	Antiviral
75	DSYVGDEAQSK	0.727108698	Antifungal
76	EDKYEEEIK	0.719936103	Antifungal
77	ILGNPSAEDMANK	0.715633099	Antifungal
78	AEFAER	0.714972822	Antiviral
79	HVETEK	0.712562562	Antifungal
80	HIEEEIK	0.712382431	Antifungal
81	ELTYQTEEDKK	0.709248031	Antiviral
82	EQDTSAHLER	0.703977541	Antiviral
83	RIQLVEEELDR	0.700332451	Antiviral
84	LKGTEDELEK	0.698666532	Antiviral
85	AELSEGK	0.698436701	Antifungal
86	SIHELEK	0.698103371	Antiviral
87	LVIIEGDLER	0.698028326	Antifungal
88	TIEDQLSELK	0.696709184	Antiviral
89	IQLVEEELDR	0.696347539	Antiviral
90	LVVIESDLER	0.69483431	Antiviral
91	NIAEEADRK	0.694415538	Antiviral
92	NIAEEADR	0.694114884	Antiviral
93	HIAEEADR	0.693571577	Antiviral
94	GTEDELEK	0.693090857	Antiviral
95	LDKENALDR	0.692792678	Antiviral
96	AMKDEEK	0.691753613	Antiviral

97	TIDDLEDELYAQK	0.691426273	Antifungal
98	QAEEAEEQANTHLSR	0.691371776	Antiviral
99	NDEHVR	0.689340721	Antiviral
100	NMKDEEK	0.683802033	Antiviral
101	KEQDTSAHLER	0.671191298	Antiviral

(Abbreviations: Alanine, A; Arginine, R; Asparagine, N; Aspartic acid, D; Cysteine, C; Glutamic acid, E; Glutamine, Q; Glycine, G; Histidine, H; Isoleucine, I; Leucine, L; Lysine, K; Methionine, M; Phenylalanine, F; Proline, P; Serine, S; Threonine, T; Tryptophan, W; Tyrosine, Y; Valine, V).

2.4 Conclusions

The aim of the present research was the development of a multitechnique analytical approach for the retrieval and the characterization of high value generating molecules from the lipid and protein fractions of tuna wastes, selecting *Thunnus albacares* as the starting material for extraction and analysis.

In detail, automated sample preparation allowed speeding up the analytical workflow, providing higher method efficiency, increased reproducibility and reducing solvent consumption and costs, compared to the conventional manual protocols. The characterization of the total FA composition, by means of GC-MS/FID, positively supported the elucidation of the native lipid content by UHPLC-MS/MS. The obtained results evidenced a higher content of PUFA-containing TAGs (mainly Dh and Ep) in waste products, compared to the edible part. Tuna waste oil was proved to be a concentrated source of ω-3 containing TAGs and represented a highly useful matrix for the implementation of the LRI lab-constructed database. A suitable analytical approach for the characterization of complex mixture of short and medium-size tryptic peptides deriving from tuna wastes was developed as well, and the use of bioinformatics tools highlighted their potential antimicrobial activity. Such findings pave the way for a promising re-use of tuna by-products as functional food ingredients in the production of nutraceuticals, thus in perfect accordance to a circular economic model.

2.5 References

1. Morseletto P. Targets for a circular economy. Resour. Conserv. Recy. 2020, 153, 104553.
2. United Nations Conference on Sustainable Development. Blue economy concept paper, 2012. https://www.unenvironment.org/resources/report/blue-economy-concept-paper.

3. FAO, Code of conduct for responsible fisheries. Rome: FAO; 2011. http://www.fao.org/3/i1900e/i1900e00.htm.
4. Herpandi N.H., Rosma A., Wan Nadiah W.A., The tuna fishing industry: a new outlook on fish protein hydrolysates. Rev. Food Sci. Saf. 2011, 10, 195-207.
5. Santini A., Tenore G.C., Novellino E. Nutraceuticals: a paradigm of proactive medicine. Eur. J. Pharm. Sci. 2017, 96, 53–61.
6. Oppedisano F., Macrì R., Gliozzi M., Musolino V., Carresi C., Maiuolo J., Bosco F., Nucera S., Zito M.C., Guarnieri L., Scarano F., Nicita C., Coppoletta A.R., Ruga S., Scicchitano M., Mollace R., Palma E., Mollace V. The anti-inflammatory and antioxidant properties of n-3 PUFAs: their role in cardiovascular protection. Biomedicines 2020, 8, 306.
7. Halim N.R.A., Yusof H.M., Sarbon N.M., Functional and bioactive properties of fish protein hydolysates and peptides: a comprehensive review. Trends Food Sci. Technol. 2016, 51, 24-33.
8. Nguyen T.M.H., Protein and lipid recovery from tuna head using industrial protease. J. Sci. Devel. 2013, 11, 1150-1158.
9. Nawaz A., Lia E., Irshad S., Xiong Z., Xiong H., Shahbaz H.M., Siddiqueg F., Valorization of fisheries by-products: challenges and technical concerns to food industry. Trends Food Sci.Technol. 2020, 99, 34-43.
10. Araujo J., Sica P., Costa C., Márquez M.C., Enzymatic hydrolysis of fish waste as an alternative to produce high value-added products. Waste Biomass Valor. 2020. DOI: https://doi.org/10.1007/s12649-020-01029-x.
11. Hsu K.C., Purification of antioxidative peptides prepared from enzymatic hydrolysates of tuna dark muscle by-product. Food Chem. 2010, 122, 42-48.
12. Sanmartín E., Arboleya J.C., Iloro I., Escuredo K., Elortza F., Moreno F.J., Proteomic analysis of processing by-products from canned and fresh tuna: identification of potentially functional food proteins. Food Chem. 2012, 134, 1211-1219.
13. Parvathy U., Binsi P.K., Visnuvinayagam S., Zynudheen A.A., Ninan G., Ravishankar C.N. Functional peptides from yellowfin tuna (*Thunnus albacares*): characterisation and storage stability assessment. Indian J. Fish. 2020, 67, 69-79.
14. Saliu F., Magoni C., Lasagni M., Della Pergola R. Labra M., Multi-analytical characterizationof perigonadal fat in bluefin tuna: from waste to marine lipid source. J. Sci. Food Agric. 2019, 99, 4571-4579.
15. de Oliveira D.A.S.B., Licodiedoff S., FurigoJr A., Ninow J.L., Bork J.A., Podestá R., Block J.M., Waszczynsky N., Enzymatic extraction of oil from yellowfin tuna (*thunnus albacares*) by-products: a comparison with other extraction methods. Int. J. Food Sci. Technol. 2017, 52, 699–705.
16. Nazir N., Diana A., Sayuti K., Physicochemical and fatty acid profile of fish oil from head of tuna (*thunnusalbacares*) extracted from various extraction method. Int. J. Adv. Sci. Eng. Inf. Technol. 2017, 7, 709-715.

17. Peng S., Chen C., Shi Z., Wang L., Amino acid and fatty acid composition of the muscle tissue of Yellowfin Tuna (*Thunnus albacares*) and Bigeye Tuna (*Thunnus obesus*). J. Food Nutr. Res. 2013, 1, 42-45.
18. Dhurmeea Z., Pethybridge H., Appadoo C., Bodin N., Lipid and fatty acid dynamics in maturefemale albacore tuna (*Thunnus alalunga*) in the western Indian Ocean. PLoS ONE. 2018, 13, e0194558.
19. Truzzi C., Annibaldi A., Illuminati S., Antonucci M., Api M., Scarponi G., Lombardo F., Pignalosa P., Carnevali O., Characterization of the Fatty Acid Composition in Cultivated Atlantic Bluefin Tuna (*Thunnus thynnus L.*) Muscle by Gas Chromatography-Mass Spectrometry. Anal.Lett. 2018, 51, 2981-2993.
20. Medina I., Aubourg S.P., Pérez Martín R., Composition of phospholipids of white muscle of six tuna species. Lipids 1995, 30, 1127-1135.
21. Tranchida P.Q., Giannino A., Mondello M., Sciarrone D., Dugo P., Dugo G., Mondello L., Elucidation of fatty acid profiles in vegetable oils exploiting group-type patterning and enhanced sensitivity of comprehensive two-dimensional gas chromatography. J. Sep.Sci. 2008, 31, 1797-1802.
22. Dugo P., Beccaria M., Fawzy N., Donato P., Cacciola F., Mondello L., Mass spectrometric elucidation of triacylglycerol content of Brevoortiatyrannus (menhaden) oil using non-aqueous reversed-phase liquid chromatography under ultra high pressure conditions. J. Chromatogr. A 2012, 1259, 227-236.
23. Beccaria M., Sullini G., Cacciola F., Donato P., Dugo P., Mondello L., High performance characterization of triacylglycerols in milk and milk-related samples by liquid chromatography and mass spectrometry. J. Chromatogr. A 2014, 1360, 172-187.
24. Rigano F., Oteri M., Russo M., Dugo P., Mondello L., Proposal of a linear retention index system for improving identification reliability of triacylglycerol profiles in different lipid samples by liquid chromatography methods. Anal.Chem. 2018, 90, 3313-3320.
25. Rigano F., Oteri M., Micalizzi G., Mangraviti D., Dugo P., Mondello L., Lipid profile of fish species by liquid chromatography coupled to mass spectrometry and a novel linear retention index database. J. Sep. Sci., 2020, 43, 1773-1780.
26. Donnarumma D., Golfieri G., Brier S., Castagnini M., Veggi D., Bottomley M.J., Delany I., Norais N., Neisseria meningitis GNA1030 is a ubiquinone-8 binding protein. FASEB J. 2015, 29, 2260-2267.
27. Amerighi F., Valeri M., Donnarumma D., Maccari S., Moschioni M., Taddei A., Lapazio L., Pansegrau W., Buccato S., De Angelis G., Ruggiero P., Masignani V., Soriani M., Pezzicoli A., Identification of a monoclonal antibody against pneumococcal pilus 1 ancillary protein impairing bacterial adhesion to human epithelial cells. J. Infect. Dis. 2016, 213, 516-522.
28. Donato P., Dugo P., Cacciola F., Dugo G., Mondello L., High peak capacity separation of peptides through the serial connection of LC columns under high temperature. J. Sep.Sci. 2009, 32, 1129-1136.

29. Donato P., Cacciola F., Sommella E., Fanali C., Dugo L., Dachà M., Campiglia P., Novellino E., Dugo P., Mondello L., Online comprehensive RPLC × RPLC with mass spectrometry detection for the analysis of proteome samples. Anal.Chem. 2011, 83, 2485–2491.
30. Micalizzi. G., Ragosta. E., Farnetti. S., Dugo P., Tranchida P.Q., Mondello L., Rigano F., Rapid and miniaturized qualitative and quantitative gas chromatography profiling of human blood total fatty acids. Anal. Bioanal.Chem. 2020, 412, 2327-2337.
31. Folch J., Lees M., Sloane-Stanley G.H. A Simple Method for the Isolation and Purification of Total Lipids from Animal Tissues. J. Biol. Chem. 1957, 226, 497-509.
32. Bligh E.G., Dyer W.J., A rapid method of total lipid extraction and purification. Can. J. Biochem. Physiol. 1959, 37, 911-917.
33. Kristinsson H.G., Lanier T.C., Halldorsdottir S.M., Geirsdottir M., Park J.W., Fish Protein Isolate by pH Shift., in: Park J. W. (3rd Ed). Surimi and surimi sea food. Taylor and Francis Group. Boca Raton 2014, 169-188.
34. Shaviklo A.R., Rezapanah S., Motamedzadegan A., Damavandi-Kamali N., Mozafari H. Optimum conditions for protein extraction from tuna processing by-products using isoelectric solubilization and precipitation processes. Iran. J. Fish.Sci., 2017, 16, 774-792.
35. Rigano F., Oteri M., Russo M., Dugo P., Mondello L. Proposal of a Linear Retention Index System for Improving Identification Reliability of Triacylglycerol Profiles in Lipid Samples by Liquid Chromatography Methods, Anal. Chem. 2018, 90, 3313-3320.
36. Sud M., Fahy E., Cotter D., Brown A., Dennis E., Glass C., Murphy R., Raetz C., Russell D., Subramaniam S., LMSD: LIPID MAPS® structure database. Nucleic Acids Research 2006, 35, D527-532.
37. Joseph S., Karnik S., Nilawe P., Jayaraman V.K., Idicula-Thomas S., ClassAMP: a prediction tool for classification of antimicrobial peptides. IEEE/ACM Trans.Comput. Biol.Bioinform.2012, 9, 1535-1538.
38. Organisation for Economic Cooperation and Development (OECD). Test No. 305: Bioaccumulation in Fish: Aqueous and Dietary Exposure. In OECD Guidelines for Testing of Chemicals; OECD: 2012.
39. Beccaria M., Inferrera V., Rigano F., Gorynskic K., Purcaro G., Pawliszyn J., Dugo P., Mondello L., Highly informative multiclass profiling of lipids by ultra-high performance liquid chromatography – Low resolution (quadrupole)mass spectrometry by using electrospray ionization and atmospheric pressure chemical ionization interfaces. J. Chromatogr. A 2017, 1509, 69–82.
40. Aguennouz M., Beccaria M., Purcaro G., Oteri M., Micalizzi G., Musumesci O., Ciranni A., Di Giorgio R.M., Toscano A., Dugo P., Mondello L., Analysis of lipidprofile in lipidstoragemyopathy, J. Chromatogr. B, 2016, 1029, 157–168.

41. Donato P., Micalizzi G., Oteri M., Rigano F., Sciarrone D., Dugo P., Mondello L., Comprehensive lipid profiling in the mediterranean mussel (*Mytilus galloprovincialis*) using hyphenated and multidimensional chromatography techniques coupled to mass spectrometry detection. Anal. Bioanal.Chem. 2018, 410, 3297–3313.
42. Wongtangtintharn S., Oku H., Iwasaki H., Toda T., Effect of branched-chain fatty acids on fatty acid biosynthesis of human breast cancer cells. J. Nutr. Sci. Vitaminol. 2004, 50, 137-143.
43. Stefanov, I., Baeten, V., Abbas, O., Colman, E., Vlaeminck, B., De Baets, B., & Fievez, V., Analysis of Milk Odd- and Branched-Chain Fatty Acids Using Fourier Transform (FT)-Raman Spectroscopy. J. Agric. Food Chem., 2010, 58, 10804–10811.
44. Cerrato A., Capriotti A.L., Capuano F., Cavaliere C., Montone A.M.I., Montone C.M., Piovesana S., Zenezini Chiozzi R., Laganà A. Identification and antimicrobial activity of medium-sized and short peptides from yellowfin tuna (Thunnus albacares) simulated gastrointestinal digestion. Foods 2020, 9, 1185.
45. Capriotti A.L., Cavaliere C., Foglia P., Piovesana S., Samperi R., Zenezini Chiozzi R., Laganà A. Development of an analytical strategy for the identification of potential bioactive peptides generated by in vitro tryptic digestion of fish muscle proteins. Anal. Bioanal.Chem. 2015, 407, 845–854.
46. Najafian L., Babji A.S. A review of fish-derived antioxidant and antimicrobial peptides: Their production, assessment, and applications Peptides, 2012, 33, 178-185.
47. Feijó Corrêa J.A., Gonçalves Evangelista A., de Melo Nazareth T., Bittencourt Luciano F., Fundamentals on the molecular mechanism of action of antimicrobial peptides Materialia 2019, 8, 100494.

3 Characterization of the lipid composition in hemp (*Cannabis sativa L.*) products by means of gas chromatography and ultra-high performance liquid chromatography coupled to mass spectrometry detection

3.1 Introduction

Cannabis sativa L. is an annual flowering herb native of Central Asia, belonging to the family of *Cannabaceae*. This species is considered one of the most ancient cultivated plants due to its extensive employment as a source of textile fiber (clothing, papermaking, sailmaking) and its use in folk medicine, to treat a wide range of ailments [1]. Nowadays its popularity is mostly related to the "recreational" use. In fact, according to the World Health Organization, Cannabis is the most commonly cultivated, trafficked, and abused illicit drug worldwide [2].

On the basis of their use, Cannabis products are generally referred as: "non-medical, retail or recreational cannabis"; "medical cannabis", when employed for therapeutic purposes; "industrial hemp", when used as starting material in the food, cosmetic, construction, biocomposite and textile fields. However, the active principles responsible for the psychotropic effects (e.g. Δ9-tetrahydrocannabinol, THC) are predominantly located in female flowers and resin-producing trichomes, which show concentration of THC as high as 20%.

Dried stems are usually characterized by amounts of psychotropic substances lower than 0.3%; instead, roots and seeds do not contain THC [3]. Nevertheless, roots and seed-derived products can be view as a valuable source of bioactive molecules and raw material for industrial purposes.

The term hemp refers to *Cannabis sativa* cultivars grown for industrial purposes, characterized by low levels of THC; particularly varieties showing a THC content <0.2% can be freely used in Europe (EU Regulation 1307/2013) [4]. The EU Plant variety database of the European Commission contains the hemp varieties (> 70) registered as agricultural species-varieties which can be cultivated in EU; among them Futura 75, Uso 31 and Finola are the most used cultivars for industrial purposes [5].

Cannabis sativa is considered a multipurpose, sustainable, and low environmental impact crop due to the reduced consume of water, the fast grow (requiring relatively low herbicide treatments), the extensive biomass production, the high quality of raw materials

and the impressive seed oil content (as high as 35%) [1,6]. Among the different parts of the plant which can be conveniently used for industrial and economic purposes, hemp seeds have shown a favorable composition in ω-6 and ω-3 PUFA, especially linoleic acid and α- and γ-linolenic acids, high-quality and easily digestible proteins rich in essential aminoacids (e.g. edestin and albumin), vitamins, especially tocopherols, antioxidant molecules (e.g. polyphenols) and minerals (e.g. potassium, magnesium and calcium) [7]. In the scientific literature, hemp seed oil has been reported to have an impressive seed oil content in unsaturated FAs, which can be as high as 90%; in detail, hemp-derived products are rich in linoleic acid (L, 18:2n6) and α-linolenic acid (Ln, 18:3n3) defined as essential fatty acids (EFAs) [8].

Moreover, hemp seed oil is reported to contain remarkable amounts of stearidonic acid (C18:4n-3, defined as SDA) commonly found in marine organisms and γ-linolenic acid (often named GLA, C18:3n-6), which has been found in primrose, borage and black currant oils. Noticeably, these two FAs are not widespread in conventional consumed edible oils. Lastly, a favorable ω-6/ω-3 ratio, around 3:1, has been reported for hempseed oil making this product highly beneficial for human consumption [9].

The considerable content in ω-6 and ω-3 PUFA represents a key factor in determining the great value of the species; in fact, as is well known, these components are involved in many biological pathways and positively affect human health, by contributing to the regulation of human metabolic activities and by preventing cardiovascular diseases [10]. For these reasons, hemp seeds and their derived products, such as oil and flour, may represent a promising source of high value molecules for the potential daily use as dietary supplements and for the production of nutraceuticals.

Diverse studies aimed at the determination of the lipid profile of *Cannabis sativa* products, concerning the composition in fatty acids (FAs) [11-14]. Concerning the analytical approaches employed for such purposes, FAs are generally investigated, in the form of fatty acid methyl esters (FAMEs) derivatives, by gas chromatography (GC) coupled to flame ionization detection (FID) and mass spectrometry (MS), for quantitative and qualitative purposes, respectively [15].

On the other hand, only a limited number of researches have focused on the characterization of complex lipids such as triacylglycerols (TAGs) in this species [16-18]. Nevertheless, TAGs represent the most abundant constituents of plant seed oils and

other derived products [19]; furthermore, the study of lipid species in their native form is proved to be crucial to obtain additional information on the role of lipids and on FAs arrangement into each lipid species. Reversed phase liquid chromatography (RP-LC) is the most suitable separation approach for TAG analysis, since hydrophobic interactions between the target analytes and the stationary phase, usually an octadecylsilica (C18) particles packed column, provide a separation of the mixture which directly depend on the TAG partition number (PN), calculated from the equation PN = CN - 2DB (carbon chain length, CN and double bonds number, DB) [20]. Nevertheless, TAG separation may represent a challenging analytical task, especially when dealing with complex mixtures in which numerous species show the same PN values and hence, a similar chromatographic behavior.

As a result, analytical methods providing high chromatographic efficiency, suitable for a large range of lipid samples and aiming to simplifying the identification procedure, are highly demanded especially in LC.

This research was aimed at the evaluation of the lipid composition of different hemp-derived products (seed oil, seed flour and seed flour waste) by means of GC-MS/FID and LC-MS analytical methods. Moreover, a recently introduced linear retention index (LRI) approach in LC [21,22] coupled to MS, was employed to achieve a reliable TAG identification in the samples investigated. The reference homologue series used for the calculation of the LC retention indices consisted of a mixture of odd carbon number TAGs (C9C9C9-C19C19C19) covering the full elution range of target analytes contained in the samples of interest.

The identification process was based on a dual filter approach, specifically concerning the information obtained from mass spectra and the retention behavior of analytes. For the latter purpose, LRI were calculated, and the obtained values were compared to an LRI TAGs labory-constructed database, considering a tolerance window of ± 15. For some components, it was possible to gain additional confirmation by using the spectral library search, achieved by recording the mass spectra of commercial standards.

The obtained results confirmed the importance of hemp-derived products for the nutraceutical usage, due to the high content in ω-6/ω-3 PUFAs and improved the knowledge about the main FA arrangements in lipids in their native form.

3.2 Material and methods

3.2.1 Reagents

Acetonitrile, 2-propanol, water (LC-MS grade), *n*-heptane, (HPLC grade), *n*-hexane, methanol (CH_3OH) (reagent grade) and potassium hydroxide (KOH) were purchased from Merck Life Science (Darmstadt, Germany). Trinonanoin (C9C9C9), triundecanoin, (C11C11C11), tritridecanoin (C13C13C13), tripentadecanoin (C15C15C15), triheptadecanoin (C17C17C17) and trinonadecanoin (C19C19C19) standards and a 1000 µg/mL C4-C24 Even Carbon Saturated FAMEs mixture in *n*-hexane were also purchased from Merck Life Science (Darmstadt, Germany). A standard mixture of the odd carbon number triacylglycerols in 2-propanol was prepared at the same concentration of the FAME mixture and the obtained solutions were employed for LRI calculation, for the LC and GC data.

3.2.2 Samples and sample preparation

Hemp seed-derived products were received by different companies based in Italy. In detail, four hemp seed oils (samples 1-4), three hemp seed flours (samples 5-7) and one hemp seed flour waste (sample 8) were investigated in this research.

Hemp seed oils were diluted in 2-propanol (1000 ppm) prior to LC-MS analysis, while seed flour and seed flour waste lipids were extracted by solvent maceration. Briefly, 50 mL of *n*-hexane were added to 40 g of flour and allowed to stand for 40 min. The hexane phase was collected apart and evaporated by rotary evaporator to obtain hemp seed flour oil; a 1000 ppm solution in 2-propanol was prepared for LC-MS analysis.

For the investigation of the FA composition, all the samples were subjected to a derivatization procedure to convert intact lipids into the corresponding FAMEs, prior to GC-MS/FID analysis. Briefly, 200 µL of KOH in methanol (2M) were added to 100 mg of oil. For FAMEs extraction, 2 mL of *n*-heptane were added to the mixture and after agitation the *n*-heptane upper layer was collected for GC-MS/FID analysis.

3.2.3 Instruments and analytical conditions

GC-MS analyses were carried out on a GCMS-QP2020 instrument (Shimadzu, Duisburg, Germany) equipped with a split-splitless injector (280 °C) and an AOC-20i autosampler.

Separations were performed on a SLB-IL60 30 m × 0.25 mm id, 0.20 μm *d.f.* medium-polarity ionic liquid (IL) capillary column (Merck Life Science) and the temperature program was set as follow: 50 °C to 280 °C at 3.0 °C/min. The injection volume was 0.5 μL, with a split ratio of 1:50. Helium was employed as carrier gas, at an average linear velocity of 30 cm s^{-1} and an initial inlet pressure of 26.6 kPa.

The following MS parameters were employed: mass range, 40–550 amu; ion source temperature, 220 °C; interface temperature, 250 °C; event time, 0.20 s. Data were acquired and processed by using GCMSsolution ver. 4.50 software (Shimadzu Europa, Duisburg, Germany), while identification was performed by using LIPIDS Mass Spectral Library ver. 1.0 (Shimadzu Europa, Duisburg, Germany) and a dedicated LRI FAME database (constructed on SLB-IL60 column, employing C4-C24 FAMEs as references homologue series). Peak assignment was based on a MS spectral similarity higher than 85% and a ± 10 LRI tolerance window.

GC-FID analyses were carried out on a GC-2010 instrument (Shimadzu, Duisburg, Germany) equipped with a split-splitless injector, an AOC-20i/s auto-sampler and a FID detector. The analytical conditions in terms of GC column, temperature program and carrier gas were the same as for the GC-MS analyses. The FID parameters were: temperature, 280 °C; sampling rate, 40 ms; gas flow rate was 40 mL min^{-1}, 30 mL min^{-1} and 400 mL min^{-1} for H_2, make-up gas (N_2) and air, respectively. Data were acquired and processed using the LabSolution ver. 5.92 software (Shimadzu, Duisburg, Germany). Analyses were performed in triplicates.

LC-MS analyses were carried out on a Nexera UHPLC system coupled to a single quadrupole LCMS-2020 spectrometer through an APCI ionization interface (Shimadzu Europa, Duisburg, Germany). The chromatographic system consisted of a CBM-20A controller, two LC-30AD dual-plunger parallel-flow pumps,a DGU-20A5R degasser, a CTO-20AC column oven, and SIL-30AC autosampler.

Separations were performed on two serially coupled Ascentis Express C18 10 cm x 2.1 mm, 2.7 μm *d.p.* columns (Merck Life Science, Darmstadt, Germany). Mobile phases were acetonitrile (A) and 2-propanol (B). The gradient program was: 0-105 min, 0-50% B, held for 5 min. The flow rate was 0.5 mL/min, the oven temperature was set at 35 °C and the injection volume was 10 μL.

The APCI interface was employed both in positive (+) and negative (-) ionization modes; the following MS parameters were used: interface temperature, 450 °C; DL temperature, 250 °C; heat block temperature, 300 °C; nebulizing gas flow (N_2), 1.5 L/min; drying gas, 5 L/min; acquisition range, 250-1200 *m/z* (+) and 100-1200 *m/z* (-).

Data were acquired and processed by using LabSolution ver. 5.95 software (Shimadzu Europa, Duisburg, Germany).

LRI were calculated by employing the mixture of odd carbon number TAGs as references homologue series, according to the following equation [22]:

$$LRI = 100\,[z + 6\frac{t_{Ri} - t_{Rz}}{t_{R(z+6)} - t_{Rz}}]$$

Equation 3.1

where z represents a value equal to the PN of the standard TAG eluting immediately before the analyte; t_{Ri} is the analyte retention time, t_{Rz} and $t_{R(z+6)}$ are the retention times of the reference compound eluting immediately before and after the analyte, respectively; 6 represents the distance in terms of PN unit between two consecutively eluted standards of the homologue series. A previous laboratory-constructed LRI database was used to identify TAGs, selecting an LRI tolerance window of ±15.

3.3 Results and Discussion

3.3.1 Fatty Acids

In this research the FA composition of hemp seed oil and hemp seed flour oil was investigated by GC-MS/FID analysis of FAMEs derivatives. By way of illustration, the GC-FID profile obtained for hemp seed oil (sample 4) is reported in Figure 3.1 (compound identification by quadrupole MS); in fact, all the samples showed almost identical qualitative FA profiles. In detail, peak at t_R 47.7 min, later identified by GC-MS as linoleic acid (C18:2n6, L) showed the higher intensity, being the most represented FA in hemp-derived products, as previously reported in the literature. Also for the peaks eluted at t_R 46.7 and 48.6 min, later identified as oleic acid (C18:1n9, O) and α linolenic acid (C18:3n3, Ln), high signal intensities were observed for the investigated samples.

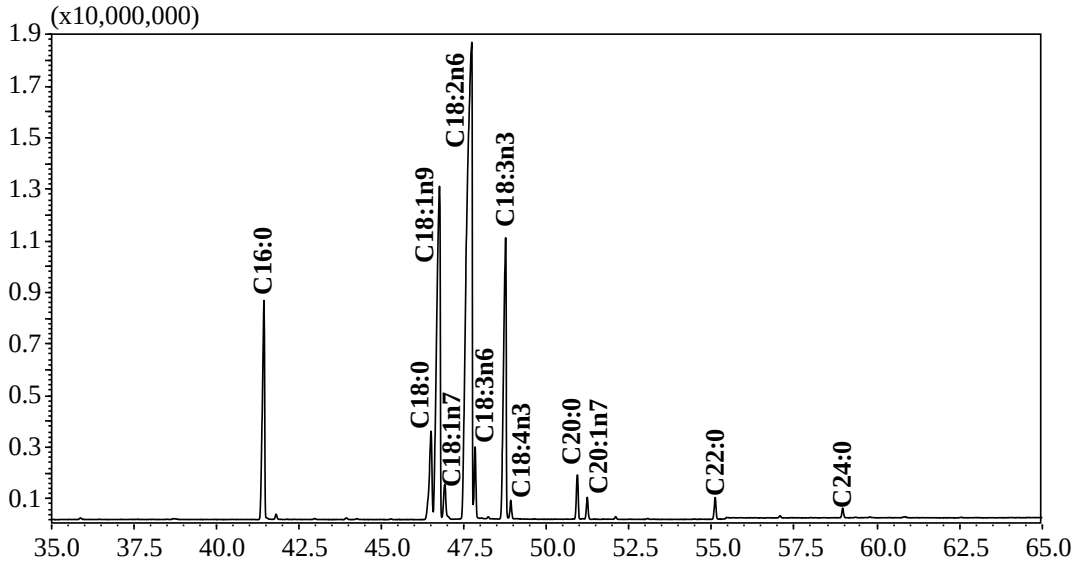

Figure 3.1 GC-FID profile of FAMEs in hemp seed oil (sample 4); peak identification was performed by Q MS.

The qualitative and quantitative results obtained for hemp-derived products are illustrated in Table 3.1. The identification was based on minimum MS spectral similarity (85%) and the comparison between experimental and theoretical LRI values. A total of 31 FAs were positively identified; a satisfactory match between the experimental MS spectra and the library was obtained, with similarity values >90% for all the compounds (only one exception for Me. C20:3n3). Furthermore, the results were confirmed by using a second filter for library search, consisting in a tolerance window of ±10 units between the experimental and theoretical LRI values; even in this case a satisfactory ΔLRI was obtained for all the identified components, with an average ΔLRI of 2.4. In detail, the most significant differences between the investigated samples were observed for the C18 FAs, which were found to be the principal components in both hemp seed oils and flours. Linoleic acid (C18:2n6) was confirmed to be the most abundant species, ranging from 53.26% (sample 8) to 56.66% (sample 5); in addition, it was found a C18:2n6/C18:3n3 ratio around 4:1, being the amount of C18:3n3 between 11.55 (sample 8) and 13.84% (sample 1). According to these results, C18:2n6 and C18:3n3 made up most of the PUFA content.

Table 3.1 Identified FAMEs in hemp derived products. For each compound, experimental (exp) and theoretical (theor) LRI values, MS spectral similarity (%), and the relative content (%) are also reported.

					Hemp seed oil				Hemp seed flour			
#	Compound	LRI_{exp}	LRI_{theor}	MS % similarity	Sample 1	Sample 2	Sample 3	Sample 4	Sample 5	Sample 6	Sample 7	Sample 8
1	Me. C14:0	1401	1400	96	0.03 ± 0.00	0.04 ± 0.01	0.04 ± 0.00	0.04 ± 0.00	0.04 ± 0.00	0.05 ± 0.00	0.05 ± 0.01	0.05 ± 0.00
2	Me. C15:0	1503	1500	95	0.02 ± 0.00	0.02 ± 0.01	0.03 ± 0.00	0.03 ± 0.00	0.02 ± 0.01	0.03 ± 0.01	0.04 ± 0.00	0.04 ± 0.01
3	Me. C16:0	1603	1600	97	6.76 ± 0.01	6.35 ± 0.03	7.01 ± 0.01	7.31 ± 0.00	7.13 ± 0.03	6.94 ± 0.01	6.86 ± 0.00	7.53 ± 0.01
4	Me. C16:1n7	1618	1609	97	0.11 ± 0.00	0.03 ± 0.00	0.11 ± 0.00	0.12 ± 0.00	0.12 ± 0.00	0.11 ± 0.00	0.11 ± 0.00	0.12 ± 0.00
5	Me. C16:2n4	1665	1663	90	0.02 ± 0.00	0.09 ± 0.00	0.02 ± 0.00	0.02 ± 0.00	0.02 ± 0.00	0.01 ± 0.00	0.02 ± 0.01	0.02 ± 0.00
6	Me. C17:0	1703	1700	95	0.04 ± 0.00	0.05 ± 0.01	0.04 ± 0.00	0.04 ± 0.00	0.05 ± 0.00	0.04 ± 0.00	0.05 ± 0.00	0.05 ± 0.00
7	Me. C17:1n7	1716	1713	94	0.02± 0.00	0.03 ± 0.00	0.03 ± 0.00	0.02 ± 0.00	0.03 ± 0.00	0.03 ± 0.01	0.03 ± 0.00	0.03 ± 0.00
8	Me. C18:0	1806	1800	97	2.77 ± 0.01	2.78 ± 0.01	2.82 ± 0.01	2.97 ± 0.00	2.73 ± 0.01	2.96 ± 0.01	2.96 ± 0.01	3.04 ± 0.01
9	Me. C18:1n9	1817	1810	94	13.84 ± 0.00	17.00 ± 0.04	14.88 ± 0.05	18.29 ± 0.02	13.76 ± 0.07	16.99 ± 0.01	17.07 ± 0.01	18.39 ± 0.00
10	Me. C18:1n7	1824	1826	96	0.98 ± 0.01	0.69 ± 0.01	0.98 ± 0.00	1.01 ± 0.01	1.02 ± 0.00	0.94 ± 0.02	0.96 ± 0.01	1.01 ± 0.00
11	Me. C18:2n6	1860	1851	98	56.06 ± 0.07	56.48 ± 0.28	55.61 ± 0.17	53.48 ± 0.17	56.66 ± 0.18	54.22 ± 0.42	54.44 ± 0.24	53.26 ± 0.32
12	Me. C18:3n6	1865	1858	96	2.57 ± 0.03	1.49 ± 0.00	1.98 ± 0.17	1.78 ± 0.18	2.87 ± 0.18	2.27 ± 0.12	2.20 ± 0.15	2.04 ± 0.14
13	Me. C18:3n3 (9Z.12E.15E)	1873	1875	92	0.03 ± 0.00	0.02 ± 0.00	0.02 ± 0.00	0.02 ± 0.00	0.03 ± 0.01	0.02 ± 0.00	0.03 ± 0.01	0.01 ± 0.00
14	Me. C18:3n3 (9Z.12E.15Z)	1883	1880	96	0.05 ± 0.00	0.04 ± 0.00	0.05 ± 0.00	0.05 ± 0.00	0.04 ± 0.00	0.04 ± 0.00	0.03 ± 0.02	0.04 ± 0.00
15	Me. C18:3n3 (9Z.12Z.15Z)	1906	1902	98	13.84 ± 0.00	12.63 ± 0.06	13.75 ± 0.04	12.12 ± 0.01	12.28 ± 0.13	12.51 ± 0.15	12.37 ± 0.07	11.55 ± 0.09
16	Me. C18:4n3	1913	1909	97	0.75 ± 0.00	0.40 ± 0.03	0.61 ± 0.01	0.44 ± 0.00	0.78 ± 0.07	0.61 ± 0.08	0.58 ± 0.06	0.52 ± 0.08
17	Me. C19:2n6	1945	1952	90	0.01 ± 0.00	0.01 ± 0.00	0.02 ± 0.00	0.01 ± 0.00	0.01 ± 0.00	0.03 ± 0.01	0.01 ± 0.00	0.01 ± 0.00

18	Me. C20:0	2002	2000	96	0.89 ± 0.00	0.72 ± 0.00	0.90 ± 0.01	0.90± 0.00	0.95 ± 0.01	0.85 ± 0.01	0.87 ± 0.01	0.89 ± 0.01
19	Me. C20:1n9	2009	2008	92	0.02 ± 0.00	0.02 ± 0.00	0.02 ± 0.00	0.02 ± 0.00	0.02 ± 0.01	0.04 ± 0.00	0.03 ± 0.01	0.03 ± 0.02
20	Me. C20:1n7	2016	2015	98	0.40 ± 0.00	0.33 ± 0.01	0.43 ± 0.00	0.44 ± 0.00	0.44 ± 0.00	0.44 ± 0.00	0.44 ± 0.00	0.47 ± 0.00
21	Me. C20:1n6	2025		90	0.02 ± 0.00	0.01 ± 0.00	0.02 ± 0.00	0.02 ± 0.00	0.02 ± 0.01	0.01 ± 0.00	0.01 ± 0.00	0.01 ± 0.00
22	Me. C20:2n6	2057	2055	96	0.06 ± 0.00	0.04 ± 0.00	0.06 ± 0.00	0.06 ± 0.00	0.06 ± 0.00	0.05 ± 0.00	0.05 ± 0.00	0.06 ± 0.00
23	Me. C21:0	2103	2102	90	0.02 ± 0.00	0.03 ± 0.02	0.02 ± 0.00	0.02 ± 0.00	0.03 ± 0.01	0.03 ± 0.01	0.02 ± 0.01	0.02 ± 0.00
24	Me. C20:3n3	2110	2109	89	0.01 ± 0.00	0.01 ± 0.00	0.01 ± 0.00	0.01 ± 0.00	0.02 ± 0.00	0.02 ± 0.01	0.01 ± 0.00	0.01 ± 0.00
25	Me. C22:0	2201	2200	91	0.37 ± 0.00	0.31 ± 0.00	0.39 ± 0.00	0.42 ± 0.00	0.47 ± 0.12	0.40 ± 0.00	0.41 ± 0.00	0.45 ± 0.01
26	Me. C22:1n9	2219	2217	91	0.03 ± 0.00	0.02 ± 0.00	0.02 ± 0.00	0.03 ± 0.00	0.03 ± 0.01	0.04 ± 0.00	0.04 ± 0.00	0.07 ± 0.00
27	Me. C23:0	2303	2301	95	0.04 ± 0.00	0.03 ± 0.01	0.04 ± 0.00	0.05 ± 0.00	0.04 ± 0.00	0.04 ± 0.00	0.04 ± 0.00	0.05 ± 0.00
28	Me. C24:0	2401	2400	93	0.16 ± 0.00	0.13 ± 0.01	0.18 ± 0.00	0.19 ± 0.00	0.19 ± 0.01	0.18 ± 0.00	0.19 ± 0.00	0.22 ± 0.00
29	Me. C24:1n9	2421	2420	90	0.02 ± 0.00	0.02 ± 0.00	0.02 ± 0.00	0.03 ± 0.00	0.03 ± 0.01	0.04 ± 0.01	0.03 ± 0.00	0.03 ± 0.00
30	Me. C25:0		2600	91	0.02 ± 0.00	0.02 ± 0.00	0.02 ± 0.00	0.03 ± 0.01	0.03 ± 0.01	0.02 ± 0.01	0.02 ± 0.00	0.02 ± 0.00
31	Me. C26:0		2600	91	0.03 ± 0.00	0.03 ± 0.01	0.03 ± 0.00	0.03 ± 0.00	0.04 ± 0.01	0.03 ± 0.01	0.03 ± 0.00	0.02 ± 0.00

High amounts of oleic (C18:1n9) and palmitic acid (C16:0) were also found in hemp seed derived products, ranging from 13.76 to 18.39% and 6.35 to 7.53%, respectively. All the samples reported a consistent GLA (18:3n6, Ln) amount, for which a high content variability was observed between samples (1.49 – 2.87%). SDA (C18:4n-3, St) was also found in hemp seed oil and flour in a range between 0.40 to 0.78%.

As a result, the contemporary presence of both the α- and ɣ-linolenic acids, the stearidonic acid content and the high amount in linoleic acid, make hemp seed-derived products high nutraceutical interest matrices. Remarkably, these samples showed a peculiar FA composition, which totally differs from the vegetable oils of common consumption and their derived food products.

As can be observed in Table 3.1, SFAs were found to be poorly present in hemp-derived products, with a percentage content lower than 12% for all the samples; among SFA, C16:0 and stearic acid (C18:0) resulted to be the predominant species. Furthermore, the high percentage of the monounsaturated MUFAs depended almost entirely on C18:1n9, while the overall content of other MUFAs was lower than 2%.

3.3.2 Triacylglycerols

In this research, TAG RP-LC separation was achieved by serially coupling two C18 (10 cm x 2.1 mm, 2.7 μm *d.p.*) narrow-bore columns, allowing the use of reduced operational flow rates (0.5 mL/min) highly compatible to MS detection. The employed analytical conditions were previously optimized [22], affording a satisfactory compromise between analysis time and chromatographic efficiency.

By way of illustration, the LC-MS TAG profiles of hemp seed oil (sample 1) and reference homologue series employed for LRI calculation are depicted in Figure 3.2; the PN values of eluted TAGs are also reported. Considering that in RP-LC, TAGs elute in order of ascending PN values, the first region of the chromatograms included PUFA-containing species, while last eluted compounds were long chain saturated or monounsaturated FAs-containing TAGs. The position of the chromatographic peaks with respect to the standard odd carbon number TAGs within the elution window, immediately highlighted the higher abundance of TAGs having PN values in the range of 38-46, as subsequently confirmed by the identification. Among the ionization techniques commonly employed in LC-MS, APCI reveal to be the most useful in TAG analysis due

to its ability in providing structural information deriving from TAG protonated species $[M+H]^+$ and fragment ions originated from the loss of the fatty acyl groups esterified to the glycerol moiety [23].

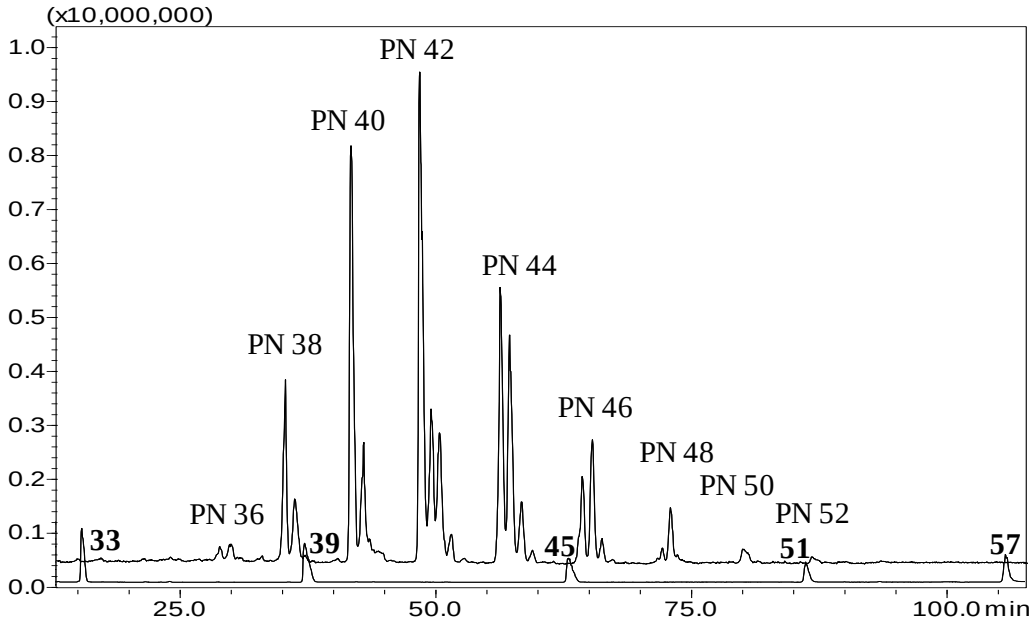

Figure 3.2 LC-MS TAG profiles of hemp seed oil (sample 1) and of the odd carbon number TAGs homologue series (PN values highlighted).

Identification was performed by combining the information deriving from the positive ion APCI-MS spectra of the individual TAGs and the retention behavior of the analytes; in detail, the $[M+H]^+$ protonated species were required for the determination of the molecular mass of each TAG, while the fragment ions were used for the determination of the FAs composition of each species. Furthermore, the experimental LRI values for each compound were calculated from Equation 3.1 and compared to the LRI theorical values from the labory-constructed database. Figure 3.3 (panel A and B) reports, as an example, the MS spectra of the compound OLLn (consisting of oleic, linoleic and α-linolenic acids). The *m/z* 879 represents the $[M+H]^+$ ion of the TAG, while *m/z* 597, 599 and 601 are the diacylglycerol-like fragment ions deriving from the loss of oleic, linoleic and linolenic acid respectively; also monoacylglycerol-like fragment ions were observed,

showing *m/z* values of 335, 337 and 339. For the TAG OLLn the average experimental LRI value was equal to 4191, which compared to the theoretical value of 4192 showed a Δ of 1 (applied tolerance window of ±15).

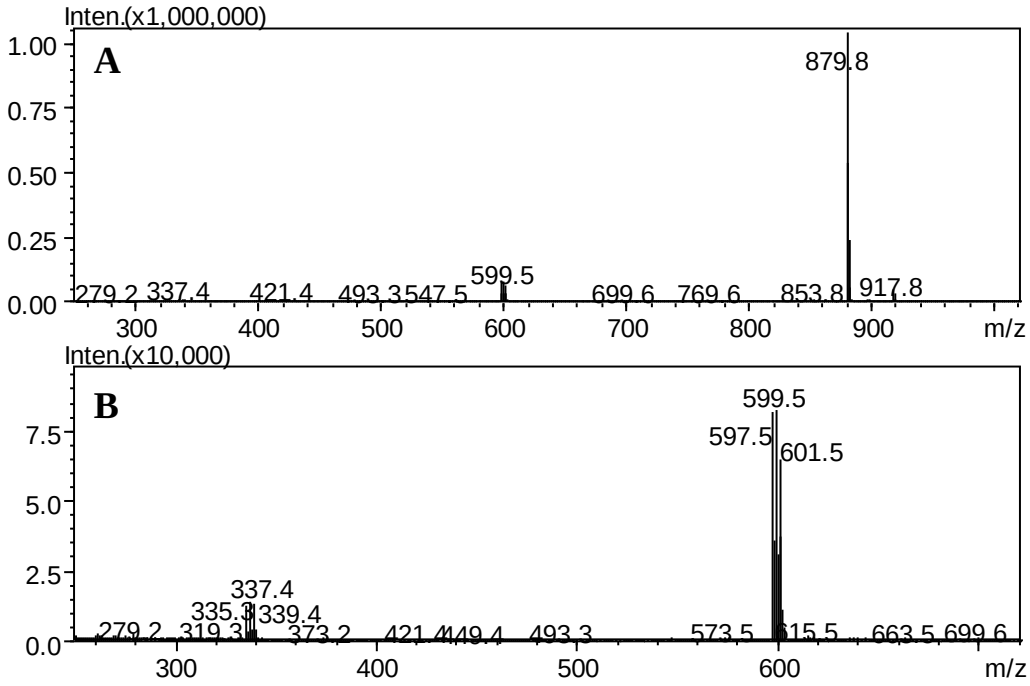

Figure 3.3 A) MS spectrum obtained by APCI (+) for the compound OLLn. B) Enlargement of the lower m/z region.

In Figure 3.4 is illustrated the comparison between the LC-MS chromatograms of hemp seed oil (sample 1) and hemp seed flour (sample 7). The investigated samples showed almost identical chromatographic profiles, with a slightly lower signal intensity in hemp seed flour compared to the oil. As can be clearly observed by the overlapping of the two total ion current chromatograms, sample 1 (hemp seed oil) showed higher peak intensities for LnLLn + γLnLLn, γLnγLnL + LLSt, LLLn + LLγLn + LnOLn, OLSt + LnLnP + LnOγLn, LLL and OLγLn + LnLP compared to sample 7 (hemp seed flour). TAG species were found to be distributed in different regions according to their PN values, ranging from 36 to 54; compounds having PN values of 54 were detected only in hemp seed oils.

In Table 3.2 are reported 62 species identified in the investigated samples, according to their PN values; the experimental and theoretical LRI values with their difference (ΔLRI) and the relative weight concentrations are also shown. For the latter case the coefficient of variation was lower than 20% for all the compounds.

The TAG profile for both hemp seed oils and hemp flour products resulted to be in agreement with the FAMEs profile obtained by GC-FID/MS; this is clearly evident from the TAG composition, which is directly related to the relative abundance of the single FAs.

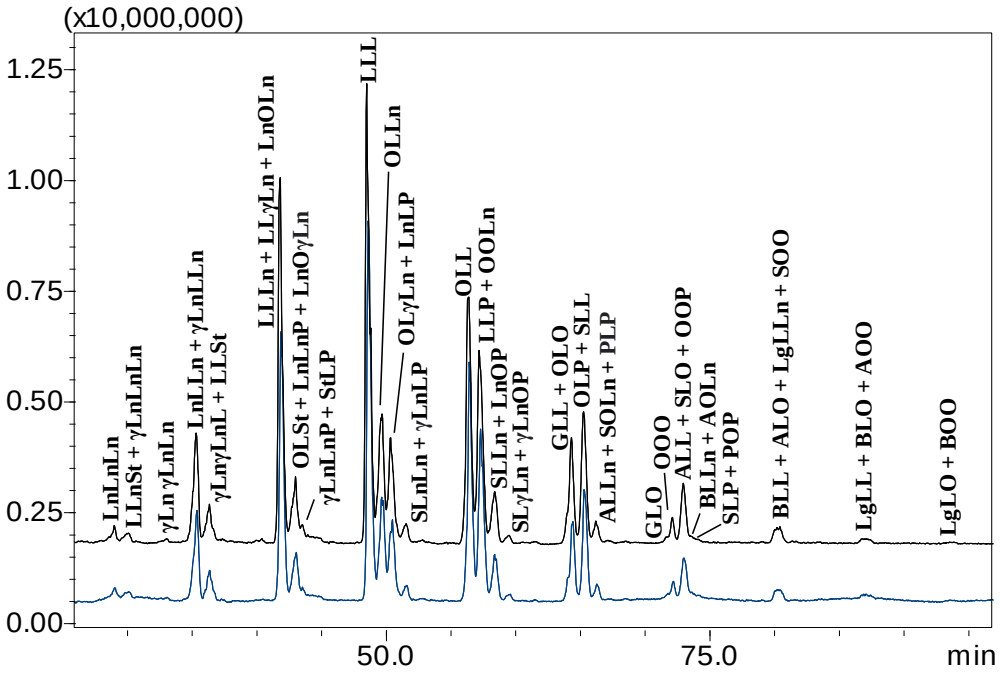

Figure 3.4 Comparison between LC-MS TAG profile of hemp seed oil (top, black, sample 1) and hemp seed flour (bottom, blue, sample 3); expansion of the TAG region.

As an example, the most abundant FA in all the analyzed samples was linoleic acid (L, C18:2n6) and the high amount of this component resulted in the predominant presence of L-containing TAGs, being LLL the most represented species in hemp seed derived products. For this compound, a discrete content variability between hemp seed oil and

flour was also observed, being LLL comprised between 18.12 and 19.34% in the first case and ranging from 16.22 and 17.84% for the latter.

Other relatively abundant TAGs found in hemp-derived products were LLLn, LLγLn, LnOLn, OLL, LLP and OOLn, reflecting the high presence of linolenic (Ln, C18:3n3 and C18:3n6, α and γ respectively), oleic (O, C18:1) and palmitic (P, C16:0) acids.

In Figure 3.5 are reported the histograms in which the identified compounds found in hemp seed oil and flour are plotted against their relative weight concentration. The bar graphs make easier and more immediate the comparison between the hemp seed derived products. In particular in panel A are reported all the identified TAGs, while panel B shows the most abundant TAGs in the samples investigated; hence this approach provided a useful fingerprint to discriminate between different hemp seed products.

Table 3.2 Identified components with their PN; experimental and theoretical LRI values and relative weight concentrations (%) are also reported.

					Hemp seed oil				Hemp seed flour			
PN	**Compound***	**LRI_{exp}**	**LRI_{theor}[a]**	**ΔLRI**	**Sample 1**	**Sample 2**	**Sample 3**	**Sample 4**	**Sample 5**	**Sample 6**	**Sample 7**	**Sample 8**
24	LnLn	-	-	-	0.30 ± 0.04	0.12 ± 0.01	0.40 ± 0.01	0.30 ± 0.04	0.87 ± 0.10	0.52 ± 0.04	0.62 ± 0.09	0.24 ± 0.01
26	LLn	-	-	-	0.54 ± 0.06	0.55 ± 0.04	0.87 ± 0.02	0.30 ± 0.03	1.56 ± 0.22	1.52 ± 0.08	1.93 ± 0.23	0.90 ± 0.00
26	OSt	-	-	-	0.10 ± 0.01	0.12 ± 0.02	0.18 ± 0.01	0.09 ± 0.00	0.79 ± 0.14	0.45 ± 0.02	0.66 ± 0.11	0.31 ± 0.04
28	LL	2895	-	-	0.97 ± 0.15	1.20 ± 0.05	1.29 ± 0.13	0.49 ± 0.02	2.84 ± 0.35	2.67 ± 0.10	3.34 ± 0.07	1.73 ± 0.04
28	OLn + LnP	2917	-	-	0.26 ± 0.02	0.30 ± 0.01	0.40 ± 0.05	0.31 ± 0.01	1.22 ± 0.20	0.79 ± 0.09	0.96 ± 0.10	0.70 ± 0.02
30	LO + LP	3100	-	-	0.52 ± 0.10	0.32 ± 0.06	0.49 ± 0.02	0.30 ± 0.01	1.47 ± 0.28	1.08 ± 0.08	1.24 ± 0.15	0.88 ± 0.12
36	LnLnLn	3675	3668	7	0.58 ± 0.02	0.75 ± 0.05	0.73 ± 0.04	0.58 ± 0.01	1.73 ± 0.18	0.57 ± 0.06	0.91 ± 0.16	0.54 ± 0.04
36	LLnSt + γLnLnLn	3703	-	-	0.73 ± 0.05	0.68 ± 0.03	0.73 ± 0.05	0.41 ± 0.08	0.76 ± 0.09	0.52 ± 0.07	0.52 ± 0.06	0.34 ± 0.01
36	γLnγLnLn	3720	-	-	0.07 ± 0.01	0.14 ± 0.02	0.12 ± 0.01	0.18 ± 0.04	-	-	-	-
38	LnLLn + γLnLLn	3845	3830/-	15/-	5.09 ± 0.27	5.00 ± 0.20	5.47 ± 0.16	4.15 ± 0.22	5.07 ± 0.13	4.57 ± 0.26	4.35 ± 0.28	4.5 ± 0.00
38	γLnγLnL + LLSt	3876	3867/3890[b]	9/14	2.73 ± 0.03	1.8 ± 0.00	2.42 ± 0.05	1.56 ± 0.01	3.65 ± 0.15	1.83 ± 0.05	1.88 ± 0.25	1.74 ± 0.04
40	LLLn + LLγLn + LnOLn	4008	3993/3999/4011	15/9/3	15.52 ± 0.49	13.63 ± 0.49	15.12 ± 0.53	14.27 ± 0.33	13.13 ± 0.25	12.84 ± 0.76	13.79 ± 1.06	12.89 ± 0.11
40	OLSt + LnLnP + LnOγLn	4036	-/4023/-	-/13/-	4.56 ± 0.13	3.05 ± 0.05	4.42 ± 0.30	2.96 ± 0.05	4.01 ± 0.04	2.71 ± 0.32	3.08 ± 0.04	2.72 ± 0.01
40	γLnLnP + StLP	4048	-	-	0.53 ± 0.06	0.56 ± 0.05	0.79 ± 0.14	0.47 ± 0.07	1.79 ± 0.02	0.39 ± 0.02	0.48 ± 0.03	0.40 ± 0.07
42	LLL	4165	4160	5	19.34 ± 0.30	18.12 ± 0.21	19.05 ± 0.50	18.60 ± 0.13	16.36 ± 0.31	17.35 ± 0.22	16.22 ± 0.37	17.84 ± 0.01
42	OLLn	4191	4192	-1	6.10 ± 0.14	6.44 ± 0.04	5.57 ± 0.04	6.37 ± 0.35	4.84 ± 0.04	6.07 ± 0.19	6.27 ± 0.20	6.20 ± 0.09
42	OLγLn + LnLP	4209	4196/4217	13/-8	5.72 ± 0.15	5.16 ± 0.38	5.13 ± 0.34	5.48 ± 0.21	4.92 ± 0.02	5.02 ± 0.18	4.49 ± 0.08	5.23 ± 0.13

42	SLnLn + γLnLP	4235	4216/4221	19/14	1.19 ± 0.03	0.81 ± 0.01	0.95 ± 0.18	0.93 ± 0.14	1.31 ± 0.01	0.91 ± 0.06	0.93 ± 0.08	1.00 ± 0.02
44	OLL	4348	4342	6	10.21 ± 0.16	11.44 ± 0.08	10.23 ± 0.43	12.88 ± 0.32	9.39 ± 0.02	11.53 ± 0.42	11.32 ± 0.2	11.85 ± 0.14
44	LLP + OOLn	4369	4358/4360	11/9	9.26 ± 0.18	9.51 ± 0.03	8.73 ± 0.60	10.47 ± 0.12	8.08 ± 0.00	9.24 ± 0.05	8.32 ± 0.21	10.16 ± 0.12
44	SLLn + LnOP	4396	4378/4383	18/13	2.57 ± 0.12	2.76 ± 0.07	2.40 ± 0.29	2.74 ± 0.13	2.15 ± 0.09	2.81 ± 0.08	2.43 ± 0.08	2.40 ± 0.07
44	SLγLn + γLnOP	4420	-/4403	-/17	0.54 ± 0.07	0.45 ± 0.01	0.48 ± 0.07	0.42 ± 0.05	0.60 ± 0.11	0.64 ± 0.12	0.45 ± 0.02	0.34 ± 0.02
46	GLL + OLO	4537	4508/4522	29/15	3.32 ± 0.23	4.72 ± 0.07	3.61 ± 0.19	4.56 ± 0.23	2.65 ± 0.14	4.18 ± 0.28	4.13 ± 0.19	4.54 ± 0.05
46	OLP + SLL	4562	4548/4548	14/14	4.69 ± 0.07	5.89 ± 0.10	4.81 ± 0.04	5.35 ± 0.44	3.90 ± 0.19	5.26 ± 0.37	4.88 ± 0.23	5.29 ± 0.03
46	ALLn + SOLn + PLP	4586	-/4570 [b]/4571	16/15	0.84 ± 0.09	1.01 ± 0.02	0.75 ± 0.04	0.86 ± 0.08	0.73 ± 0.12	0.95 ± 0.03	0.89 ± 0.06	0.89 ± 0.07
48	GLO	4728	4708	20	0.12 ± 0.01	0.17 ± 0.00	0.24 ± 0.03	0.14 ± 0.00	0.12 ± 0.02	0.19 ± 0.02	0.13 ± 0.01	0.25 ± 0.02
48	OOO	4740	4729	11	0.40 ± 0.05	0.81 ± 0.04	0.66 ± 0.00	0.83 ± 0.02	0.42 ± 0.10	0.66 ± 0.03	0.59 ± 0.07	0.91 ± 0.04
48	ALL + SLO + OOP	4761	-/4746/4756	-/15/5	1.84 ± 0.29	2.61 ± 0.13	2.14 ± 0.07	2.48 ± 0.07	1.84 ± 0.11	2.36 ± 0.07	2.16 ± 0.36	2.88 ± 0.28
48	BLLn + AOLn	4777	-	-	0.17 ± 0.01	0.20 ± 0.02	0.23 ± 0.00	-	-	-	-	-
48	SLP + POP	4789	-/4776	-/13	0.06 ± 0.01	0.10 ± 0.00	0.10 ± 0.01					
50	BLL + ALO +LgLLn+ SOO	4948	-/-/-/4948	-/-/-/0	0.82 ± 0.03	1.10 ± 0.05	0.99 ± 0.02	1.08 ± 0.03	0.86 ± 0.16	0.9 ± 0.16	0.97 ± 0.1	1.08 ± 0.01
52	LgLL + BLO + AOO	5126	-	-	0.27 ± 0.00	0.41 ± 0.00	0.40 ± 0.02	0.46 ± 0.05	0.37 ± 0.04	0.39 ± 0.06	0.37 ± 0.03	0.48 ± 0.00
54	LgLO + BOO	5336	-	-	0.06 ± 0.00	0.11 ± 0.01	0.11 ± 0.01	-	-	-	-	-

*Ln: linolenic acid (C18:3); L: linoleic acid (C18:2); O: oleic acid (C18:1); St: stearidonic acid (C18:4); P: palmitic acid (C16:0); S: stearic acid (C18:0); G: gadoleic acid (C20:1); A: arachidic acid (C20:1), B: behenic acid (C22:0), Lg: lignocericacid (C24:0).

[a] LRI theoretical values according to Rigano et al. Anal. Chem. 2018 [22]; [b] LRI theoretical values according to Rigano et al. Anal. J Sep Sci 2020 [25].

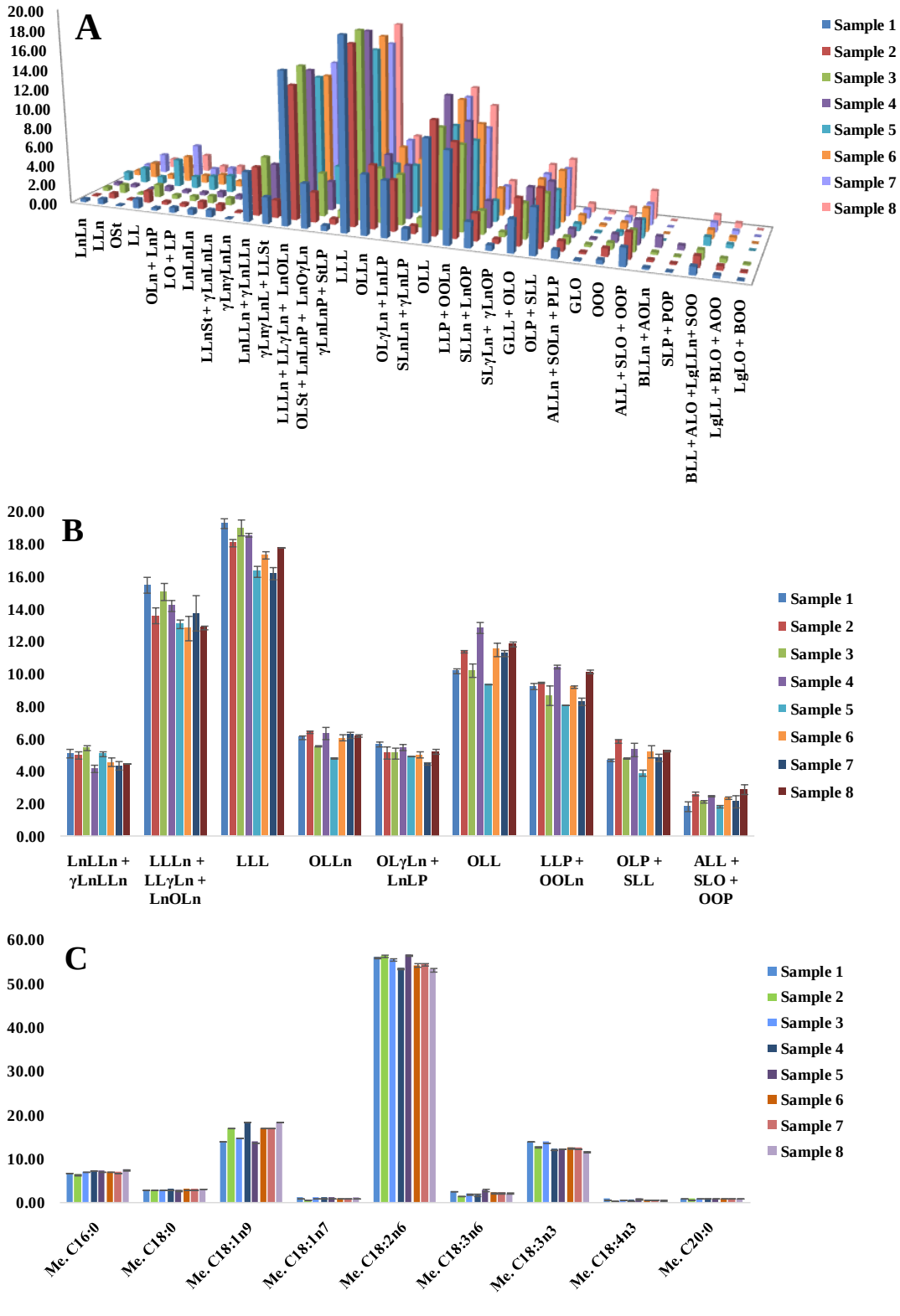

Figure 3.5 Identified compounds in hemp products and their relative amounts. A) all the identified TAGs; B) and C) most abundant TAGs and FAs, respectively.

In fact, as can be easily appreciated from the histogram (panel B), hemp seed oil samples, compared to hemp seed flour samples, resulted to be richer in the following peaks: LLLn + LLγLn + LnOLn, LLL and OLγLn + LnLP; furthermore, considerable variability was observed between samples of the same type but produced by different companies. As an example, sample 4 resulted to significantly differ from other hemp seed oil samples for the higher amount of OLL, LLP and OOLn. Samples 1 and 3 resulted to be more similar, with comparable quantities of the peaks LLLn + LLγLn + LnOLn, LLL, OLL and LLP + OOLn; sample 2 was found to be richer in the peaks OLLn, OLL and LLP + OOLn compared to sample 1 and 3, while the content in peaks LLLn + LLγLn + LnOLn and LLL was the lowest among hemp seed oil samples. Among hemp seed flour samples, sample 8 resulted to have the highest amount of the peaks LLL, OLγLn + LnLP, OLL, LLP + OOLn and ALL + SLO + OOP, but showed the lowest percentage of diacylglycerols and minority compounds compared to the other samples. Sample 5 reported the highest concentration of the peak LnLLn + γLnLLn of the hemp seed flour samples and the lowest concentration of the peaks OLL, LLP + OOLn and OLP + SLL in all the samples investigated.

In panel C is reported the histogram inherent to the most abundant FAs identified in hemp derived products. As easily foreseeable, the comparison between panel A/B and panel C clearly highlights the usefulness of the evaluation of the TAG profiles to discriminate between samples. In fact, TAG composition represents an effective fingerprint which is unique for each lipid matrix due to the highest combinations of fatty acids that are arranged in the formation of triglycerides. From panel C in Figure 3.5 only minor differences between hemp seed derived products can be appreciated, especially concerning C18:1n9, C18:2n6 and C18:3n6; the first resulted to be more abundant in samples 2 and 4 for the hemp seed oils and in samples 6, 7 and 8 for the hemp seed flours counterpart, showing comparable amounts in all of them. The compound C18:2n6 was found to be more abundant in samples 1 and 2 among the hemp seed oils and sample 5 for hemp seed flours. The latter FA was found to be less abundant in samples 4, 6 and 8. As is quite evident, the differences in the FAME profile are not so relevant to clearly differentiate oil and flour samples, and especially to differentiate similar samples produced by different companies.

The calculation of the experimental LRI represented an additional strategy to improve the identification process and further implement the laboratory-constructed database through the addition of the new identified TAGs. The ΔLRI value between LRI_{exp} and LRI_{th} remained inside the tolerance window for all the compounds, with few exceptions resulting from the coelutions between minor components and higher abundant species. Regarding TAGs containing at least two moieties of Ln, the previous LRI database [22] reported species exclusively constituted by αLn or alternatively by γLn, while the investigated samples resulted to be reach in TAGs containing both the α and γ isomers, as reported by Lisa *et al.* [16]. In such cases, the experimental LRI showed intermediate values between TAGs containing exclusively αLn isomers and exclusively γLn ones, depending by the different retention behavior of the analytes, which in turn is directly related to the position of the double bonds. In fact, it is well known that in non-aqueous reversed phase conditions, as in this research, TAGs containing γLn show higher retention compared to TAGs containing the αLn isomer counterpart [24] and this is obviously reflected in the LRI values.

In accordance with the above considerations, the species LnLnLn (containing three αLn isomers) and γLnγLnγLn were reported in the database with LRI_{th} values of 3668 and 3747, respectively, and the first of the two TAGs was identified in the hemp-derived products with a ΔLRI value of 7 (LRI_{exp} 3675). Consistently other two components were identified as γLnLnLn and γLnγLnLn on the basis of the additional information given by their LRI_{exp}, equal to 3703 and 3720, respectively.

Another point to consider concerns the coelution of two or more species, which inevitably determines minor variations in LRI_{exp} with respect to LRI_{theor}; the latter were obtained through the analysis of samples of reduced complexity, containing just one of the coeluted TAGs. This is the case of the peak containing OLSt, LnLnP and LnOγLn for which the LRI_{exp} was equal to 4036, as a result of the contribution to retention of the three TAGs (only LnLnP was previously reported in the database with a LRI_{th} value of 4023; Δ=13). Moreover, in accordance with the previous statement, LRI_{th} of the compounds LnOLn and γLnOγLn are 4011 and 4052, respectively; thus, an intermediate LRI_{exp} value of 4036, as obtained for the TAG LnOγLn which contain both the α and γ-Ln isomers, is perfectly plausible.

3.4 Conclusions

In this research, eight different hemp seed-derived products were investigated by using GC-MS/FID and LC-MS analytical techniques, and a total of 31 FAs and 62 glycerolipids were positively identified.

As a result, the favorable composition in lipid components of *Cannabis sativa*, especially in terms of ω-6/ω-3 FAs, was confirmed, suggesting the great economic interest of the species, even for nutritional and nutraceutical purposes. The remarkable content in unconventional FAs, as GLA and SDA, together with the high presence in linoleic acid contribute to the great value of these products, differentiating them from traditionally consumed edible oils and foods.

The investigation of the TAG composition resulted to be highly beneficial to clearly differentiate hemp seed oils and meals produced by different companies, since the TAG profile is unique for each lipid matrix. Moreover, such findings increase the knowledge on FAs distribution in glycerolipids, providing additional information on their native form, both in hemp seed oil and hemp seed flour samples.

Concerning the LC-MS analytical workflow, the already existing LRI database was further implemented and the LRI approach was succesfully confirmed to be an indispensable strategy to obtain a reliable identification of TAGs in combination to MS, capable of reducing the number of possible candidates for compounds showing the same $[M+H]^+$ ions by APCI-MS (+).

Such findings may be the basis for the extension of the LRI approach to other lipid classes and, in the near future, for a fully automatization of the identification process in liquid chromatography.

3.5 References

1. Ranalli P., Venturi, G. Hemp as a raw material for industrial applications. Euphytica 2004, 140, 1-6.
2. Alcohol, Drugs and Addictive Behaviours Unit, WHO, www.who.int.
3. European Monitoring Centre for Drugs and Drug Addiction 2017, Cannabis legislation https://www.emcdda.europa.eu/publications/adhoc/cannabis-legislation-europe_en
4. EU Regulation 1307/2013 https://eur-lex.europa.eu/legal-content/EN/TXT/?uri=celex:32013R1307

5. EU Plant variety database of the European Commission (v.3.4) https://ec.europa.eu/food/plant/plant_propagation_material/plant_variety_catalogues_databases/search/public/index.cfm?event=SearchForm&ctl_type=A
6. Farinon B., Molinari R., Costantini L., Merendino N. The Seed of Industrial Hemp (Cannabis sativa L.): Nutritional Quality and Potential Functionality for Human Health and Nutrition, Nutrients, 2020 12, 1935.
7. Rupasinghe H.P.V., Davis A., Kumar S.K., Murray B., Zheljazkov V.D. Industrial Hemp (Cannabis sativa subsp. sativa) as an Emerging Source for Value-Added Functional Food Ingredients and Nutraceuticals. Molecules 2020, 25, 4078.
8. Dimić E., Romanić R., Vujasinović V. Essential Fatty Acids, Nutritive Value and Oxidative Stability of Cold Pressed Hempseed (*Cannabis Sativa L.*) Oil from Different Varieties. Acta Alimentaria 2009, 38, 229–36.
9. Callaway, J C. Hempseed as a Nutritional Resource: An Overview, Euphytica 2004, 140, 65–72.
10. Saini R.K., Keum Y., Omega-3 and omega-6 polyunsaturated fatty acids: Dietary sources, metabolism, and significance — A review, Life Sci. 2018, 203, 255-267.
11. Vonapartis E., Aubin M., Seguin P., Mustafa A.F., Charron J. Seed composition of ten industrial hemp cultivars approved for production in Canada. J. Food Compos. Anal 2015, 39, 8–12.
12. Marzocchi S., Caboni M.F. Effect of harvesting time on hemp (cannabis sativa l.) seed oil lipid composition, Ital. J. Food Sci. 2020, 32, 1018-1029.
13. Da Porto C., Decorti D., Tubaro, F. Fatty acid composition and oxidation stability of hemp (Cannabis sativa L.) seed oil extracted by supercritical carbon dioxide, Industrial Crops and Products, 2012, 36, 401-404.
14. Leizer C., Ribnicky D., Poulev A. The Composition of Hemp Seed Oil and Its Potential as an Important Source of Nutrition 2017, 4179, 35-53.
15. Beale D.J., Pinu F.R., Kouremenos K.A., Poojary M.M., Narayana V.K., Boughton B.A., Kanojia K., Dayalan S., Jones O.A.H., Dias D.A. Review of recent developments in GC–MS approaches to metabolomics-based research. Metabolomics 2018, 14, 152.
16. Lísa M., Holčapek M., Boháč M. Statistical Evaluation of Triacylglycerol Composition in Plant Oils Based on High-Performance Liquid Chromatography−Atmospheric Pressure Chemical Ionization Mass Spectrometry Data J. Agric. Food Chem. 2009, 57, 15, 6888-6898.
17. Tringaniello C., Cossignani L., Blasi F. Characterization of the Triacylglycerol Fraction of Italian and Extra-European Hemp Seed Oil. Foods 2021, 10, 916.
18. Mungure T.E., Birch E.J. Analysis of Intact Triacylglycerols in Cold Pressed Canola, Flax and Hemp Seed Oils by HPLC and ESI-MS. SOP Transactions Anal. Chem. 2014, 1, 48–61.
19. Indelicato, S., David Bongiorno, Rosa Pitonzo, Vita D., Calabrese V., Indelicato S., Avellone G. Triacylglycerols in Edible Oils: Determination, Characterization,

Quantitation, Chemometric Approach and Evaluation of Adulterations. J. Chromatogr. A 2017, 1515, 1–16.
20. Ruiz-Gutidrrez V., Barron L.J.R. Methods for the analysis of triacylglycerols. J. Chromatogr. B 1995, 671, 133-168.
21. Rigano F., Arigò A., Oteri M., La Tella R., Dugo P., Mondello L. The retention index approach in liquid chromatography: An historical review and recent advances. J. Chromatogr. A. 2021, 1640, 461963.
22. Rigano F., Oteri M., Russo M., Dugo P., Mondello L. Proposal of a Linear Retention Index System for Improving Identification Reliability of Triacylglycerol Profiles in Lipid Samples by Liquid Chromatography Methods, Anal. Chem. 2018, 90, 3313-3320.
23. Rezanka T., Sigler K. The Use of Atmospheric Pressure Chemical Ionization Mass Spectrometry with High Performance Liquid Chromatography and Other Separation Techniques for Identification of Triacylglycerols. Curr. Anal. Chem. 2007, 3, 252-271.
24. Lísa M., Holčapek M. Triacylglycerols in Nut and Seed Oils: Detailed Characterization Using High-Performance Liquid Chromatography/Mass Spectrometry. In Nuts and Seeds in Health and Disease Prevention, Preedy V.R., Watson R.R., Patel V.B. (Eds.), Academic Press, 2011, 43–54.
25. Rigano F., Oteri M., Micalizzi G., Mangraviti D., Dugo P., Mondello L. Lipid profile of fish species by liquid chromatography coupled to mass spectrometry and a novel linear retention index database. J Sep Sci. 2020, 43, 9-10.

4 Assessment of the colon availability of delphinidin and cyanidin-3-O-sambubioside from *Hibiscus sabdariffa* and 6-gingerol from *Zingiber officinale* extracts by means of liquid chromatography coupled to photodiode array and mass spectrometry detection

4.1 Introduction

The gut microbiota is the main responsible for the production of many toxic molecules (e.g., methylglyoxal) at the colon level [1]. The production of such harmful components for human health, results from the anaerobic microbial fermentation of undigested carbohydrates in the small intestine, thus, leading to the lactose intolerance condition, which determines a wide range of gut and systemic symptoms [2]. As a consequence, the produced toxic metabolites may affect bacterial growth, determining an alteration of the gut microbiota [3].

Bioactive components deriving from foods and natural sources have gained increasing importance as an alternative to pharmaceutical products, to treat different types of ailments and to exert beneficial effects which contribute to the improvement of human health. Among them, polyphenols, which naturally occur in a wide variety of vegetables, fruits and flowers, have been classified as carbonyl stress inhibitors, due to their ability in trapping electrophilic species (e.g., aldehydes), determining the formation of coupling products, including oligomers [4,5].

Hibiscus sabdariffa L. (*H.s.*), also known as roselle, karkade or bissap, belongs to the family of Malvaceae and is world widely cultivated in tropical and subtropical regions, especially in Egypt, India, Thailand and Mexico. This species has been traditionally used as hot herbal or cold drink beverage due to the content in anthocyanins, water-soluble flavonoids, generally found in glycosylated forms [6-10], in plants and fruits. Anthocyanins have been proved to have antioxidants properties, preventing or inhibiting the oxidation processes by scavenging free radicals and reducing oxidative stress; in detail, the two most important anthocyanins in *H.s.* are cyanidin-3-O-sambubioside (C3S) and delphinidin-3-Osambubioside (D3S) [11].

Zingiber officinale L. (*Z.o.*), which belongs to the family of Zingiberaceae, is highly rich in gingerols, shogaols, paradols and zingerone, which confer the pungent taste of ginger [12]. Among them, 6-gingerol is the most abundant component in ginger fresh rhizomes, while 6-shogaol is the main compound in dried rhizomes [13].

Most of the *in vivo* studies on polyphenols bioavailability were focused on the availability of the unmetabolized cyanidin-3-O-glucoside (C3G) in plasma and urine samples [14]. Nevertheless, it should be noted that although polyphenols are poorly absorbed in the bloodstream after their administration, a large fraction of them transits to the intestine, reaching the colon lumen. To this concern, scarce literature is available, even if some researches have demonstrated that a wide portion of ingested polyphenols (up to 90%) results to be available at the colon level [15]. Furthermore, *in vitro* studies on *H.s.* and *Z.o.* metabolites have shown anti-inflammatory effects and trapping properties toward toxic molecules locally produced in the colon [5, 16], highlighting the close relationship between the biological activities of polyphenols and their availability at the site of action. In this context, the present research aimed at assessing the availability at the colon level of *H.s.* anthocyanins, C3S and D3S and the availability of 6-gingerol from *Z.o.*, being the biological effects of such components directly depending on their availability at the site of action. The availability of non-absorbed and intact or partially metabolized polyphenols, would perform, according to *in vitro* outcomes, highly antioxidant activity and trapping effect towards toxic molecules produced by the gut microbiota.

For such purposes, Wistar rats were subjected to the oral administration of *H.s.* and *Z.o.* plant extracts; their faeces were collected and extracted through solid-liquid extraction with methanol:water (60:40 *v/v*), followed by solid-phase extraction (SPE) on a C18 cartridge. Finally, the colon availability of the polyphenols was assessed through the analysis of faeces extracts by using liquid chromatography coupled to photodiode array and mass spectrometry detection (LC-PDA/MS).

4.2 Material and methods

4.2.1 Reagents and plant material

All solvents, reagents, and standard materials were purchased from Merck Life Science. Water, acetonitrile, methanol, ethyl acetate, trifluoroacetic acid (TFA) and formic acid (FA) LC-MS grade were used for polyphenol extraction and analysis. Capsaicin (purity ≥ 99.0%, 6-gingerol analogue [17-19]) and cyanidin-3-O-glucoside (purity ≥ 95.0%) were employed for semi-quantification; 1000 mg/L stock solutions were prepared by dissolving 10 mg in 10 mL of pure methanol for capsaicin [19] and 0.1% HCl in methanol for C3S [20]. Calibration curves were constructed by triplicate injections of six different

concentration levels of the standards and using a linear regression model; determination coefficients (R^2) of 0.998 and 0.972 were obtained, respectively.

Solid-phase extraction (SPE) was performed on a Sep-Pak Vac C18 octadecyl cartridge (3 mL, 200 mg) (VWR International Srl, Milan, Italy).

The basic ration for Wistar rats employed in this research was a composed-feeding stuff, consisting of cereals and derivatives, oilseeds meal, alfalfa and a mineral-vitamin supplement, with the following composition: moisture content, 13%; crude proteins, 14%; ash, 10%; crude fibre, 14%; fat, 2%; vitamins, A, D3, E; calcium and phosphorus.

The dried calyces of H.s. and fresh rhizomes of Z.o. were purchased in Meknes, Morocco and the identification of such plant materials was conducted at the Department of Biology, Faculty of Sciences, Moulay Ismail University, Meknes, Morocco.

H.s. dried calyces were ground using a blender equipped with a mesh of 2 mm, while fresh Z.o. rhizomes were washed with water, peeled and sliced. All the samples were stored at + 4 °C for 12 h in darkness before the extraction [21].

4.2.2 Sample preparation

In this research, three different concentrations of *H.s.* calyces and *Z.o.* rhizomes were evaluated, i.e. 2% (*w/v*), 4% (*w/v*) and 6% (*w/v*). In detail, 200, 400, and 600 mg of *H.s.* calyx powder were weighed, considering the dry matter of 93% (RSD = 0.11%) and 10 mL of distilled water were added to each amount. After a decoction of 10 min, samples were filtered separately through a muslin cloth in a conical flask. Afterwards, the filtrate was centrifuged at 2060×*g* for 10 min and the supernatant was filtered through a 0.45 μm Acrodisc nylon membrane (Merck Life Science) prior to LC-PDA/MS analysis.

Fresh *Z.o.* slices were weighed into 200, 400 and 600 mg, considering the dry matter of 9% (RSD = 0.03%), which was measured by heating a representative sample at 100 °C for 12 h [22]. The zingiber samples were squeezed with 10 mL of cold distilled water in a mortar for 10 min. Then, the extract was filtered through muslin cloth in a conical flask and centrifuged at 2060×*g* for 15 min. Finally, the supernatant was filtered through a 0.45 μm Acrodisc nylon membrane prior to LC-PDA/MS analysis.

The aqueous extracts of *H.s.* and *Z.o.* at concentrations of 2%, 4% and 6% (*w/v*) were stored for 48 h at + 4 °C, prior to rats' administration [21].

4.2.3 Experimental design

Wistar rats, 3-4 week old, distributed equally in female and male with an average weight between 277 and 521 g respectively, were used for the experiment. The animals were housed in individual metabolism cages, at a temperature of 22 °C (± 1 °C) and hygrometry of 50–60%, with night and day alternation every 12 h. Before the experiment, an adaptation period to the rats' diet and to the metabolism cages was observed, in which and tap water were distributed ad libitum, measuring the consumed water and food and assessing the amount of faeces excreted each 12 h for 4 days. The sufficient and non-waste meal amount was determined as 15 g twice a day. After a 4-day adaptation period to food and metabolism cage, rats were randomly distributed into three treatment groups, each containing three rats.

At the beginning of each treatment, all rats received, through the gavage, a single oral dose of one random extract concentration, followed by the collection of the faecal matter. The collected faeces were immediately stored at -80 °C, every 6 h over 4 days, to avoid the bacterial deterioration of polyphenols. Specifically, the control group received tap water, the second group received H.s. aqueous extract and the third group received Z.o. aqueous extract. The treatments were repeated for four periods and the quantities of consumed food and water were noted. The three groups received a different random concentration of 2, 4 or 6% (*w/v*) of both *H.s.* and *Z.o.* extracts for each period, after being subjected to another adaptation-collection cycle. Before to be moved to the subsequent cycle, rats were rested for a few days. The experimental design was a split plot in a randomized complete block.

4.2.4 Faeces collection and composite

During the faecal matter collection, rats were deprived of food to avoid faeces contamination. Faeces were collected from the groups every 12 h for 4 days. The 6-h collections were promptly put together with the other following 6-h collection under -80 °C to avoid polyphenol degradation. In detail, faecal samples were weighed, sealed in polyethylene bag and stored at -80 °C until the analysis. Prior to preparation of the composites, faeces dry matter was determined by drying a representative small amount of each collected faeces in the oven at 135 °C for 2 h [22], such material was not subjected to polyphenol extraction, but exclusively used for dry matter determination. The frozen

faecal samples of rats which received the same treatment and the same concentration of plant extract, were thawed, broken into small pieces with spatula, pooled together and homogenized in a mortar to obtain the composite samples.

4.2.5 Faeces extraction

The extraction of the faecal matter was carried out by using a previously reported [23] procedure, with minor modifications. Briefly, 20 mL of methanol:water 60:40 *v/v* were added to 1 g of faecal composite (total amount in the range 3.0-12.1 g min-max); for the faeces of rats which received *H.s* the solvent mixture was acidified with 1% TFA. The extraction was performed in a stirrer for 20 min, then the samples were sonicated for 10 min. The faecal slurry was centrifugated at 1000 ×*g* for 15 min and the supernatant was collected, while and the pellet was re-extracted twice, firstly with 20 mL and then with 10 mL of the solvent extraction mixture. All supernatants were pooled together and evaporated by EZ-2 Envi evaporator at +20 °C. Afterwards, the *H.s.* faeces extracts were dissolved in 1 mL of 1%TFA in water, while the Z.o. faeces were dissolved in 1 mL of water. Afterwards, samples were subjected to SPE on a C18 cartridge, which was preconditioned with two column volumes of pure methanol, followed by three column volumes of 1% TFA in water with, to remove the remaining methanol. The aqueous extracts were loaded on the cartridge and washed with two column volumes of 1% TFA in water, to remove unadsorbed compounds. Anthocyanins were eluted with two column volumes of 1% TFA in methanol, while polyphenols were eluted with two column volumes of ethyl acetate, from the faeces of rats which received *H.s.* and *Z.o.*, respectively. The eluates were evaporated, and the dried samples were redissolved in 1 mL of 1% TFA or 1 mL of pure water, for anthocyanins and polyphenols extracts, respectively, prior to the LC-PDA/MS analysis. The extraction procedures were performed in duplicate.

4.2.6 Instrumentats and analytical conditions

The analyses were performed on a Prominence LC-20A system (Shimadzu, Kyoto, Japan), consisting of a CBM-20A controller, a DGU-20 A5 degasser, two LC-20AD dual-plunger parallel-flow pumps, a SIL-20A autosampler, a CTO-20AC column oven. The LC system was coupled to an SPDM20A photo diode array detector and an LCMS-2020

single quadrupole mass spectrometer through an ESI ionization interface. Data acquisition and processing was performed using the LCMS solution ver. 5.65 software (Shimadzu, Kyoto, Japan).

LC separations were performed on an Ascentis Express C18 column 150 × 4.6 mm, 2.7 μm *d.p.* (Merck Life Science, Darmstadt, Germany). For analysis of the anthocyanins, both in *H.s.* aqueous and faeces extracts, mobile phases were A) water/F.A. (95/5 *v/v*) and B) ACN, under the following gradient program: 0 min, 12% B; 25 min, 30% B; 34 min, 100% B [24, 25]. PDA acquisition was performed in the range of 200-550 nm; *H.s.* anthocyanins in the aqueous extract were monitored at 520 nm (sampling frequency: 40 Hz; time constant: 0.025 s).

Concerning the analysis of polyphenols, both in *Z.o.* aqueous extract and faeces, mobile phases were: A) 0.1% FA in water and B) ACN, under the following gradient program: 0 min, 0% B; 5 min, 5% B; 15 min, 10% B; 30 min, 20%B; 60 min, 50% B and 70 min, 100% B. PDA acquisition was performed in the range of 200-350 nm; *Z.o.* polyphenols in aqueous extract were monitored at 280 nm (sampling frequency: 40 Hz; time constant: 0.025 s).

The injection volume was 5 μL, the flow rate was 1 mL/min and a T piece was used after PDA to direct 0.2 mL/min of the flow to the ESI interface.

The ESI source was used both in positive and negative ionization modes and the MS parameters were set as follows: acquisition range, 100–1200 *m/z*; scan speed, 1154 μ/s; event time, 500 and 1000 ms; nebulizing gas (N_2) flow rate, 1.5 L/min; drying gas (N_2) flow rate, 5 L/min; interface temperature, 350 °C; heat block temperature, 350 °C; DL temperature, 280 °C; DL voltage, -34 V; interface voltage, -4.5 kV; Qarray DC voltage, 1.0 V; Qarray RF voltage, 60 V.

4.3 Results and Discussion

In Figure 4.1 are shown the LC-PDA analyses (λ= 520 nm) of the delphinidin-3-O-sambubioside and cyanidin-3-O-sambubioside anthocyanins in *H.s.* aqueous extract and in the faeces extracts of rats which received different concentrations of *H.s.*, i.e. 6% (*w/v*), 4% (*w/v*) and 2% (*w/v*). The anthocyanins were confirmed by MS detection, by single-ion monitoring (SIM), in positive ionization mode, of the corresponding $[M+H]^+$ ions, at *m/z* 597 and 581 for D3S and C3S, respectively. The tentative identification was

supported by the anthocyanins UV spectra and the correspondence of retention times (with %RSD values lower than 2%), between the anthocyanins found in the aqueous *H.s.* extract and faeces extracts. Furthermore, the investigated compounds were semi-quantified at 520 nm (D3S, C3S) and 280 nm (6-gingerol), using the external calibration curves obtained from analogue compounds; the semi-quantitative results are showed in Table 4.1 and the amounts were expressed in μg/g of dried extract and faeces.

In detail, the amounts of the oral administered C3S as C3G equivalent were found to be equal to 2.19 μg/g and 0.97 μg/g (*w/w*) for the 6% and 4% of *H.s.* calyces concentrations, while the anthocyanins content in faeces extracts were equal to 1.58 μg/g and 0.17 μg/g (*w/w*), respectively. As a result, the availability at the colon level of C3S after 12 h, expressed as percentage of the total ingested and total excreted polyphenol, was equal to 72.15% and 17.52% for the administered *H.s.* concentrations of 6% and 4%, respectively. On the other hand, D3S, with a content of 0.21 μg/g (*w/w*) as C3G equivalent in the 6% of *H.s.* calyces concentration, showed a colon availability of 76.19%, since the corresponding amount found in faeces was equal to 0.16 μg/g (*w/w*).

Conversely, D3S was not available in the colon at 4% of *H.s.* concentration, and both the anthocyanins were not available at the 2% (*w/v*) administered concentration; the latter finding was probably due to the metabolization by the gut microbiota [19, 26]. In detail, compared to the other polyphenols, C3S and D3S resulted to be available in the colon in higher amounts; as a confirmation of this, the lack of anthocyanins absorption in such portion of the intestine, has been reported in previous researches [27–29].

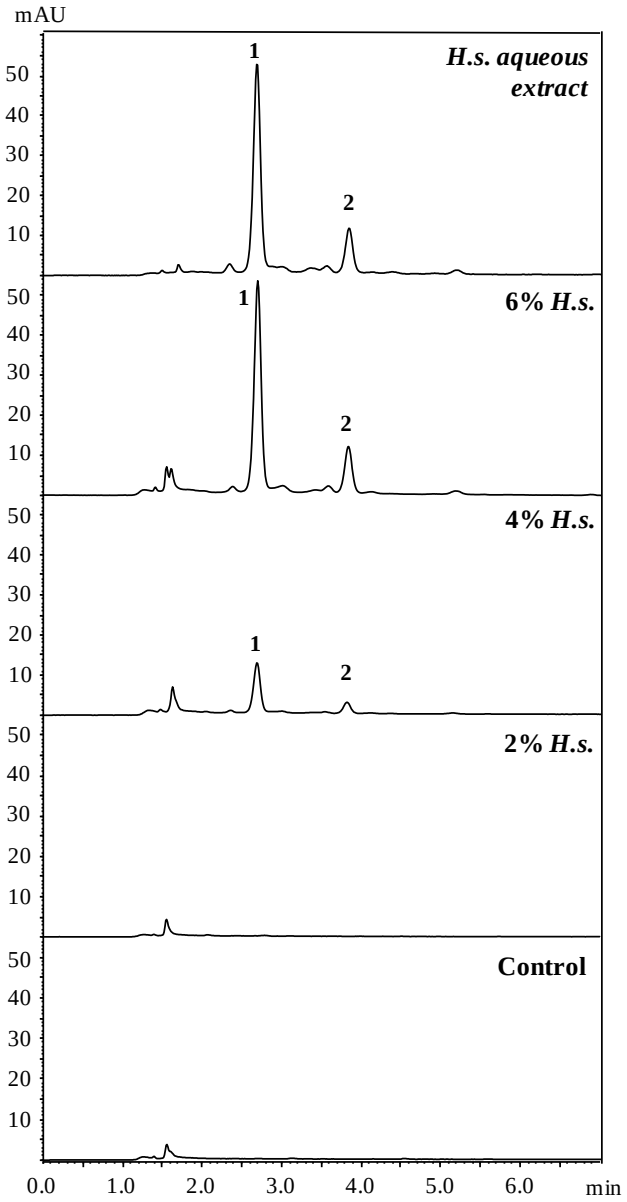

Figure 4.1. LC–PDA chromatograms (at 520 nm) of cyanidin-3-O-sambubioside (1) and delphinidin-3-O-sambubioside (2) anthocyanins in H.s. aqueous extract and their intact availability in the rat's colon at different administered concentrations 6%, 4% and 2% (w/v).

Table 4.1 Quantification (μg/g ± RSD) of H.s. anthocyanins and Z.o. gingerol at 2, 4 and 6% (w/v) of oral administered plant extracts and their availability in the colon.

	Oral administered plant extract (μg/g)*			**Colon availability (μg/g)***		
	6% (*w/v*)	**4% (*w/v*)**	**2% (*w/v*)**	**6% (*w/v*)**	**4% (*w/v*)**	**2% (*w/v*)**
C3S	2.19 ± 0.21	0.97 ± 0.17	0.24 ± 0.08	1.58 ± 0.52	0.17 ± 0.00	-
D3S	0.21 ± 0.09	0.09 ± 0.14	0.02 ± 0.10	0.16 ± 0.00	-	-
6-gingerol	56.45 ± 0.16	125.46 ± 0.1	62.73 ± 0.09	0.85 ± 0.11	-	-

* *Capsaicin or cyanidin-3-O-glucoside equivalent 2, 4 and 6% (w/v) represent the orally administered concentration of the crude extract.*

Although anthocyanins may be degraded by the gut microbiota at the colon level [19, 26, 30], the destiny of such metabolites is closely related to their chemical structures and most of them have been reported to not undergo a metabolism of the parent glycoside to glucurono-, sulfo-, or methyl- derivatives [14, 31–34]. Furthermore, anthocyanins absorption, metabolism and excretion directly depend on the nature of both the sugar moiety but also on the structure of the aglycone [31, 35]. These results are consistent with the intact availability of anthocyanins at the colon level (at 6% and 4% (*w/v*) of administered *H.s.* concentrations) which may be justified by the presence of the sambubiose glycone moiety, which restrains the methylation or the glucuronidation of the molecule. As a consequence, in accordance with previous works, the most recovered anthocyanin, in its intact/native form, within the gastrointestinal tract was cyanidin-3-O-sambubioside compared to the other glycone moieties. In detail, C3S showed a recovery of 78% with respect to cyanidin-3-O-glucoside, which had a recovery around the 2% [29]. Nevertheless, anthocyanins availability within the colon, is reduced with the passing of time, due to the microbial catabolism [36, 37] which result in breaking down of aglycones by fission of the C-ring, with the A- and B- ring fragments conversion into different metabolites [36, 38, 39]. In this research, the presence of the available anthocyanins in the colon was monitored for a short period of time, 12 h.

In Figure 4.2 are reported the LC-PDA analyses (λ= 280 nm) of *Z.o.* extract (A), faeces extract (B) and control sample (C). In detail, 6-gingerol, which is the main bioactive compound in fresh ginger, was detected at retention time of 55.0 min and confirmed through MS detection by monitoring the $[M-H]^-$ ion at *m/z* 293, in negative ionization mode. In this case, only the highest administered concentration (i.e. 6% of *Z.o.*) was detected in rat faeces. As reported in Table 4.1, an amount of 56.45 μg/g (*w/w*) as capsaicin equivalent was detected in the 6% (*w/v*) of fresh *Z.o.*, while a lower concentration equal to 0.85 μg/g (*w/w*), as capsaicin equivalent, was found in rat's faeces for the same administered concentration (at the same retention time of the reference peak in the *Z.o.* crude extract). Therefore, a very low colon availability was obtained for 6-gingerol, equal to 1.50%, considering the total ingested and total excreted polyphenol; 6-gingerol was not detected in faeces of rats which received the other *Z.o.* concentrations (i.e., 4% and 2%) and in the control sample. These results highlighted that the highest administered *Z.o.* concentration (i.e., 6%) allowed for a partial bypass of the

deconjugation and the metabolism by the gut microbiota, resulting in the 6-gingerol availability at the colon level. In fact, according to Jiang *et al.*, after oral administration, 6-gingerol is highly distributed in the gastrointestinal tract compared to the other examined tissues; furthermore, it was found to be available in its intact form 4h after the administration, being brain, heart, lung, spleen, liver, kidney, stomach and small intestine tissues collected 5, 15, 30 min and 1, 2, 4 h after dosing [40]. In another research, approximately 48% of the 6-gingerol administered 50-mg/kg dose was excreted in the bile as glucuronide, while the 16% was excreted in urine within 60 h, suggesting that the gut flora and liver enzymes play an important role in the metabolism of the polyphenolic compound [41]. As a consequence, the lower availability at the colon level of 6-gingerol, compared to the *H.s.* anthocyanins, may be related to its conversion into other metabolites, such as glucuronide conjugates [42-43].

4.4 Conclusions

In the present research, the availability of the most representative intact *H.S.* anthocyanins and 6-gingerol from *Z.o.* at the colon level was evaluated. As a result, such components have been found in faeces extracts when administered in plant concentrations higher than 6% for all the investigated polyphenols, while only C3S was detected at administered concentration of 4%; further, the colon availability of the investigated compounds in their intact form resulted to be limited to 12 h. In the faecal extracts of rats which received the 2% plant concentration, no polyphenols have been detected.

C3S and D3S of *H.s.* showed high availability at the colon level (72.15% and 76.19%, respectively for the administered *H.s.* concentrations of 6%) compared to 6-gingerol from *Z.o.* (with lower availability, equal to 1.50%). These results positively encourage the research on the polyphenol activities at the gastrointestinal level, with particular emphasis on the antioxidant activities and the trapping effect towards toxic molecules produced in the colon (e.g., methylglyoxal), since the biological activities of such components is tightly related to their availability at the site of action. As a result, the presence of bioactive compounds available at the colon site after oral administration, highlights the possibility to use *H.s.* extracts as dietary supplements.

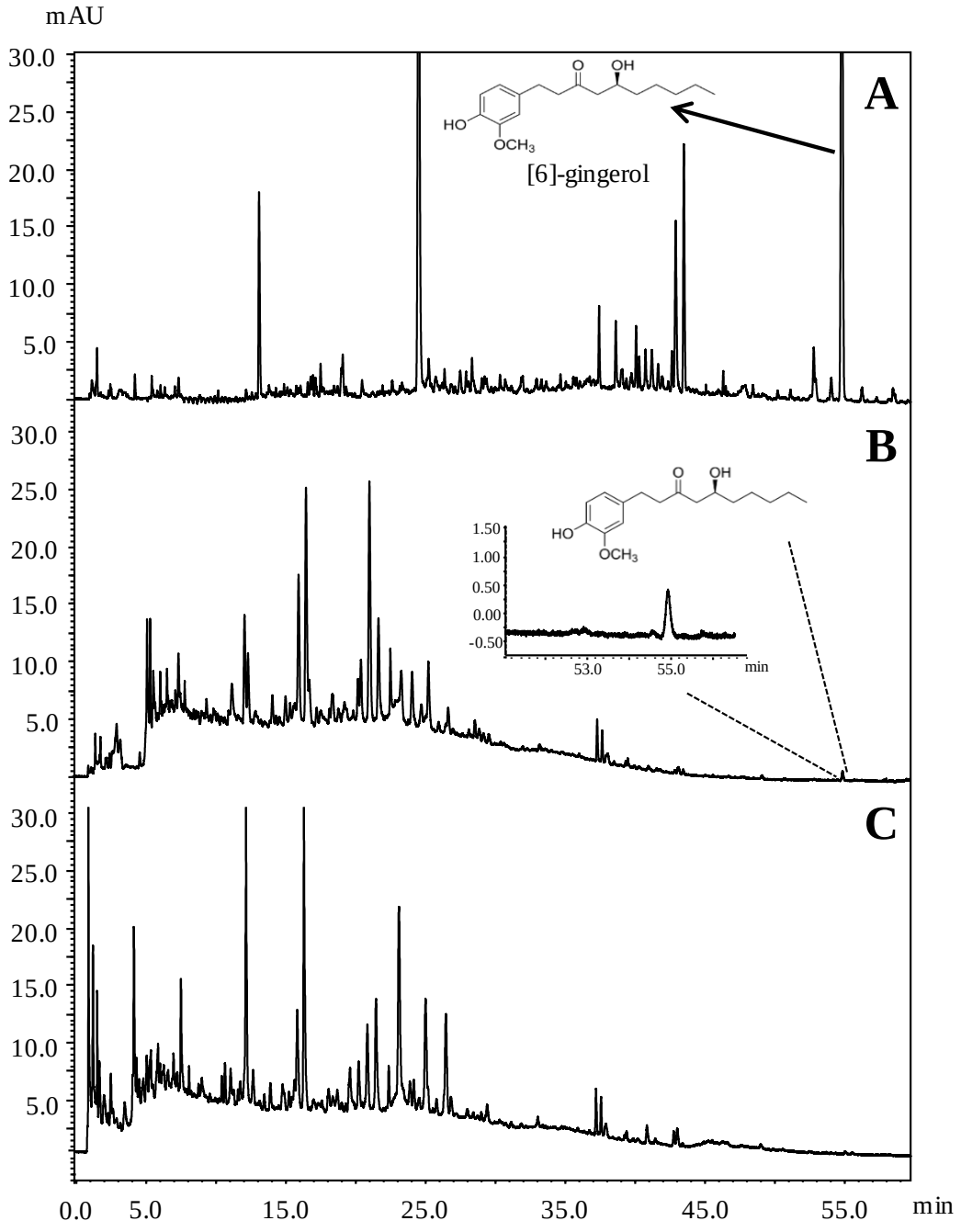

Figure 4.2. HPLC-PDA chromatograms extracted at 280 nm of 6% (w/v) Z.o. aqueous extract (A); faeces extract of rats which received 6% (w/v) Z.o. (B) and control (C).

4.5 References

1. Campbell A.K., Matthews S.B., Vassel N., Cox C.D., Naseem R., Chaichi J., Holland I.B., Green J., Wann K.T. Bacterial metabolic 'toxins': a new mechanism for lactose and food intolerance. and irritable bowel syndrome. Toxicol. 2010, 278, 268-276.
2. Campbell A.K., Waud J.P., Matthews S.B. The molecular basisof lactose intolerance. Sci. Prog, 2009, 92, 241-287.
3. Campbell A.K., Naseem R., Holland I.B., Matthews S.B., Wann K.T., Methylglyoxal and other carbohydrate metabolites induce lanthanum-sensitive Ca^{2+} transients and inhibit growth in E. coli. Arch. Biochem. Biophys. 2007, 468, 107-113.
4. Ho C., Wang M. Dietary phenolics as reactive carbonyl scavengers: potential impact on human health and mechanism of action. J. Trad. Complement. Med. 2013, 3, 139-141.
5. Zhu Y., Zhao Y., Wang P. Ahmedna M. Sang S. Bioactive ginger constituents alleviate protein glycation by trapping methylglyoxal. Chem. Res. Toxicol. 2015, 28, 1842-1849.
6. Kumar S., Pandey A.K., Chemistry and biological activities of flavonoids: an overview. Sci. World J. 2007, 73, 637–670.
7. Tsao R. Chemistry and biochemistry of dietary polyphenols. Nutrients 2010. 2, 1231-1246.
8. Crozier A., Jaganath I.B., Clifford M.N. Dietary phenolics: chemistry. bioavailability and effects on health. Nat. Prod. Rep. 2009, 26, 1001-1043.
9. Morohashi K., Casas M.I., Ferreyra M.L.F., Mejia-Guerra M.K., Pourcel L., Yilmaz A., Feller A., Carvalho B., Emiliani J., Rodriguez E. A genome-wide regulatory framework identifies maize pericarp Color1 controlled genes. Plant Cell 2012, 24, 2745-2764.
10. Fantini M., Benvenuto M., Masuelli L., Frajese G., Tresoldi I., Modesti A., Bei R. In vitro and in vivo antitumoral effects of combinations of polyphenols. or polyphenols and anticancer drugs, perspectives on cancer treatment. Int. J. Mol. Sci. 2015, 16, 9236-9282.
11. Grajeda-Iglesias C., Figueroa-Espinoza M.C., Barouh N. Isolation and characterization of anthocyanins from Hibiscus sabdariffa flowers. J. Nat. Prod. 2016, 79, 1709-1718.
12. Baliga M.S., Latheef L., Haniadka R., Fazal F., Chacko J., Arora R. Ginger (*Zingiber officinale Roscoe*) in the treatment and prevention of arthritis. In Bioactive food as dietary interventions for arthritis and related inflammatory diseases. Preedy R.R.W.R. (ed) Academic Press, San Diego, 2013, 529–544.
13. Jolad S.D., Lantz R.C., Solyom A.M. Fresh organically grown ginger (*Zingiber officinale*), composition and effects on LPS-induced PGE_2 production. Phytochemistry 2004, 65,1937-1954.

14. Ichiyanagi T., Shida Y., Rahman M.M., Hatano Y., Konishi T. Extended glucuronidation is another major path of cyanidin 3-O-b-D-glucopyranoside metabolism in rats. J. Agric. Food. Chem. 2005, 53, 7312-7319.
15. Cardona F., Andrés-Lacueva C., Tulipani S. Benefits of polyphenols on gut microbiota and implications in human health. J. Nutr. Biochem. 2013, 24, 1415-1422.
16. Sogo T., Terahara N., Hisanaga A. Anti-inflammatory activity and molecular mechanism of delphinidin 3-sambubioside, a Hibiscus anthocyanin, anti-inflammatory effects of delphinidin 3-sambubioside. BioFactors 2015, 41, 58–65.
17. Zick S.M., Ruffin M.T., Djuric Z., Normolle D., Brenner D.E. Quantitation of 6-,8- and 10-gingerols and 6-shogaol in human plasma by high performance liquid chromatography with electrochemical detection. Int. J. Biomed. Sci. 2010, 6, 233-240.
18. National Sanitation Foundation (NSF) HPLC Analysis of Gingerols and Shogaols in Zingiber officinale (Ginger) INA Method 114,000 International, http: //www.nsf.org/busin ess/ina/ginger.asp. Accessed 9 Jul 2010.
19. Oyedemi B.O.M. Maria K.E., Stapleton P.D., Gibbons S. Capsaicin and gingerol analogues inhibit the growth of efflux multidrug resistant bacteria and R-plasmids conjugal transfer. J. Ethnopharmacol. 2019, 245, 111871.
20. Kallam K., Appelhagen I., Luo J., Albert N., Zhang H., Deroles S., Hill L., Findlay K., Andersen Ø.M., Davies K., Martin C. Aromatic decoration determines the formation of anthocyanic vacuolar inclusions. Curr. Biol. 2017, 27, 945–957.
21. Ghasemzadeh A., Jaafar H.Z.E., Rahmat A. Changes in antioxidant and antibacterial activities as well as phytochemical constituents associated with ginger storage and polyphenol oxidase activity. BMC Complement Altern. Med. 2016, 16, 382.
22. Official Methods of Analysis of Analysis Association of Official Analytical Chemists International AOAC, 1996. Moisture in animal feed, method 930,15 (16th edn), Gaithersburg, MD, References-Scientific Research Publishing. n.d. Accessed 4 Dec 2018.
23. He J., Magnuson B.A., Giusti M.M. Analysis of anthocyanins in rat intestinal contents impact of anthocyanin chemical structure on fecal excretion. J. Agric. Food Chem. 2005, 53, 2859-2866.
24. Fanali C., Dugo L., D' Orazio G., Lirangi M., Dachà M., Dugo P., Mondello L. Analysis of anthocyanins in commercial fruit juices by using nano-liquid chromatography-electrospray-mass spectrometry and high-performance liquid chromatography with UV–vis detector. J. Sep. Sci. 2011, 34, 150–159.
25. Cesa S., Carradori S., Bellagamba G. Evaluation of processing effects on anthocyanin content and colour modifications of blueberry (*Vaccinium spp.*) extracts, comparison between HPLC-DAD and CIELAB analyses. Food Chem. 2017, 232, 114–123.
26. Aura A.M., Martin-Lopez P., O'Leary K.A., Williamson G., Oksman-Caldentey K.M., Poutanen K., Santos-Buelga C. In vitro metabolism of anthocyanins by human gut microflora. Eur. J. Nutr. 2005, 44, 133–142.

27. Matuschek M.C., Hendriks W.H., McGhie T.K., Reynolds G.W. The jejunum is the main site of absorption for anthocyanins inmice. J. Nutr. Biochem. 2006, 17, 31-36.
28. Williamson G., Kay C.D., Crozier A. The bioavailability, transport and bioactivity of dietary flavonoids, a review froma historical perspective, dietary flavonoids, a historical review. Compr. Rev. Food Sci. 2018, 17, 1054-1112.
29. Wu X., Pittman H.E., Prior R.L. Fate of anthocyanins andantioxidant capacity in contents of the gastrointestinal tract ofweanling pigs following black raspberry consumption. J. Agric. Food Chem. 2006, 54, 583–589.
30. Esposito D., Damsud T., Wilson M., Grace M.H., Strauch R., Li X., Lila M.A., Komarnytsky S. Black currant anthocyanins attenuate weight gain and improve glucose metabolism in diet induced obese mice with intact, but not disrupted, gut microbiome. J. Agric. Food Chem. 2015, 63, 6172-6180.
31. McGhie T.K., Ainge G.D., Barnett L.E., Cooney J.M., Jensen J.D. Anthocyanin glycosides from berry fruit are absorbed and excreted unmetabolized by both humans and rats. J. Agric. Food Chem. 2003, 51, 4539-4548.
32. Miyazawa T., Nakagawa K., Kudo M., Muraishi K., Someya K. Direct intestinal absorption of red fruit anthocyanins, cyanidin-3-glucoside and cyanidin-3,5-diglucoside, into rats and humans. J Agric Food Chem 1999, 47, 1083-1091.
33. Milbury P., Cao G., Prior R.L., Blumberg J. Bioavailability of elderberry anthocyanins. Mech Ageing Dev. 2002, 123, 997-1006.
34. Cooney J.M., Jensen J.D., McGhie T.K. LC-MS identification of anthocyanins in boysenberry extract and anthocyanin metabolites in human urine following dosing. J. Sci. Food Agric. 2004, 84, 237–245.
35. Wu X., Pittman H.E., Mckay S., Prior R.L. Aglycones and sugar moieties alter anthocyanin absorption and metabolism after berry consumption in weanling pigs. J. Nutr. 2005, 135, 2417-2424.
36. Gonzalez-Barrio R., Edwards C.A., Crozier A. Colonic catabolism of ellagitannins, ellagic acid, and raspberry anthocyanins. In vivo and in vitro studies. Drug Metab. Dispos. 2011, 39,1680-1688.
37. McDougall G.J., Conner S., Pereira-Caro G., Gonzalez-Barrio R., Brown E.M., Verrall S., Stewart D. Tracking (poly)phenol components from raspberries in ileal fluid. J. Agric. Food Chem. 2014, 62, 7631-7641.
38. Feliciano R.P., Boeres A., Massacessi L., Istas G., Ventura M.R., dosSantos C.N., Heiss C., Rodriguez-Mateos A. Identificationand quantification of novel cranberry-derived plasma and urinary(poly)phenols. Arch Biochem Biophys 2016, 599, 31-41.
39. Rodriguez-Mateos A., Vauzour D., Krueger C.G., ShanmuganayagamD., Reed J., Calani L., Mena P., Del Rio D., Crozier A. Bioavailability, bioactivity and impact on health of dietary flavonoids and related compounds, an update. Arch Toxicol 2014, 88, 1803-1853.
40. Jiang S.Z., Wang N.S., Mi S.Q. Plasma pharmacokinetics and tissue distribution of [6]-gingerol in rats. Biopharm. Drug Dispos. 2008, 29, 529-537.

41. Nakazawa T., Ohsawa K. Metabolism of [6]-gingerol in rats. Life Sci. 2002, 70, 2165-2175.
42. Ahmed R.S., Seth V., Banerjee B.D. Influence of dietary ginger (*Zingiber officinale Rose*) on antioxidant defense-system in rat, comparison with ascorbic acid. Indian J. Exp. Biol. 2000, 38, 604-606.
43. Zick S.M., Djuric Z., Ruffin M.T., Litzinger A.J., Normolle D.P., Alrawi S., Feng M.R., Brenner D.E. Pharmacokinetics of 6-gingerol, 8-gingerol, 10-gingerol and 6-shogaol and conjugate metabolites in healthy human subjects. Cancer Epidemiol. Biomark. Prev. 2008, 17, 1930-1936.

5 The on-line coupling of silver thiolate and octadecylsilica monodisperse material for triacylglycerol analysis by comprehensive liquid chromatography

5.1 Introduction

In recent years, lipid analysis has become one of the most promising research fields, given the extensive involvement of lipids components in in multiple biological processes and in determining the nutritional value, the organoleptic features and the technological properties of different foods and natural products. As a result, the development of suitable analytical methods allowing for the comprehensive elucidation of the lipid composition in different matrices is highly demanded [1].

Among lipid species, triacylglycerols (TAGs) are the main components of edible oils and animal fats. Such compounds have a pivotal role in human diet since they represent a concentrated store of metabolic energy and a source of essential fatty acids (FAs) and fat-soluble vitamins. TAGs components, which consist of three FAs esterified to a glycerol molecule, may differ for the total carbon number (CN), unsaturation degree, position and configuration of double bonds (DBs) and the stereochemical positions (*sn*-1, -2 and -3) of FAs on the glycerol backbone. The high number of possible FAs combinations in TAG molecules results in a unique TAG profile for each lipid matrix, which can serve as fingerprint to ensure the quality and authenticity of food products [2].

Liquid chromatography (LC) represents the election technique for TAG analysis, followed by super critical fluid chromatography (SFC) and thin-layer chromatography (TLC) [3,4]. Among the LC separation modes, normal-phase (NP) LC and hydrophilic interaction liquid chromatography (HILIC) have been extensively investigated to achieve lipid class separation, also affording a partial discrimination of lipid species within each class [5]. On the other side, silver ion (Ag^+)- and non-aqueous reversed phase-LC (NARP-LC) have been the most widely used separation approaches for TAG analysis [6].

In Ag^+-LC, the retention mechanism is based on the capability of unsaturated organic compounds to complex with transition metals bonded to the stationary phase, by forming charge-transfer type organometallic complexes in which the unsaturated compound acts as an electron donor and the silver ion as an electron acceptor [7]. Specifically, Ag^+-LC separations occur based on the differences in the strength of such weak reversible complexes formed during the elution process. As a consequence, the separation of TAGs

is ruled by the differences in unsaturation degree and DB position; in general the retention increases with the increase in the number of DBs and the distance among them. Conversely, retention decreases with the increasing chain-length and with an increasing number of substituents at the DB, being such conditions responsible for the reduction of organometallic complexes' stability.

As far as the stationary phase material is concerned, silver ions have been traditionally embedded in the LC system by three different techniques: the first involves binding the Ag^+ ions to an ion-exchange medium in which silver ions replace the protons of the functional groups and form stable ionic interactions. A second technique consists in impregnating a support with a silver salt (e.g. silica gel and silver nitrate), while in the third procedure the silver salt is added to the mobile phase during a conventional RP-LC separation (incompatible with MS) [7,8]. The most relevant issue of the conventional silver ion columns is related to the difficulty in obtaining a stable and reproducible systems, with a controlled Ag^+ content. In fact, the quality of column packing, especially in terms of density, stability and accessibility of Ag^+ ions, plays an important role in the retention process.

Another drawback is related to the limited operational life of such stationary phases, resulting from the potential loss of silver ions. In order to overcome such limitations, Ag^+-LC columns of silica gel functionalized with thiol groups have been more recently introduced for lipid separation, especially for TAG analysis [9,10]. In silver thiolate chromatographic materials (AgTCM), thiol groups are capable of forming stable covalent complexes with Ag(I), offering advantages such as higher stability, controlled Ag^+ content, longer operational life, reproducibility across extended use, lack of silver leaking from the stationary phases allowing for MS detection. A recent work of Aponte *et al.* reported the comparison between AgTCM and other Ag^+ impregnated stationary phases to test olefinic interactions, proving the effectiveness of the silver thiolate columns for the separation of unsaturated organic compounds [11].

The high complexity of many food matrices often makes untargeted elucidation of lipid species a challenging task; thus, the combination of two separation techniques, aiming at enhancing the resolving power of the chromatographic system may be highly recommendable [12]. For this purpose, NARP-LC separation mode, based on analytes hydrophobicity, may effectively complement Ag^+-LC. In NARP-LC, TAGs elute

according to the increasing partition number (PN), calculated from the equation PN = CN - 2DB (carbon chain length, CN and double bonds number, DB) [13]. NARP-LC has been widely used for TAG analysis, since the employment of non-aqueous solvents makes this technique highly suitable for non-polar compounds separation, also providing an easy coupling to MS detection [3,14].

The coupling between Ag^+- and NARP-LC can be conveniently exploited in multidimensional separation approaches, aiming to increase the number of resolved compounds. As an example, Holčapek *et al.* developed an off-line setup using NARP-LC in the first dimension (^{1}D), followed by Ag^+-LC analysis of the collected fractions in the second dimension (^{2}D), for the analysis of TAGs in plant oils and animal fats, with atmospheric pressure chemical ionization (APCI) MS detection [15]. The orthogonality of the two separation modes resulted in the highest number of identified TAGs ever reported for the investigated samples. Despite the high potential of the developed multidimensional approach, the off-line techniques present inherent drawbacks as longer analysis time and the risks associated with sample manipulation. Conversely, on-line comprehensive LC approaches (2D-LC, LC×LC), using a modulator (switching valve) for the transfer of ^{1}D eluate to the second dimension, minimize sample losses and contamination; another advantage consists in the capability for system automation [16]. An on-line Ag^+-LC×NARP-LC set-up coupled to evaporative light scattering detection (ELSD) was exploited by Mondello *et al*., for the elucidation of the TAG composition in *Borago officinalis* oil [17]. In the work, 78 TAGs were tentatively identified identified based on their chromatographic behavior, since ELSD response, which is dependent upon the size and the shape of the analyte particles, was unable to provide information related to the molar masses. Furthermore, TAG species show limited UV absorbance at low wavelengths (205 or 210 nm) and the low sensitivity especially observed for saturated lipids makes the employment of UV detectors less useful in TAG analysis. As a result, MS is considered the most powerful technique to attain highly informative data for TAG identification and the employment of APCI interfaces provides a high ionization efficiency of non-polar analytes and an easier coupling to NARP-LC [18].

In this work, the TAG composition of a borage seed oil sample was investigated using an LC×LC set-up, based on the coupling of silver thiolate (^{1}D) and octadecylsilica (^{2}D) columns, in combination to ion trap-time of flight (IT-ToF) MS. The coupling of

orthogonal separation mechanism resulted to be useful strategy when dealing with highly complex food matrices. In addition, the group-type separation afforded by the proposed analytical approach may be useful to quickly fingerprint TAG components of oil samples. Finally, the use of MS represents an added dimension to the LC separation system, unravelling post-column co-eluting components and enabling the identification of a high number of TAGs in the examined sample.

5.2 Material and methods

5.2.1 Reagents and sample preparation

LC-MS grade butyronitrile (BN), *n*-hexane, acetonitrile (ACN) and 2-propanol employed for TAG analysis were obtained from Merck Life Science (Darmstadt. Germany). Borage oil was purchased at a local market, diluted in n-hexane (1000 ppm) and filtered through a 0.45 μm Whatman nylon membrane (Merck Life Science).

5.2.2 Instruments and analytical conditions

The analyses were performed on a Nexera LC-30A system consisting of a CBM-20A controller, a DGU-20A5R degassing unit, four LC-30AD parallel-flow pumps, a SIL-30AC autosampler and a CTO-20A column oven; the LC system was coupled to an LCMS-IT-ToF mass spectrometer through an APCI interface (Shimadzu Europa, Duisburg, Germany). The two LC dimensions were connected using two electronically controlled two-position, six-port high-pressure FCV-32AH switching valves, placed inside the column oven and equipped with two 11 μL empty loops. The entire system was controlled by the LCMSsolution software ver. 3.50.346 (Shimadzu Europa, Duisburg, Germany), while the LC×LC data were visualized and handled employing Chromsquare ver. 1.3 software (Shimadzu Europa, Duisburg, Germany).

^{1}D separations were performed on a lab-made silver thiolate column, 150 × 1.0 mm I.D., 5 μm *d.p.* and the employed mobile phases were: A) 1% BN in *n*-hexane and B) 10% BN in *n*-hexane. The flow rate was 7 μL/min and the gradient program was: 0 min, 10% B; 76 min, 25% B; 120 min, 35% B; 160 min, 85%B; the injection volume was 2 μL and the column oven was set at 30 °C. The modulation time was 1.5 min, corresponding to the ^{2}D gradient time.

^{2}D separations were carried out on a Titan C18 column, 50 × 4.6 mm I.D., 1.9 μm *d.p.* (Merck Life Science, Darmstadt, Germany) and the employed mobile phases were: A)

ACN and B) 2-propanol. The flow rate was 4 mL/min and the following repetitive gradient program was used: 0 to 0.12 min, 30% B; 0.16 min, 50% B; 1.20 min, 70% B; 1.21 min, 30% B (hold for 0.29 min). Concerning the MS detection, 1 mL of the ^{2}D flow was directed to an APCI source operated in positive ionization mode and the following parameters were set: detector voltage, 1.60 kV; interface temperature, 350 °C; CDL temperature, 250 °C; block heater temperature, 200 °C; nebulizing gas flow (N_2), 2.5 L/min; ion accumulation time, 30 msec; full scan range, 500 to 1100 m/z; event time, 300 ms (repeat, 3; ASC, 70%). Repeatability studies of the Ag^{+}-LC×NARP-UHPLC separation were performed by three injections of the borage seed oil sample (5 µL) over three consecutive days.

5.3 Results and Discussion

Vegetable oils, derived from plant sources, represent natural matrices predominantly constituted from TAGs. In detail, a high number of both saturated and unsaturated FAs are arranged in the formation of TAG species, being oleic, linoleic, linolenic, palmitic and stearic acids the most common FAs occuring in vegetable oils; in this field an extensive work has been carried out by Holčapek's research group [19].

Borago officinalis L. (borage) seed oil is considered one of the most complex plant oils and further represents a valuable source of γ-linolenic acid; thus, such product has a higher commercial value compared to conventional consumed edible oils [20, 21]. Given the high complexity of borage oil, highly efficient analytical approaches allowing for the comprehensive elucidation of borage TAG components have been exploited. As an example, octadecylsilica (ODS) columns were serially coupled in NARP-LC attaining additional separation power; however, the resulting increase in the identification capability was obtained at the price of long analysis times (e.g., two hours were required for the separation of 88 TAGs on a total column length of 45 cm) [14, 22, 23]. Another analytical strategy employed for borage oil analysis consisted in the use of an LC×LC set-up based on the coupling of micro-Ag^{+} and partially porous ODS columns, in ^{1}D and ^{2}D. respectively [17]. The combined use of the two separation mechanisms, with a complementary separation selectivity, allowed to allocate in the 2D-LC retention plane a total of 78 TAGs. Nevertheless, the employment of the ELSD as detection did not provide any structural information of the lipid components.

In this research, a pattern-type separation of borage seed oil TAGs was achieved by the development of an LC×LC approach, based on the coupling of Ag^+-LC and NARP-LC; further, the conditions of the latter technique ensured full compatibility with APCI-MS detection.

Given the independent separation mechanisms operating on the two stationary phases, the Ag^+-LC×NARP-LC represent one of the most orthogonal approaches in LC×LC. Separations in the two chromatographic dimensions were optimized separately and subsequently combined in the comprehensive approach, in which some stringent requirements needed to be met. In fact, Ag^+-LC and NARP-LC coupling is not straightforward due to the incompatibility of the solvents employed in the two dimensions and the possible lack of peak focusing at the head of the ^{2}D column. In the proposed approach, the potential mismatch between incompatible solvents and the possible lack of peak focusing were partially avoided by using a microbore column as ^{1}D. The latter in fact allowed the use of low operational flow rates (i.e. 7 μL/min), enabling the transfer of a very small ^{1}D eluent fraction to the ^{2}D dimension separation, in each modulation (i.e. 11 μL/min). The instrumental coupling was obtained through the employment of two electronically activated two-position, six-ports switching valves for within-loop automated fraction collection/re-injection, equipped with two identical storage loops of 11 μL; a schematic representation of the LC×LC setup is illustrated in Figure 5.1 (panel A and B).

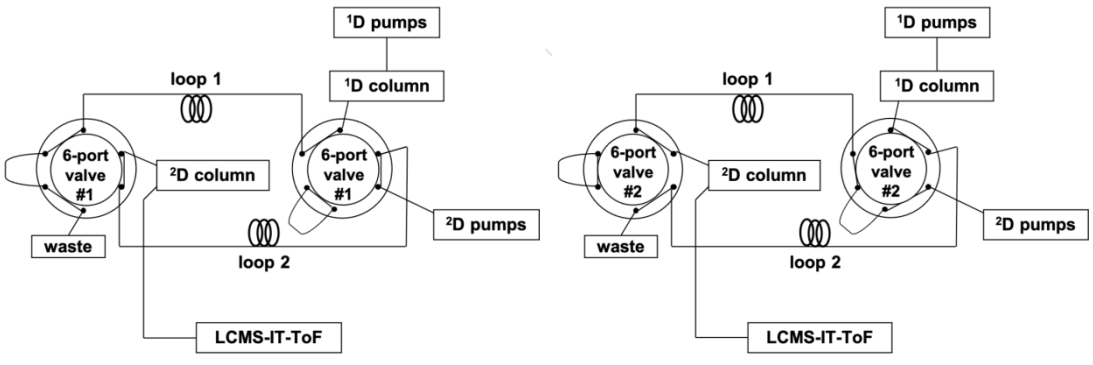

(**A**) (**B**)

Figure 5.1 Schematic representation of the LC×LC system, showing the routes for each ^{2}D separation, corresponding to different positions of the two six-port, two-position switching valves. (A) Loop 1 becomes filled with the ^{1}D eluent, while the ^{2}D pumps flush the content of loop 2 towards the ^{2}D column. (b) Loop 2 becomes filled with the ^{1}D eluent, while the ^{2}D pumps flush the content of loop 1 towards the ^{2}D column.

The modulation time of the switching valves was equal to the ^{2}D analysis time, enabling for the fractionation and the transfer of the ^{1}D effluent to the ^{2}D every 1.5 min. In fact, in LC × LC, the separation occurring in the second dimension must be completed before the injection of the subsequent fraction eluting from the first column; furthermore, the ^{2}D analysis should be fast enough to permit at least the transfer of three to four cuts, since undersampling of the ^{1}D peaks would determine a serious loss of information in the ^{2}D separation. As a result, the ^{2}D separation required a high mobile phase flow rate, i.e. 4 mL/min and a gradient starting with a very high percentage of the weaker solvent (ACN), to provide better on-column focusing. Furthermore, given the large differences of the sample components in terms of polarity and hydrophobicity, the employment of fast repetitive gradients revealed to be mandatory to enable components separation in a very short timeframe. Finally a fast ramp up to 70% of the stronger solvent (2-propanol) at the end of each gradient ensured the complete compound elution. A proper time for the column reconditioning (i.e. 17 s) within each gradient cycle was also allotted.

The need for very fast and efficient ^{2}D separation was accomplished by the use of a monodisperse silica column packed with sub-2 µm fully porous particles. Regarding the latter, it is acknowledged that the reduced particle size together with the ultra-narrow particle size distribution enable an increase of efficiency and allow for faster separation and short reconditioning times, as previously demonstrated [24–27].

In Figure 5.2 is showed the Ag^{+}-LC×NARP-UHPLC separation of a borage seed oil sample; the contour plot was obtained by APCI-MS in the positive ionization mode. As can be easily observed, TAG components are located in a distinctive way in the 2D space on the basis of their DB and PN values, as a result of the separations occurred in the ^{1}D and ^{2}D, respectively. In detail, TAGs identified in the borage oil sample covered an extensive range of DBs (0-9) and PN values (36-56); the components were resolved through the complementary separation mechanisms of Ag^{+}-LC×NARP-UHPLC.

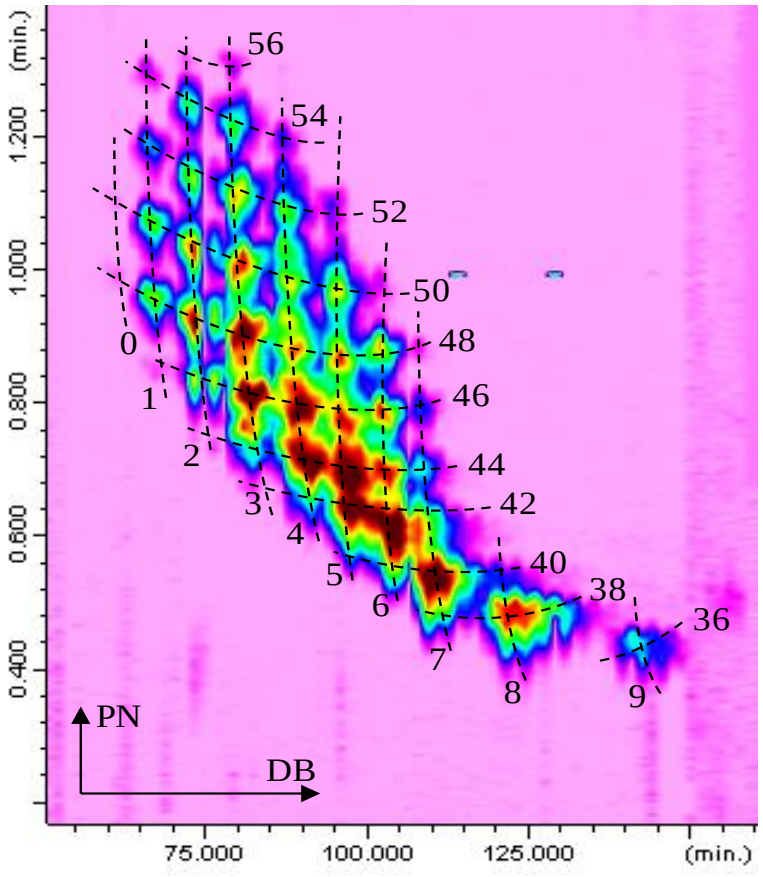

Figure 5.2 Ag^+-LC×NARP-UHPLC separation of a borage seed oil, relevant part of the TAGs elution region (total ion chromatogram obtained by APCI-MS in positive ion mode).

The Ag^+-LC×NARP-UHPLC system performances were evaluated in terms of peak capacity (n_C), calculated according to the method defined by Neue [28]:

$$n_C = 1 + \frac{t_g}{\left(\frac{1}{n}\right)\sum_1^n \omega}$$

Equation 5.1

where t_g represents the gradient time, n is the number of peaks selected for the calculation, and ω is the average peak width. The peak widths in the raw chromatograms, before interpolation by the 2D software, were employed for the calculation of the peak capacity in ^{1}D and ^{2}D. The theoretical $n_{C,2D}$ of the system obtained with a modulation

time of 1.5 min was calculated as equal to 925, being multiplicative of the values obtained in the two separation dimensions ($n_{C1} \times n_{C2}$). Nevertheless, the obtained values result to be overestimated if they do not take into account the degree of correlation between ^{1}D and ^{2}D separations (the "product rule") and the undersampling of the ^{1}D peaks, which practically lower the final peak capacity.

Specifically, the first factor has a significant influence on the RP×RP 2D LC systems, in which the retention mechanisms are substantially identical. Nevertheless, the system employed in this research consisted of truly orthogonal separation dimensions (Ag^{+} and RP), at least in principle. Conversely, the actual peak capacity achieved in ^{1}D was significantly affected by the undersampling effect and the contribution of this factor was quantitatively estimated by γ, according to the number of fractions effectively transferred for each peak. The undersampling effect was calculated on the basis of the approach proposed by Guiochon [29] and further developed by Carr [30,31], employing the following equation:

$$\gamma = \frac{\sqrt{r^2 + 3.424}}{r}$$

Equation 5.2

in which r is the fraction collection ratio, resulting by the relationship between the sampling time (i.e., the total analysis time in ^{2}D. $^{2}t_{cyc}$) and the average peak widths ($^{1}\omega$):

$$^{2}t_{cyc} = \frac{^{1}\omega}{r}$$

Equation 5.3

Given that the ^{2}D cycle time was 1.5 min (equal to the ^{2}D gradient time plus the reconditioning time) and the average first dimension peak widths was 3.89 min, the number of colleted fractions per average peak width was equal to 2.59. As a result, the peak capacity in ^{1}D was reduced by a γ factor of 1.23, obtaining a "practical" value of approximately 31. Equation 5.4 was applied for the calculation of the peak capacity of the Ag^{+}-LC×NARP-UHPLC system:

$$n_{C.2D} = \frac{{}^1t_G\,\lambda}{{}^2w}\frac{1}{\sqrt{r^2+3.424}}$$

Equation 5.4

in which ${}^1t_G$ represents the ^{1}D gradient time, λ is the ^{2}D gradient time (fraction of the ^{2}D cycle time devoted to the separation) and ${}^2w$ is the average peak width in ^{2}D (equal to 0.12 min in the employed system). Finally, the practical peak capacity value was calculated as equal to 507.

The intermediate precision or within-lab reproducibility of the Ag^+-LC×NARP-UHPLC approach was calculated by performing three analyses over three days; the retention times and peak areas of five selected peaks, corresponding to TAGs eluted within the 160 min ^{1}D gradient and covering the whole ^{2}D gradient duration, are reported in Table 5.1. The values were taken from the raw (non-interpolated) ^{2}D chromatogram.

TAG components were identified on the basis of their APCI-MS spectra, by evaluating $[M+H]^+$ ions for the molecular weight determination; furthermore, the in-source fragmentation obtained under positive ionization was employed for the structure elucidation. In fact the FAs composition of each TAG was inferred by the evaluation of diacylglycerol-like fragment ions (DG^+), resulting from the loss of a single FA moiety from the glycerol backbone. Specifically non-polar TAGs were easily ionized by APCI-MS and more abundant in-source fragmentation was observed for such components.

Table 5.1 Inter-day variabilities for TAGs retention times and peak areas (three injections).

	Retention Time (Minutes)		**Peak Area**	
Peak	$\bar{t}_R \pm s$	%RSD	$Average \pm s$	%RSD
1	141.005 ± 1.23	0.92	37,513,401 ± 2,479,635.81	6.61
2	111.005 ± 2.01	1.81	712,277,629 ± 40,314,913.8	5.66
3	97.505 ± 0.84	0.86	677,656,664 ± 45,470,762.2	6.71
4	73.505 ± 0.75	1.02	483,139,425 ± 29,906,330.4	6.19
5	61.505 ± 0.20	0.33	9,674,556 ± 248,636.089	2.57

$\bar{t}_R \pm s$, average retention time ± standard deviation; %RSD, relative standard deviation percentage.
* Total retention times are given by the sum of ^{1}D retention time + ^{2}D retention time.

As is well known, the cleavage of the FAs from the *sn*-2 position is less preferred compared to the *sn*-1/3 positions; such assumption is clearly evident from the higher abundance of the corresponding $[M+H\text{-}R_1COOH]^+$ and $[M+H\text{-}R_3COOH]^+$ fragment ions.

Hence $[M+H-R_2COOH]^+$ ions of lower intensity may be used for the determination of the FAs esterified at the *sn*-2 position [23]. Furthermore, the predominance of unsaturated FAs, as for the linoleic acid, in the *sn*-2 position of the TAGs found in vegetable oils has been extensively reported in literature [32].

In Table 5.2 a total of 94 TAGs identified in the borage seed oil sample are reported, as well as their DB and PN values, theoretical and experimental $[M+H]^+$ ions, mass accuracy (ppm) and observed DG^+ ions for each species. The investigated compounds were annotated employing initials of FA trivial names and the *sn*-1/3 positions were considered as equivalent; therefore, TAGs were named according to the decreasing molecular masses of the FAs, except for the central position assigned to unsaturated FAs, as commonly observed in plant oils [32].

As expected, three DG^+ ions were observed for those TAGs resulting from the combination of three different FAs, while only two or one DG^+ ions were observed for TAGs consisting of two or three moieties of the same FA, respectively. Accordingly, the TAG showing a $[M+H]^+$ ion of *m/z* 857.7504 and DG^+ ions at *m/z* 575.5003 (PL^+), 577.5140 (PO^+) and 601.5109 (LO^+) was assigned as the combination of oleic, palmitic and linoleic acid (i.e., the TAG OLP, #32 in Table 5.2).

Table 5.2 Triacylglycerols identified in borage seed oil, with their DB and PN values. For each species, m/z values of the theoretical and the experimental protonated molecular ions ([M+H]$^+$ theor and [M+H]$^+$ exp, respectively), the experimental mass accuracy (error in ppm) and the observed diglyceride ions (DG+ exp), are reported.

#	TAG	DB	PN	[M+H]$^+$ theor	[M+H]$^+$ exp	DG$^+$ exp	DG$^+$ exp	DG$^+$ exp	Error (ppm)
1	PPP	0	48	807.7436	nd	PP, 551.4641	-	-	-
2	SPP	0	50	835.7749	nd	SP, 579.5520	PP, 551.4970	-	-
3	POP	1	48	833.7593	nd	PP, 551.4877	PO, 577.5152	-	-
4	SOP	1	50	861.7906	nd	OP, 577.5122	SP, 579.5578	SO, 605.5433	-
5	SOS	1	52	889.8219	nd	SO, 605.5468	SS, 607.5575	-	-
6	AOP	1	52	889.8219	nd	AO, 633.5779	OP, 577.5107	AP, 607.5575	-
7	BOP	1	54	917.8532	nd	BO, 661.5996	OP, 577.5149	BP, 635.5797	-
8	AOS	1	54	917.8532	nd	AO, 633.5785	OS, 605.5499	AS, 635.5797	-
9	LgOP	1	56	945.8845	nd	LgO, 689.6104	OP, 577.5140	LgP, 663.6274	-
10	BOS	1	56	945.8845	nd	BO, 661.6147	SO, 605.5388	BS, 663.62840	-
11	PLP	2	46	831.7436	831.7494	PP, 551.5020	PL, 575.4978	-	6.9
12	OOP	2	48	859.7749	859.7733	PO, 577.5152	OO, 603.5265	-	1.9
13	SLP	2	48	859.7749	859.7733	SL, 603.5265	LP, 575.4973	SL, 603.5265	1.9
14	GOP	2	50	887.8062	887.8080	GO, 631.5566	OP, 577.5161	GP, 605.5420	2.0
15	ALP	2	50	887.8062	887.8080	AL, 631.5565	LP, 575.505	AP, 607.5447	2.0
16	SLS	2	50	887.8062	887.8080	SL, 603.5271	SS, 607.5447	-	2.0
17	SOO	2	50	887.8062	887.8080	OO, 603.5271	SO, 605.5420	-	2.0
18	C22:1OP	2	52	915.8375	915.8354	C22:1O, 659.5895	OP, 577.5151	C22:1P, 633.5715	2.3
19	AOO	2	52	915.8375	915.8354	AO, 633.5715	OO, 603.5296	-	2.3
20	GOS	2	52	915.8375	915.8354	GO, 631.5572	SO, 605.5437	GS, 633.5715	2.3
21	BLP	2	52	915.8375	915.8354	BL, 659.5895	LP, 575.4986	BP, 635.6066	2.3
22	ALS	2	52	915.8375	915.8354	AL, 631.5572	LO, 601.5243	AO, 633.5715	2.3
23	C24:1OP	2	54	943.8688	943.8705	C24:1O, 687.6199	OP, 577.5144	C24:1P, 661.6041	1.8
24	C22:1OS	2	54	943.8688	943.8705	C22:1O, 659.5888	OS, 605.5433	C22:1S, 661.6041	1.8

25	BOO	2	54	943.8688	943.8705	BO, 661.6041	OO, 603.5324	-	1.8
26	LgLP	2	54	943.8688	943.8705	LgL, 687.6196	LP, 575.4772	LgP, 663.6432	1.8
27	BLS	2	54	943.8688	943.8705	BL, 659.5888	LS, 603.5324	BS, 663.6432	1.8
28	C24:1OS	2	56	971.9001	nd	C24:1O, 687.5943	OS, 605.5515	C24:1S. 689.6465	-
29	LgOO	2	56	971.9001	nd	LgO, 689.6465	OO, 603.4264	-	-
30	LgLS	2	56	971.9001	nd	LgL, 687.5943	LS, 603.4264	LgS, 691.6627	-
31	PγLnP	3	44	829.7280	829.7257	PP, 551.5008	PγLn, 573.4831	-	2.8
32	OLP	3	46	857.7593	857.7545	PL, 575.5003	PO, 577.5140	LO, 601.5109	5.6
33	SγLnP	3	46	857.7593	857.7545	SγLn, 601.5109	PγLn, 573.4830	SP, 579.5282	5.6
34	OOO	3	48	885.7906	885.7939	OO, 603.5292	-	-	3.7
35	GLP	3	48	885.7906	885.7939	GL, 629.5392	LP, 575.5004	GP, 605.5375	3.7
36	SLO	3	48	885.7906	885.7939	LO, 601.5169	SL, 603.5292	SO, 605.5375	3.7
37	SγLnS	3	48	885.7906	885.7939	SS, 607.5575	SγLn, 601.5169	-	3.7
38	ALO	3	50	913.8219	913.8202	AL, 631.5587	LO, 601.5143	AO, 633.5729	1.9
39	BγLnP	3	50	913.8219	913.8202	BγLn, 657.5726	PγLn, 573.4856	BP, 635.5901	1.9
40	GLS	3	50	913.8219	913.8202	GL, 629.5421	LS, 603.5285	GS, 633.5729	1.9
41	GOO	3	50	913.8219	913.8202	GO, 631.5587	OO, 603.5285	-	1.9
42	C22:1OO	3	52	941.8532	941.8515	C22:1O, 659.5901	OO, 603.5278	-	1.8
43	C24:1LP	3	52	941.8532	941.8515	C24:1L, 685.6038	LP, 575.4989	C24:1P, 661.6040	1.8
44	C22:1OG	3	54	969.8845	969.8789	C22:1O, 659.5889	OG, 631.5591	C22:1G, 687.6163	5.8
45	C24:1OO	3	54	969.8845	969.8789	C24:1O, 687.6163	OO, 603.5286	-	5.8
46	C24:1LS	3	54	969.8845	969.8789	C24:1L, 685.6038	LS, 603.5286	C24:1S, 689.6339	5.8
47	LgLO	3	54	969.8845	969.8789	LgL, 687.6163	OL, 601.5146	LgO, 689.6339	5.8
48	C22:1OC22:1	3	56	997.9158	nd	C22:1O, 659.5894	C22:1C22:1, 715.648(	-	-
49	C24:1OG	3	56	997.9158	nd	C24:1O, 687.6221	OG, 631.5586	C24:1G, 715.6480	-
50	LLP	4	44	855.7436	855.7401	LP, 575.5005	LL, 599.4967	-	4.1
51	γLnOP	4	44	855.7436	855.7401	OγLn, 599.4967	PγLn, 573.4853	PO, 577.5146	4.1
52	OLO	4	46	883.7749	883.7694	OO, 603.5799	OL, 601.5135	-	6.2
53	SLL	4	46	883.7749	883.7694	LL, 599.4969	SL, 603.5799	-	6.2

54	GγLnP	4	46	883.7749	883.7694	GγLn, 627.5231	PγLn, 573.4848	GP, 605.5386	6.2
55	SOγLn	4	46	883.7749	883.7694	OγLn, 599.4969	SγLn, 601.5135	SO, 605.5386	6.2
56	GLO	4	48	911.8062	911.7993	GO, 631.5567	OL, 601.5146	GL, 629.5449	7.6
57	C22:1γLnP	4	48	911.8062	911.7993	C22:1γLn, 655.5573	γLnP, 573.4834	C22:1P, 633.5735	7.6
58	ALL	4	48	911.8062	911.7993	LL, 599.5042	AL, 631.5567	-	7.6
59	GγLnS	4	48	911.8062	911.7993	GγLn, 627.5336	SγLn, 601.5146	GS, 633.5735	7.6
60	C22:1LO	4	50	939.8375	939.8345	C22:1L, 657.5740	LO, 601.5142	C22:1O, 659.5886	3.2
61	GLG	4	50	939.8375	939.8345	GL, 629.5450	GG, 659.5886	-	3.2
62	BLL	4	50	939.8375	939.8345	BL, 659.5886	LL, 599.5040	-	3.2
63	C24:1γLnP	4	50	939.8375	939.8345	C24:1γLn, 683.5854	PγLn, 573.4833	C24:1P, 661.6029	3.2
64	C24:1LO	4	52	967.8688	967.8639	C24:1L, 685.6038	LO, 601.5137	C24:1O, 687.6177	5.1
65	LgLL	4	52	967.8688	967.8639	LgL, 687.6177	LL, 599.4961	-	5.1
66	C24:1γLnS	4	52	967.8688	967.8639	C24:1γLn, 683.5891	SγLn. 601.5137	C24:1S. 689.6338	5.1
67	C22:1LC22:1	4	54	995.9001	995.8919	C22:1L, 657.5935	C22:1C22:1, 715.6518	-	8.2
68	C24:1LG	4	54	995.9001	995.8919	C24:1G, 715.6449	GL, 629.5437	C24:1L, 685.6041	8.2
69	C24:1LC22:1	4	56	1023.9314	nd	C24:1C22:1, 743.7023	C22:1L, 657.5960	C24:1L, 685.6038	-
70	γLnLP	5	42	853.7280	853.7251	PγLn, 573.4852	LP, 575.4991	LγLn, 597.4786	3.4
71	OLL	5	44	881.7593	881.7557	LL, 599.4979	LO, 601.5102	-	4.1
72	OOγLn	5	44	881.7593	881.7557	OO, 603.5791	OγLn, 599.4979	-	4.1
73	SLγLn	5	44	881.7593	881.7557	SL, 603.5791	LγLn, 597.4829	SγLn, 601.5102	4.1
74	GLL	5	46	909.7906	909.7893	LL, 599.4985	GL, 629.5434	-	1.4
75	GOγLn	5	46	909.7906	909.7893	GO, 631.5538	OγLn, 599.4985	GγLn, 627.5617	1.4
76	ALγLn	5	46	909.7906	909.7893	AL, 631.5538	LγLn, 597.4820	ALn, 629.5434	1.4
77	C22:1LL	5	48	937.8219	937.8167	LL, 599.4983	C22:1L, 657.5733	-	5.5
78	BLγLn	5	48	937.8219	937.8167	BL, 659.5866	LγLn, 597.4889	BLn, 657.5733	5.5
79	C24:1LL	5	50	965.8532	965.8522	C24:1L, 685.6172	LL, 599.4981	-	1.0
80	C24:1OγLn	5	50	965.8532	965.8522	C24:1O, 687.6172	OγLn, 599.4981	C24:1γLn, 683.5902	1.0
81	C22:1γLnC22:1	5	52	993.8845	993.8809	C22:1γLn, 655.5937	C22:1C22:1, 715.6605	-	3.6
82	γLnγLnP	6	40	851.7123	851.7112	γLnγLn, 595.4679	PγLn, 573.4847	-	1.3

83	LLL	6	42	879.7436	879.7394	LL, 599.4968	-	-	4.8
84	OLγLn	6	42	879.7436	879.7394	OL, 601.5088	LγLn, 597.4845	OγLn, 599.4968	4.8
85	SγLnγLn	6	42	879.7436	879.7394	γLnγLn, 595.4684	SγLn, 601.5088	-	4.8
86	GLγLn	6	44	907.7749	907.7733	GL, 629.5408	LγLn, 597.4845	GγLn, 627.5283	1.8
87	C22:1LγLn	6	46	935.8062	935.8065	C22:1L, 657.5728	LγLn, 597.4825	C22:1γLn, 655.561	0.3
88	C24:1LγLn	6	48	963.8375	963.8337	C24:1L, 685.6049	LγLn, 597.4802	C24:1γLn, 683.590	3.9
89	γLnγLnPo	7	38	849.6967	849.6957	γLnγLn, 595.4453	PoγLn, 571.4680	-	1.2
90	LLγLn	7	40	877.7280	877.7222	γLnL, 597.4834	LL, 599.4971	-	6.6
91	γLnOγLn	7	40	877.7280	877.7222	OγLn, 599.4971	γLnγLn, 595.4707	-	6.6
92	GγLnγLn	7	42	905.7593	905.7592	GγLn, 627.5271	γLnγLn, 595.4721	-	0.1
93	γLnLγLn	8	38	875.7123	875.7076	LγLn, 597.4819	γLnγLn, 595.4669	-	5.4
94	γLnγLnγLn	9	36	873.6967	873.6966	γLnγLn, 595.4670	-	-	0.1

Abbreviations of FAs: P, palmitic (C16:0); Po, palmitoleic (C16:1); S, stearic (C18:0); O, oleic (C18:1); L, linoleic (C18:2); Ln, linolenic (C18:3); A, arachidic (C20:1); G, gadoleic (C20:1); B, behenic (C22:0); Lg, lignoceric (C24:0).

Conversely, for the TAG showing a $[M+H]^+$ of *m/z* 885.7939 a single DG^+ ion at *m/z* 603.5292 (OO^+) was observed, therefore, such species was identified as triolein (i.e., the TAG OOO, #34 in Table 5.2).

The TAG composition of borage seed oil highlighted the high content in ω-6 polyunsaturated FAs (PUFAs), with regard to linoleic acid and γ-linolenic acid (18:2 and 18:3, respectively), in agreement with previous works [20,23].

As proof of the usefulness of the LC×LC approach in the resolution of the complex TAG mixture of the investigated sample, the species LLP, OLO, GLO, GLG, C24:1LO (#50, #52, #56, #61 and #64, in Table 5.2) are reported by way of example. The above-mentioned TAGs are characterized by the same unsaturation degree (DB = 4) and would coelute under monodimensional Ag^+-LC conditions; however, they were successfully separated under the ^{2}D NARP-UHPLC conditions, according to their different PN values (i.e., 44, 46, 48, 50 and 52). Furthermore, the retention mechanism in Ag^+-LC also enables separation on the basis of the distribution of the unsaturations within the FAs contained in the TAG components [33]; as a consequence, it was possible to partially separate species showing the same DB and PN values. In detail, among TAGs with the same number of DBs, the species in which the unsaturations are concentrated in one acyl moiety are generally retained more strongly [34,35]. As an example, the TAGs OLP and SγLnP (#32 and #33 in Table 5.2) are characterized by the same DB and PN value (3 and 46, respectively), but show a different distribution of the unsaturations in the FA chains. Specifically, in OLP the three DBs are distributed in two FA moieties (i.e., one in O and two in L), while in SγLnP all the unsaturations are located in a single FA (i.e., γLn). Due to these differences, the TAGs were partially separated by Ag^+-LC×NARP-UHPLC, being SγLnP more strongly retained, compared to OLP [36].

In Figure 5.3 are reported the APCI-MS spectra of OLP (panel A) and SγLnP (panel B); as can be observed, the two isobaric molecules generated identical $[M+H]^+$ ions, but different DG^+ fragment ions. For the species OLP, the ions at *m/z* 577.5140 (PO^+), 575.5003 (PL^+) and 601.5109 (LO^+) were observed, while the ions at *m/z* 601.5109 ($S\gamma Ln^+$), 573.4830 ($P\gamma Ln^+$) and 579.5282 (SP^+) were observed for SγLnP.

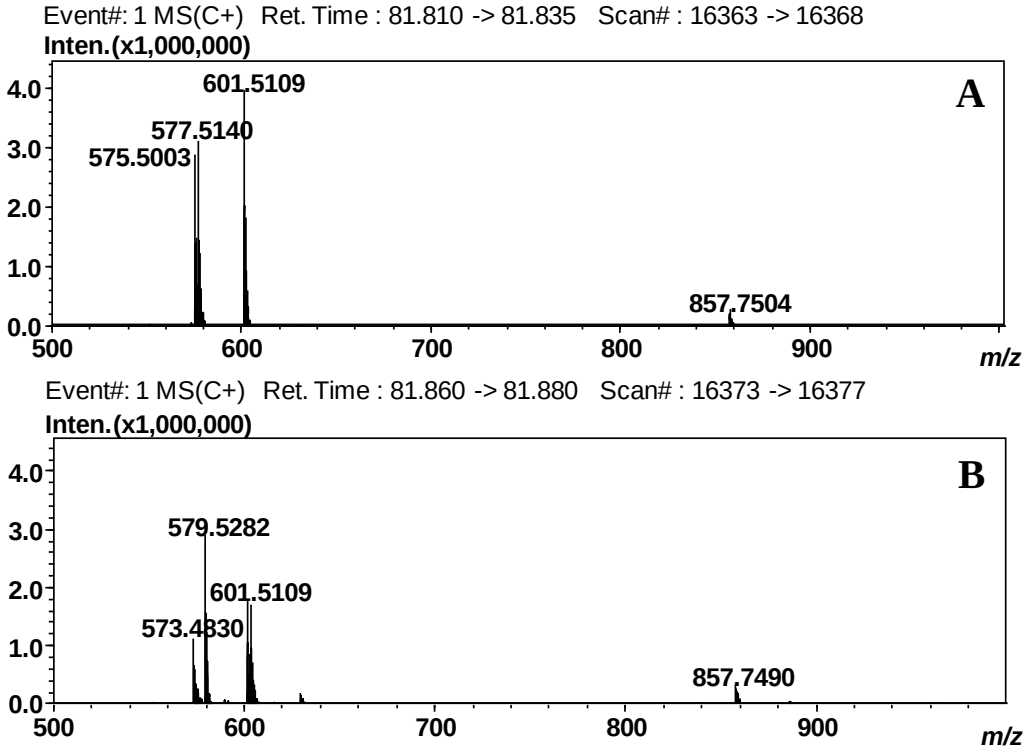

Figure 5.3 APCI-MS spectra obtained for the peaks of OLP (panel A) and SγLnP (panel B).

5.4 Conclusions

In this work, the TAG composition of a borage seed oil was investigated by Ag^+-LC×NARP-UHPLC coupled to APCI-MS detection, enabling the identification of 94 lipid species. The coupling of two orthogonal separation techniques provided a characteristic pattern-type distribution of the TAG components in the 2D space, according to their DB (ranging from 0 to 9) and PN values (ranging from 36 to 56). The proposed approach may represent a useful strategy when dealing with complex matrices; furthermore, the obtained group-type separation allows for a quick TAG fingerprint which may serve to discriminate different samples.

5.5 References

1. Donato P., Cacciola F., Beccaria M., Dugo P., Mondello L. Lipidomics, In Comprehensive Analytical Chemistry, Advanced Mass Spectrometry for Food Safety and Quality, Picó Y., Ed., Elsevier: Amsterdam, The Netherlands, 2015, Volume 68, pp. 395–439.

2. Buchgraber M., Franz U., Hendrik E., Elke A. Triacylglycerol profiling by using chromatographic techniques. Eur. J. Lipid Sci. Technol. 2004, 106, 621–648.
3. Donato P., Dugo P., Mondello L. Separation of Lipids, In Liquid Chromatography. Fanali S., Haddad P.R., Poole C.F., Schoenmakers P., Lloyd D., Eds., Elsevier: Amsterdam, The Netherlands, 2013, pp. 203–248.
4. Donato P., Inferrera V., Sciarrone D., Mondello L. Supercritical fluid chromatography for lipid analysis in foodstuffs. J. Sep. Sci. 2017, 40, 361–382.
5. Donato P., Micalizzi G., Oteri M., Rigano F., Sciarrone D., Dugo P., Mondello L. Comprehensive lipid profiling in the mediterranean mussel (*Mytilus galloprovincialis*) using hyphenated and multidimensional chromatography techniques coupled to mass spectrometry detection. Anal. Bioanal. Chem. 2018, 410, 3297–3313.
6. Holčapek. M., Liebisch. G., Ekroos. K. Lipidomic Analysis. Anal. Chem. 2018. 90. 4249−4257.
7. Holčapek M., Lísa M. Silver-ion liquid chromatography–mass spectrometry, In Handbook of Advanced Chromatography/Mass Spectrometry Techniques. Holčapek M., Byrdwell W.C., Eds., Elsevier: London, UK, 2017, Volume 3, pp. 115–140.
8. Dobson G., Christie W.W., Nikolova-Damyanova B. Silver ion chromatography of lipids and fatty acids. J. Chromatogr. B Biomed. Appl. 1995, 671, 197–222.
9. Momchilova S.M., Nikolova-Damyanova B.M. Advances in silver ion chromatography for the analysis of fatty acids and triacylglycerols-2001 to 2011. Anal. Sci. 2012, 28, 837–844.
10. Dillon J.T., Aponte J.C., Tarozo R., Huang Y. Efficient liquid chromatographic analysis of mono-, di-, and triglycerols using silver thiolate stationary phase. J. Chromatogr. A 2012, 1240, 90–95.
11. Aponte J.C., Dillon J.T., Tarozo R., Huang Y. Separation of unsaturated organic compounds using silver–thiolate chromatographic material. J. Chrom. A 2012, 1240, 83–89.
12. Cacciola F., Donato P., Sciarrone D., Dugo P., Mondello L. Comprehensive liquid chromatography and other liquid-based comprehensive techniques coupled to mass spectrometry in food analysis. Anal. Chem. 2017, 89, 414−429.
13. Dugo P., Beccaria M., Fawzy N., Donato P., Cacciola F., Mondello L. Mass spectrometric elucidation of triacylglycerol content of Brevoortia tyrannus (menhaden) oil using non-aqueous reversed-phase liquid chromatography under ultra high pressure conditions. J. Chromatogr. A 2012, 1259, 227–236.
14. Lísa M., Holčapek M. Triacylglycerols in nut and seed oils: Detailed characterization using high-performance liquid chromatography/mass spectrometry, In Nuts and Seeds in Health and Disease Prevention. Preedy V.R., Watson R.R., Patel V.B., Eds., Academic Press: London, UK, 2011, pp. 43–54.
15. Holčapek M., Velínská H., Lísa M., Cesla P. Orthogonality of silver-ion and non-aqueous reversed-phase HPLC/MS in the analysis of complex natural mixtures of triacylglycerols. J. Sep. Sci. 2009, 32, 3672–3680.

16. Stoll D.R., Carr P.W. Two-Dimensional liquid chromatography: A state of the art tutorial. Anal. Chem. 2017, 89, 519−531.
17. Mondello L., Beccaria M., Donato P., Cacciola F., Dugo G., Dugo P. Comprehensive two-dimensional liquid chromatography with evaporative light scattering detection for the analysis of triacylglycerols in Borago officinalis. J. Sep. Sci. 2011, 34, 688–692.
18. Holčapek M., Lísa M., Jandera P., Kabátová N. Quantitation of triacylglycerols in plant oils using HPLC with APCI-MS. evaporative light-scattering. and UV detection. J. Sep. Sci. 2005, 28, 1315–1333.
19. Holčapek M., Jandera P., Zderadička P., Hrubá L. Characterization of triacylglycerol and diacylglycerol composition of plant oils using high-performance liquid chromatography-atmospheric pressure chemical ionization mass spectrometry. J. Chromatogr. A 2003, 1010, 195–215.
20. Eskin N.A.M. Borage and evening primrose oil. Eur. J. Lipid Sci. Technol. 2008, 110, 651–654.
21. Asadi-Samani M., Bahmani M., Rafieian-Kopaei M. The chemical composition, botanical characteristic and biological activities of Borago officinalis: A review. Asian Pac. J. Trop. Med. 2014, 7, S22–S28.
22. Lísa M., Holčapek M., Boháč M. Statistical Evaluation of Triacylglycerol Composition in Plant Oils Based on High-Performance Liquid Chromatography Atmospheric Pressure Chemical Ionization Mass Spectrometry Data. J. Agric. Food Chem. 2009, 57, 6888–6898.
23. Lísa M., Holčapek M. Triacylglycerols profiling in plant oils important in food industry. dietetics and cosmetics using high-performance liquid chromatography–atmospheric pressure chemical ionization mass spectrometry. J. Chromatogr. A 2008, 1198–1199, 115–130.
24. Ismail O.H., Catani M., Pasti L., Cavazzini A., Ciogli A., Villani C., Kotoni D., Gasparrini F., Bell D.S. Experimental evidence of the kinetic performance achievable with columns packed with the new 1.9 μm fully porous particles Titan C18. J. Chromatogr. A 2016, 1454, 86–92.
25. Sommella E., Pepe G., Ventre G., Pagano F., Manfra M., Pierri G., Ismail O., Ciogli A., Campiglia P. Evaluation of two sub-2 μm stationary phases, core-shell and totally porous monodisperse, in the second dimension of on-line comprehensive two dimensional liquid chromatography, a case study: Separation of milk peptides after expiration date. J. Chromatogr. A 2015, 1375, 54–61.
26. Broeckhoven K., Desmet G. Advances and Innovations in Liquid Chromatography Stationary Phase Supports. Anal. Chem. 2021, 93, 257−272.
27. Catani M., Ismail O.H., Cavazzini A., Ciogli A., Villani C., Pasti L., Bergantin C., Cabooter D., Desmet G., Gasparrini F. Rationale behind the optimum efficiency of columns packed with new 1.9 μm fully porous particles of narrow particle size distribution. J. Chromatogr. A 2016, 1454, 78–85.

28. Neue U.D. Theory of peak capacity in gradient elution. J. Chromatogr. A 2005, 1079, 153–161.
29. Horváth K., Fairchild J.N., Guiochon G. Generation and Limitations of Peak Capacity in Online Two-Dimensional Liquid Chromatography. Anal. Chem. 2009, 81, 3879–3888.
30. Gu H., Huang Y., Carr P.W. Peak capacity optimization in comprehensive two dimensional liquid chromatography: A practical approach. J. Chromatogr. A 2011, 1218, 64–73.
31. Davis J.M., Stoll D.R., Carr P.W. Effect of First-Dimension Undersampling on Effective Peak Capacity in Comprehensive Two-Dimensional Separations. Anal. Chem. 2008, 80, 461–473.
32. Lísa M., Netušilová K., Franěk L., Dvořáková H., Vrkoslav V., Holčapek M. Characterization of fatty acid and triacylglycerol composition in animal fats using silver-ion and non-aqueous reversed-phase high-performance liquid chromatography/mass spectrometry and gas chromatography/flame ionization detection. J. Chromatogr. A 2011, 1218, 7499–7510.
33. Nikolova-Damyanova B. Retention of lipids in silver ion high-performance liquid chromatography: Facts and assumptions. J. Chromatogr. A 2009, 1216, 1815–1824.
34. Christie W.W. Separation of molecular species of triacylglycerols by high-performance liquid chromatography with a silver ion column. J. Chromatogr. A 1988, 454, 273–284.
35. Neff W.E., Adlof R.O., List G.R., El-Agaimy M. Analyses of Vegetable Oil Triacylglycerols by Silver Ion High Performance Liquid Chromatography with Flame Ionization Detection. J. Liq. Chromatogr. 1994, 17, 3951–3968.
36. Pattern-type separation of triacylglycerols by silver thiolate×non-aqueous reversed phase comprehensive liquid chromatography. Arena P., Sciarrone D., Dugo P., Donato P., Mondello L. Separations 2021, 8, 88.

6 Characterization of triacylglycerols in plant oils by means of subcritical solvent chromatography

6.1 Introduction

In recent times, considerable scientific efforts have been put in the development of analytical approaches allowing for triacylglycerols (TAGs) analysis and profiling, due to the importance of this task in different research fields [1-3] including food, pharmaceutical and clinical applications.

TAG components have a fundamental role in human nutrition, since they represent the main source of free fatty acids (FAs) and polyunsaturated fatty acids (PUFAs); in fact, the latter represent the direct substrates for energy production via the beta oxidation pathway and are involved in genes regulations and in the constitution of biological membranes [4-5]. Furthermore, PUFAs are precursors of biologically active metabolites, as the eicosanoids, while FAs such as α-linolenic acid (ALA, C18:3, omega-3) and linoleic acid (LA, C18:2, omega-6) are essential for humans, and their deficiency can result in retarded growth, dermatitis, kidney diseases, and several brain disorders [6-8].

TAGs represent the major constituents of most animal fats and vegetable oils of commercial relevance; as a result, their characterization may be highly useful to confirm authenticity of such products or detect possible adulterations, as well as for the prediction of physical/physiological properties of foods. For all these reasons the development of suitable analytical methods for TAG analysis and profiling is highly demanded in food industry [9,10].

Different chromatographic techniques have been traditionally employed for TAG analysis, including thin layer chromatography (TLC), liquid chromatography (LC), capillary electrochromatography (CEC), gas chromatography (GC), and supercritical/subcritical fluid chromatography (SFC/SubFC) [11]. Multidimensional approaches have also been exploited for the analysis of complex samples, aiming at enhancing the resolving power of the chromatographic systems [12-14]. As for detection, the coupling to mass spectrometry (MS) results to be highly useful since it provides complementary information to retention data, consisting of molecular weight and eventually fragment ions [15,16].

HPLC approaches employing reversed-phase (RP) and silver ion (Ag^+) separation modes have been widely applied for the separation of TAGs, either independently, or in off-line

or on-line combinations; the latter exploiting the complementary nature of the two retention mechanisms and, thus, of the information attainable. In RP-LC, retention of TAGs increases with the increasing degree of hydrophobicity, commonly expressed in terms of partition number (PN), as given by the sum of the total carbon number of all acyl chains (CN), minus twice the number of double bonds (DB): PN=CN-2DB [17]. Conversely, in Ag^+LC TAG separation is ruled by the unsaturation degree, and the distribution of DBs in the FA chains. Both RP- and Ag^+LC rely on the use of low polarity, non-aqueous (NA) mobile phases, well suited to the non-polar nature of TAGs; one main advantage of both techniques consists in the use of mild temperatures, so that degradation risks of the more labile long-chain PUFAs are minimized [18].

On the other hand, SFC is much suitable for lipid analysis, and the reduced organic solvent consumption with respect to LC has favourable fallout in terms of toxicity, costs, and environmental impact. Furthermore, the low mobile phase viscosity and higher diffusion coefficients allow for faster or more efficient separations to be attained, by the use of high linear velocities or longer columns, respectively. Additionally, shorter re-equilibration times are needed, after each gradient elution in SFC, allowing for faster separations and/or better resolution to be achieved [19]. Advantages of the use of SFC over other chromatographic techniques practised for lipid analysis, and notably for TAG analysis have been extensively discussed [20-22]. Furthermore, most recent instrumental developments, together with the employment of sub-2 μm and superficially porous particles columns, the higher pressure capabilities and novel design of backpressure regulators have contributed to make efficiency and sensitivity of modern SFC comparable to that of HPLC or ultra-high pressure HPLC (UHPLC). At the same time, a number of packing materials specifically tailored for SFC have been introduced, affording improved selectivity, peak shape, and sample capacity [23-29].

In recent years SFC has decisively shifted its focus on the use of carbon dioxide mixed with other co-solvents (or modifiers). The addition of small percentages of a polar organic co-solvent to the CO_2 mobile phase results to be highly convenient to allow the solubility of more polar analytes, in such way extending the range of amenable analytes. In detail, the use of a modifier affects the selectivity, by introducing additional hydrogen bonding or dipole-dipole interactions; however it determines an increase of the critical temperature and pressure of pure CO_2. A practical consequence is that, under a typical gradient

program at the mild temperatures adopted for the separations, a subcritical fluid will be obtained very quickly, while the conditions required to maintain a supercritical mobile phase would be impracticable. As a result, most of SFC separations are performed under subcritical conditions [30].

Applications of packed SFC (pSFC) to the task of TAG profiling in foodstuffs have been recently described [31], mainly using octadecylsilica (ODS) columns. Retention of TAGs on ODS stationary phases closely resembles that observed under NARP-LC conditions, being PN the main factor which rules the separation; further, for TAGs within the same PN group, a linear relationship between TAG retention and their DB values has been demonstrated.

The aim of this research work was the elucidation of the TAG profile in vegetable oils of different origin, using CO_2 as the main mobile phase solvent, under subcritical conditions. In addition, the coupling to quadrupole time of flight (Q-ToF) MS detection through APCI ionization allowed for the identification of the investigated compounds. The proposed approach, compared to the conventional LC separations, allowed for a consistent reduction of the analysis time, organic solvent consumption and environmental impact.

6.2 Material and methods

6.2.1 Reagents

Compressed CO_2 (99.9% grade) used as the main mobile phase was from Rivoira (Milan, Italy); LC-MS grade solvents (acetonitrile (AcN), ethanol (EtOH), *n*-hexane, isopropyl alcohol (IPA), and methanol (MeOH), used as the modifier or sample diluent) and standard TAGs (trilinolein (C18:2/C18:2/C18:2) and 1,3-palmitin-2-olein (C16:0/C18:1/C16:0)) were from Merck Life Science (Darmstadt, Germany).

6.2.2 Samples and sample preparation

Samples of borage oil (*Borago officinalis*), corn oil (*Zea mays*), refined hazelnut oil (*Corylus colurna*), extravirgin olive oil (*Olea europaea*), palm oil (*Elaeis guineensis*), peanut oil (*Arachishypogaea*), and soybean oil (*Glycine max*) were from a local market. All samples were filtered through 0.45 µm Acrodisc nylon membrane filter (Pall Life

Sciences, Ann Arbor, MI, USA) and diluted with IPA (around 1000 ppm) prior to SubFC-MS analyses.

6.2.3 Instruments and analytical conditions

SubFC-MS analyses were performed on an Acquity UPC^2 (Ultra Performance Convergence Chromatography) system consisting of: UPC^2 Binary Solvent Manager (BSM), Sample Manager-FL, UPC^2 Convergence Manager, Column Manager-A. The system was hyphenated to Synapt G2-S quadrupole time of flight (Q-ToF) mass spectrometer through an atmospheric pressure chemical ionization (APCI) interface. All instruments were from Waters Corporation (Milford, MA, USA).

Chromatographic separations were carried out on Ascentis Express C18 (100×30 mm i.d., 2.0 μm *d.p.*, partially porous) column Merck Life Science (Darmstadt, Germany), at a constant mobile phase flow rate of 1.0 mL/min. The injection volume was 2 μL. The following experimental parameters were investigated: nature and percentage of modifier (AcN, EtOH, IPA) into compressed CO_2, type of elution (isocratic *vs.* gradient), gradient steepness, pressure of the active backpressure regulator (ABPR, 1500 psi and 3000 psi), and column temperature (20° C and 30° C). Under optimized experimental conditions, SubFC separation of the vegetable oil samples was achieved under the following conditions: column temperature, 20° C; ABPR set, 1500 psi; gradient elution of AcN into CO_2, 0-5 min, 5% B, 5-20 min, to 30% B, hold for 3 min.

Q-ToFMS spectra were acquired under the following conditions: ionization mode, APCI positive; scan range, 100 to 1200 *m/z*; source temperature, 120° C; probe temperature, 400° C; desolvationgas (N_2) flow, 400 L/h; nebulizer gas flow (N_2), 4.5 bar; corona current, 4 μA; sampling cone, 40 V.

The effluent from the SFC system was delivered to the MS interface by means of the shortest length (about 30 cm) of insulated peek tubing (0.005 in i.d). Leucine enkephalin was used as the lock mass and detected at *m/z* 556.2771 (positive ionization). The SFC and MS instruments were controlled by separate processors, both using MassLynxsoftware V4.1 (SCN916) for data acquisition and processing; an external trigger event was set, to start the MS acquisition right after SFC analysis start.

6.3 Results and Discussion

Analysis of plant oil samples (borage, corn, hazelnut, olive, palm, peanut, and soybean oil) was carried out by means of SFC on a 10-cm ODS column consisting of superficially porous particles (2.7 μm), under subcritical conditions. Detection by APCI-Q-ToF MS allowed the identification in the vegetable oils of a total of 122 different TAGs, listed in Table 6.1, on the basis of the observed protonated molecular ions and in-source originated fragment ions (diacylglycerols, DAGs).

For method optimization, in terms of TAG separation, peak shape, and analysis time, the effect of selected parameters was investigated, i.e.: column temperature (20-30 °C), nature and percentage of the organic modifier (AcN, EtOH, IPA) into compressed CO_2, type of elution (isocratic *vs.* gradient), gradient steepness, ABPR setting (1500 psi and 3000 psi, corresponding to 103 and 207 bar, respectively). The retention behaviour of TAGs on RP ODS columns as a function of the temperature has been previously investigated, with neat CO_2 as the mobile phase (at a pressure of 150 bar) [32]. It has been demonstrated that in the supercritical region (35-45 °C) TAG retention increases with increasing temperature, due to the decrease of density, while an opposite behaviour was observed by lowering the temperature below the critical point of 31.3 °C. In the subcritical region employed in this work (20-30 °C) and in the presence of low modifier contents (< 20%) added to CO_2 mobile phase it was observed that TAG retention decreased with increasing temperature, in a similar way to HPLC, but to a lesser extent. In accordance with previous research [33], the separation of TAGs containing saturated FAs (such as miristic acid, palmitic acid, and stearic acid) was more affected by changes in the temperature, with respect to the other molecules, probably as a result of the larger changes in the solubility. On the basis of the results obtained, all subsequent experiments were carried out at a column temperature of 20 °C. Concerning the mobile phase to be employed for TAG separation, in search of optimum selectivity, AcN, EtOH and IPA were evaluated as co-solvents. The best results were obtained using the solvent mixture AcN/CO_2; the selected mobile phase, compared to the others, provided the reduction of the coelutions of TAGs showing different PN values and allowed for the separation of the most abundant TAGs belonging to the same PN.

In detail, a steep gradient was employed, starting from 5% AcN, and increasing the modifier percentage into CO_2 to 30% in 20 min, linearly.

Table 6.1 TAG composition of different vegetable oil samples, reported according to the increasing PN and DB values, obtained by SubFC on a C18 column. The theoretical m/z values of the protonated molecular ions are also reported.

#	TAGs	PN	DB	$[M+H]^+_{theor.}$	Borage	Corn	Olive	Hazelnut	Palm	Peanut	Soybean
1	γLnγLnγLn	36	9	873.6967	*						
2	γLnγLnPo	38	7	849.6967	*						
3	LnLLn	38	8	875.7123							*
4	γLnLγLn	38	8	875.7123	*						
5	LnLnP	40	6	851.7123							*
6	γLnγLnP	40	6	851.7123	*						
7	LLLn	40	7	877.728		*			*		*
8	LLγLn	40	7	877.728	*						
9	LnOLn	40	7	877.728							*
10	γLnOγLn	40	7	877.728	*						
11	LLPo	42	5	853.728		*					
12	LnLP	42	5	853.728		*				*	*
13	γLnLP	42	5	853.728	*						
14	LLL	42	6	879.7436	*	*		*	*	*	*
15	OLLn	42	6	879.7436		*	*	*		*	*
16	SLnLn	42	6	879.7436						*	*
17	OLγLn	42	6	879.7436	*						
18	SγLnγLn	42	6	879.7436	*						
19	GγLnγLn	42	7	905.7593	*						
20	PLM	44	2	803.7123					*		
21	PLnP	44	3	829.728		*			*		*
22	PγLnP	44	3	829.728	*						
23	OLM	44	3	829.728					*		
24	PPoL	44	3	829.728							

25	LLP	44	4	855.7436	*	*	*	*	*	*	*
26	OLPo	44	4	855.7436			*	*		*	
27	LnOP	44	4	855.7436		*	*		*	*	*
28	γLnOP	44	4	855.7436	*						
29	OLL	44	5	881.7593	*	*	*	*	*	*	*
30	OOLn	44	5	881.7593			*	*	*		*
31	SLLn	44	5	881.7593							*
32	OOγLn	44	5	881.7593	*						
33	SLγLn	44	5	881.7593	*						
34	GLγLn	44	6	907.7749	*						
35	C20:2LL	44	6	907.7749							*
36	PPM	46	0	779.7123					*		
37	POM	46	1	805.728					*		
38	POPo	46	2	831.7436			*	*	*		
39	PLP	46	2	831.7436	*	*	*	*	*	*	*
40	OOM	46	2	831.7436					*		
41	OOPo	46	3	857.7593			*	*			
42	OLP	46	3	857.7593	*	*	*	*	*	*	*
43	SLnP	46	3	857.7593						*	*
44	SγLnP	46	3	857.7593	*						
45	OLO	46	4	883.7749	*	*	*	*	*	*	*
46	SLL	46	4	883.7749	*	*				*	*
47	SOLn	46	4	883.7749		*	*			*	*
48	SOγLn	46	4	883.7749	*						
49	GγLnP	46	4	883.7749	*						
50	GLL	46	5	909.7906	*	*				*	*
51	GOγLn	46	5	909.7906	*						
52	ALγLn	46	5	909.7906	*						

53	C22:1LγLn	46	6	935.8062	*							
54	PPP	48	0	807.7436						*	*	
55	POP	48	1	833.7593	*	*	*	*	*	*	*	*
56	OOP	48	2	859.7749	*	*	*	*	*	*	*	*
57	SLP	48	2	859.7749	*	*		*	*	*	*	*
58	OOO	48	3	885.7906	*	*	*	*	*	*	*	*
59	GLP	48	3	885.7906	*	*					*	*
60	SLO	48	3	885.7906	*	*	*	*	*	*	*	*
61	SγLnS	48	3	885.7906	*							
62	GγLnS	48	4	911.8062	*							
63	GLO	48	4	911.8062	*	*	*	*			*	*
64	ALL	48	4	911.8062	*	*					*	*
65	C22:1γLnP	48	4	911.8062	*							
66	C22:1LL	48	5	937.8219	*						*	
67	BLLn	48	5	937.8219								*
68	BLγLn	48	5	937.8219	*							
69	C24:1LγLn	48	6	963.8375	*							
70	SPP	50	0	835.7749						*		
71	SOP	50	1	861.7906	*	*	*	*	*	*	*	*
72	GOP	50	2	887.8062	*	*	*			*	*	*
73	ALP	50	2	887.8062	*	*	*			*	*	*
74	SLS	50	2	887.8062	*	*					*	*
75	SOO	50	2	887.8062	*	*	*	*	*	*	*	*
76	GOO	50	3	913.8219	*	*	*	*			*	*
77	ALO	50	3	913.8219	*	*	*			*	*	*
78	GLS	50	3	913.8219	*							
79	BγLnP	50	3	913.8219	*							
80	C22:1LO	50	4	939.8375	*						*	

81	GLG	50	4	939.8375	*							
82	BLL	50	4	939.8375	*	*	*				*	*
83	C24:1γLnP	50	4	939.8375	*							
84	C24:1OγLn	50	5	965.8532	*							
85	C24:1LL	50	5	965.8532	*							
86	LgLLn	50	5	965.8532								*
87	C23:0LL	51	4	953.8532							*	
88	APP	52	0	863.8062						*		
89	SSP	52	0	863.8062						*		
90	AOP	52	1	889.8219	*	*	*	*		*	*	
91	SOS	52	1	889.8219	*	*	*	*		*	*	
92	GOS	52	2	915.8375	*							
93	AOO	52	2	915.8375	*	*	*	*		*	*	*
94	BLP	52	2	915.8375		*				*	*	*
95	ALS	52	2	915.8375	*	*						*
96	C22:1OP	52	2	915.8375	*							
97	C22:1OO	52	3	941.8532	*						*	
98	C24:1LP	52	3	941.8532	*							
99	BLO	52	3	941.8532		*	*			*	*	*
100	C24:1LO	52	4	967.8688	*							
101	LgLL	52	4	967.8688	*	*	*				*	*
102	C24:1γLnS	52	4	967.8688	*							
103	C22:1γLnC22:1	52	5	993.8845	*							
104	BOP	54	1	917.8532			*			*	*	
105	AOS	54	1	917.8532			*			*	*	
106	C22:1OS	54	2	943.8688	*							
107	C24:1OP	54	2	943.8688	*							
108	BOO	54	2	943.8688	*	*	*			*	*	*

109	LgLP	54	2	943.8688		*			*	*	*
110	BLS	54	2	943.8688						*	*
111	C24:1OO	54	3	969.8845	*						
112	C24:1LS	54	3	969.8845	*						
113	C22:1OG	54	3	969.8845	*						
114	LgLO	54	3	969.8845	*	*	*		*	*	*
115	C23:0OO	55	2	957.8845						*	
116	LgOP	56	1	945.8845						*	
117	BOS	56	1	945.8845						*	
118	LgOO	56	2	971.9001	*	*	*		*	*	
119	LgLS	56	2	971.9001						*	
120	C24:1OS	56	2	971.9001	*						
121	C22:1OC22:1	56	3	997.9158	*						
122	C24:1OG	56	3	997.9158	*						

Fatty acid abbreviations: M= miristic acid (C14:0), P= palmitic acid (C16:0), Po= palmitoleic acid (C16:1), $C_{17:0}$= margaric acid, $C_{17:1}$= eptadecenoic acid, S= stearic acid (C18:0), O= oleic acid (C18:1), L= linoleic acid (C18:2), Ln= linolenic acid (C18:3), A= arachidic acid (C20:0), G= gadoleic acid (C20:1), B= behenic acid (C22:0), $C_{22:1}$= erucic acid, Lg= lignoceric acid (C24:0), $C_{24:1}$= nervonic acid.
Note: the standard notation of TAGs was adopted, using trivial names of FAs arranged according to the literature on plant oils: the sn-1, sn-2 and sn-3 positions were designated according to FAs decreasing molecular weights, and placing an unsaturated FA in the sn-2 position (preferably, linoleic acid) [34].

The different selectivity afforded by the use of the AcN/CO_2 mobile phase, over the ones containing alcohol modifiers may be explained on the basis of additional dipole-dipole interactions established with the TAG molecules, especially the more unsaturated compounds. As is well known, pressure affects the density of supercritical CO_2 and therefore, influences the eluotropic strength of supercritical fluid. A backpressure value of 103 bar was selected for the UPC2 analysis.

With the optimized SubFC separation conditions, for all the samples investigated, elution of the TAG species was achieved within 10 min, as shown in the chromatograms in Figure 6.1 (panels A-F), the only exception being borage oil (14 min run), shown in Figure 6.2. Specifically, the latter sample was characterized by TAGs spanning in a wide range of PN (36-56), differing for the unsaturation degree (DB 1-9). Table 6.1 lists PN, DB, and theoretical *m/z* values of the 122 TAGs components identified in the 7 vegetable oil samples. Among these, 81 were detected in the borage oil, while the other samples showed lower complexity.

According to what reported in the literature [34,35], borage oil showed the highest complexity, in terms of FA and TAG composition, and for such reason it was selected as a model sample, to demonstrate the extension of the relationships between retention properties of TAGs and chemical structures generally observed in NARP-LC and SubFC with neat CO_2, to SubFC with CO_2/modifier mobile phases exploited in this work. Retention of the sample TAG constituents occurred according to their increasing PN, which may well describe molecules' hydrophobicity, as determined by the length of hydrocarbon chain and the polar contribution given by the number of unsaturations. From the chromatogram in Figure 6.2 it can be seen that all the TAG species contained in borage oil were eluted within 14 minutes, with a mobile phase containing around 20% of the modifier (AcN). The list of identified compounds in Table 6.1 shows that the elution order of TAGs was mainly governed by hydrophobicity of the solutes, since retention increases from PN 36 (γLnγLnγLn) to PN 56 (C24:1OG). Similarly to what observed in RP-LC on ODS columns and in SubFC with neat CO_2, the apolar character of TAGs becomes dominant at the higher PN values, providing more interaction with the separation medium and diminished solubility in the mobile phase; as a result, the retention increases.

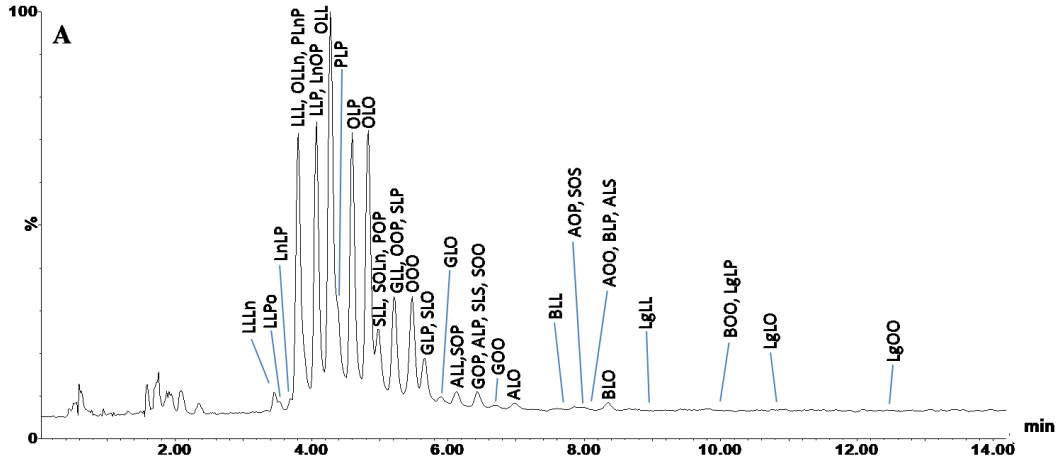
A
100
%
0
LLLn
LLPo
LnLP
LLL, OLLn, PLnP
LLP, LnOP
OLL
PLP
OLP
OLO
SLL, SOLn, POP
GLL, OOP, SLP
OOO
GLP, SLO
GLO
ALL,SOP
GOP, ALP, SLS, SOO
GOO
ALO
BLL
AOP, SOS
AOO, BLP, ALS
BLO
LgLL
BOO, LgLP
LgLO
LgOO
2.00
4.00
6.00
8.00
10.00
12.00
14.00
min

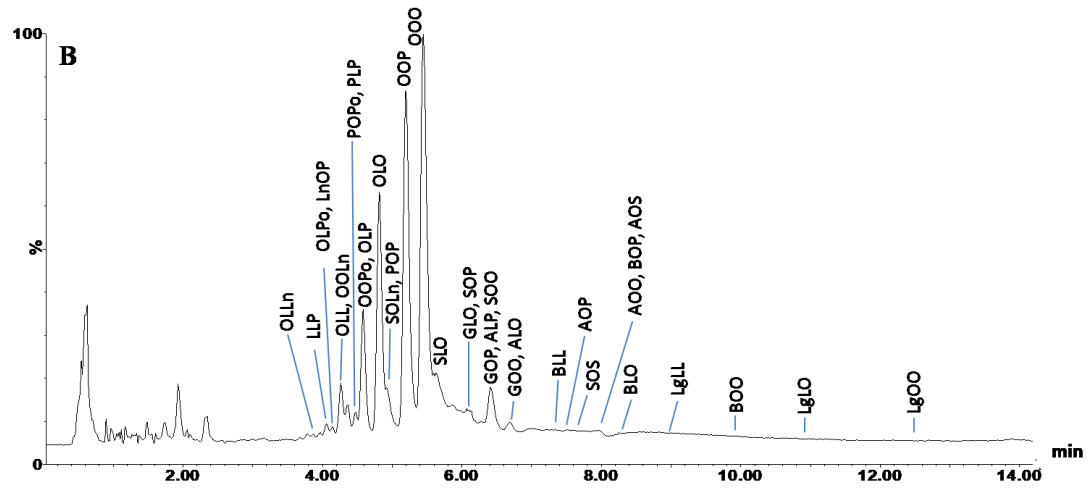
B
100
%
0
OLLn
LLP
OLPo, LnOP
OLL, OOLn
OOPo, OLP
POPo, PLP
SOLn, POP
OLO
OOP
OOO
SLO
GLO, SOP
GOP, ALP, SOO
GOO, ALO
BLL
AOP
SOS
AOO, BOP, AOS
BLO
LgLL
BOO
LgLO
LgOO
2.00
4.00
6.00
8.00
10.00
12.00
14.00
min

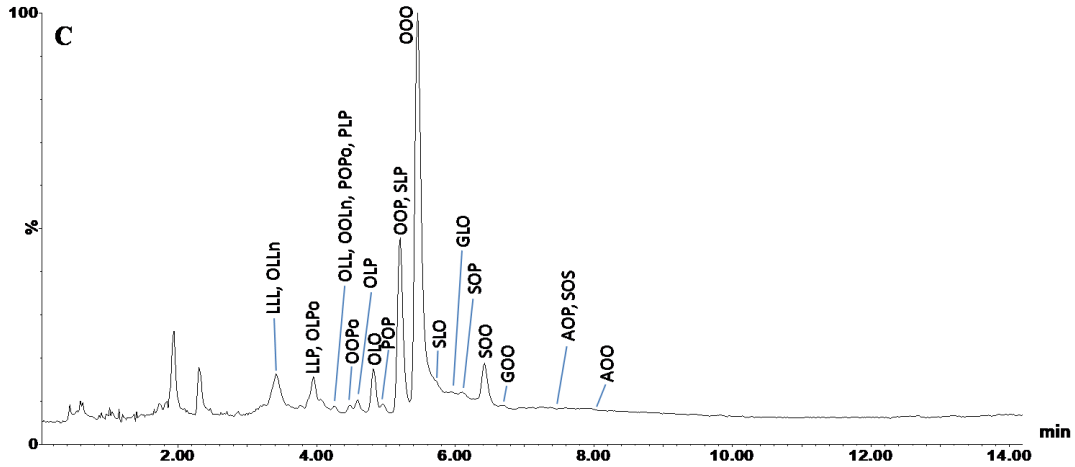
C
100
%
0
LLL, OLLn
LLP, OLPo
OLL, OOLn, POPo, PLP
OOPo
OLP
OLO
POP
OOP, SLP
OOO
SLO
GLO
SOP
SOO
GOO
AOP, SOS
AOO
2.00
4.00
6.00
8.00
10.00
12.00
14.00
min

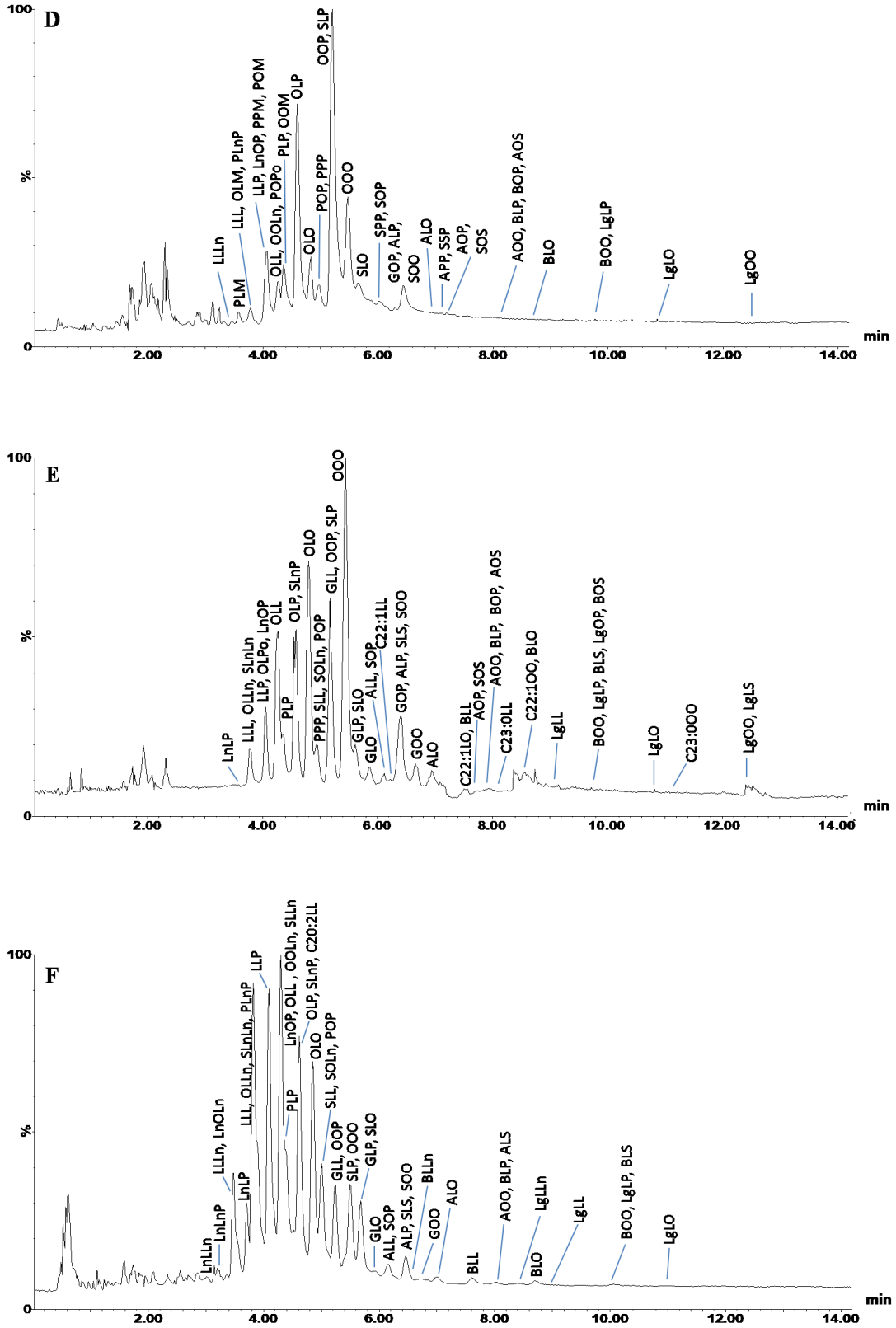

Figure 6.1 UHPSFC-APCI-MS TAG profile of Corn oil (A) Olive oil (B), Hazelnut oil (C), Palm oil (D) Peanut oil, (E), Soybean oil (F).

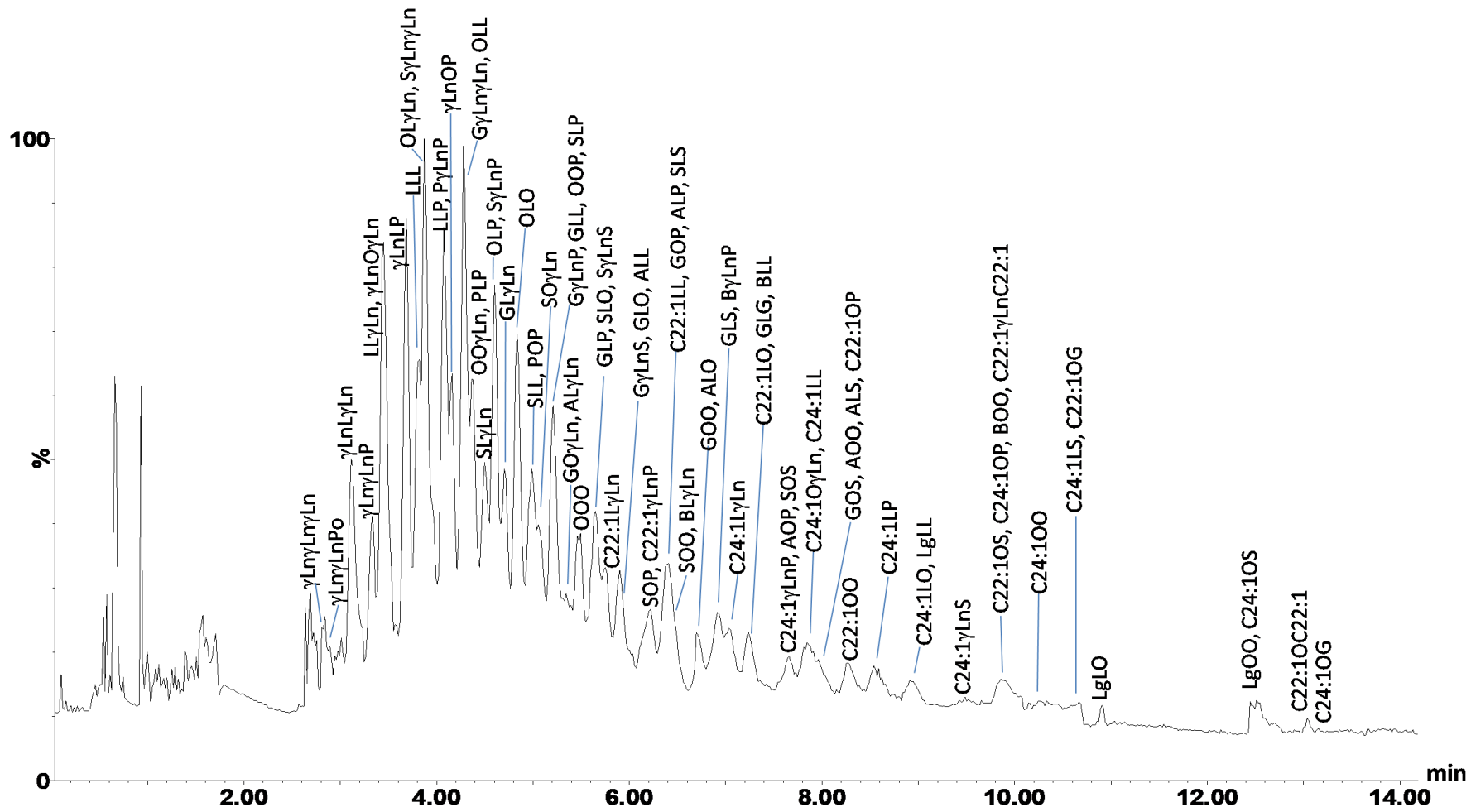

Figure 6.2 UHPSFC-APCI-MS TAG profile of a Borage seed oil sample.

According to what reported in the literature [34,35], borage oil showed the highest complexity, in terms of FA and TAG composition, and for such reason it was selected as a model sample, to demonstrate the extension of the relationships between retention properties of TAGs and chemical structures generally observed in NARP-LC and SubFC with neat CO_2, to SubFC with CO_2/modifier mobile phases exploited in this work. Retention of the sample TAG constituents occurred according to their increasing PN, which may well describe molecules' hydrophobicity, as determined by the length of hydrocarbon chain and the polar contribution given by the number of unsaturations. From the chromatogram in Figure 6.2 it can be seen that all the TAG species contained in borage oil were eluted within 14 minutes, with a mobile phase containing around 20% of the modifier (AcN). The list of identified compounds in Table 6.1 shows that the elution order of TAGs was mainly governed by hydrophobicity of the solutes, since retention increases from PN 36 (γLnγLnγLn) to PN 56 (C24:1OG). Similarly to what observed in RP-LC on ODS columns and in SubFC with neat CO_2, the apolar character of TAGs becomes dominant at the higher PN values, providing more interaction with the separation medium and diminished solubility in the mobile phase; as a result, the retention increases. Likewise, for compounds having identical PN (but differing in CN and DB), reversion of the retention's order was observed, e.g. the OLL-LLP (PN 44) elution order reported in RP-LC, became LLP-OLL in SubFC with AcN. An increase in the DB value resulted in faster elution of TAGs within the same PN, due to the increase in the TAG polarity and the resulting increase of solubility in the mobile phase, e.g. the TAG OLO (PN 46, DB 4) was more strongly retained compared to the TAG SγLNP (PN 46, DB 3).

Furthermore, the presence of higher alkyl chain lengths such as C20, C22, C24 leads to numerous additional TAGs and specifically, for long saturated and monounsaturated FAs- containing lipids, a stronger retention was observed, as for the case of GγLnγLn with a PN value of 42 which eluted in the PN 44 region (being OLL the most representative compounds) and GLγLn with a PN value of 44, which eluted in the PN 46 region (being OLP the most representative compound).

TAGs components have been identified on the basis of their APCI-MS spectra by evaluating $[M+H]^+$ ions for the molecular weight determination and the diacylglycerol-like fragment ions (DG^+), resulting from the loss of a single FA moiety

from the glycerol backbone, for the identification of individual FAs constituting each TAG species. TAGs were notated employing initials of FA trivial names and the sn-1/3 positions were considered as equivalent; therefore, TAGs were named according to the decreasing molecular masses of the FAs, except for the central position assigned to unsaturated FAs, as commonly observed in plant oils.

6.4 Conclusions

In this research, a SubFC approach for the comprehensive characterization of TAG components in different vegetable oils, using CO_2 as the main mobile phase solvent and Q-ToF MS detection was developed. A total of 122 TAG species were positively identified based on their APCI-MS spectra, without the need of post-column make-up solvent/pump.

Compared to LC approaches, the low viscosity and high diffusivity of the mobile phase employed in SubFC allowed for a consistent reduction of the analysis time (less than 14 min); furthermore, the drastic reduction in the use of organic solvents makes this SubFC-based approach less toxic, less expensive, and more environmental-friendly over conventional techniques.

The employment of subFC-MS approach for the the study of vegetable oil samples was confirmed to be a useful strategy for the investigation of non-polar lipids in complex matrices.

6.5 References

1. Christie, W.W., Han, X., *Lipid Analysis*. 4th Edition, Oily Press, Bridgewater 2010.
2. Gunstone, F. D., Harwood, J. L., Dijkstra, A. J., The Lipid Handbook, 3rd Edition, CRC Press, Boca Raton 2007.
3. Li M., Yang L., Liu H. Analytical Methods in Lipidomics and Their Applications. Anal. Chem. 2014, 86, 1, 161–175
4. Brown H.A., Marnett LJ. Introduction to lipid biochemistry, metabolism, and signaling. Chem. Rev. 2011, 111, 5817-5820.
5. Vance J. E., Vance D. E., Biochemistry of Lipids, Lipoproteins and Membranes. 4th Edition, Elsevier, Amsterdam 2002.
6. Lusis A. J., Atherosclerosis. Nature 2000, 407, 233–241.
7. Bazinet R. P., Layé S. Polyunsaturated fatty acids and their metabolites in brain function and disease. Nature Reviews Neuroscience 2014, 15, 771–785.

8. Aguennouz M., Beccaria M., Purcaro G., Oteri M., Micalizzi G., Musumesci O., Ciranni A., Di Giorgio R.M., Toscano A., Dugo P., Mondello L. Analysis of lipid profile in lipid storage myopathy. J. Chromatogr. B, 2016, 1029, 157–168.
9. Gunstone F.D. Vegetable Oils in Food Technology: Composition, Properties and Uses, Second Edition, Blackwell Publishing Ltd. 2011.
10. FEDIOL, The European Vegetable Oil and Protein meal Industry, Brussells, http://www.fediol.be/.
11. Triacylglycerols in edible oils: Determination, characterization, quantitation, chemometric approach and evaluation of adulterations Indelicato S., Bongiorno D., Pitonzoc R., Di Stefano V., Calabrese V., Indelicato S., Avellone G. J. Chromatogr. A, 2017, 1515, 1–16.
12. Tranchida P.Q., Donato P., Dugo P., Dugo G., Mondello L. Comprehensive Chromatographic Methods for the Analysis of Lipids Trend Anal. Chem. 2007, 26, 191-205.
13. Mondello L., Beccaria M., Donato P., Cacciola F., Dugo G., Dugo P. Comprehensive two-dimensional liquid chromatography with evaporative light scattering detection for the analysis of triacylglycerols in *Borago officinalis*. J. Sep. Sci. 34, 2011, 688-692.
14. Donato P., Micalizzi G., Oteri M., Rigano F., Sciarrone D., Dugo P., Mondello L. Comprehensive lipid profiling in marine organisms by hyphenated and multidimensionalchromatography techniques coupled to mass spectrometry detection. Anal. Bioanal. Chem. 2018, 410, 3297-3313.
15. Kallio H., Nylund M., Bostrom P., Yang B. Triacylglycerol regioisomers in human milk resolved with an algorithmic novelelectrospray ionization tandem mass spectrometry method. Food Chem. 2017, 233, 351-360.
16. Murphy R.C., Challenges in mass spectrometry-based lipidomics of neutral lipids. Trends Anal. Chem. 2018, 107, 91-98.
17. Beccaria M., Sullini G., Cacciola F., Donato P., Dugo P., Mondello L. High performance characterization of triacylglycerols in milk and milk-related samples by liquid chromatography and mass spectrometry. J. Chromatogr. A, 2014, 1360, 172–187.
18. Lisa M., Denev R., Holcapek M. Retention behaviour of isomeric triacylglycerols in silver-ion HPLC: effects of mobile phase composition and temperature. J. Sep. Sci. 2013, 36, 2888–2900.
19. Donato P., Giuffrida D., Oteri M., Inferrera V., Dugo P., Mondello L.. Supercritical fluid chromatography×ultrahigh pressure liquid chroma- tography for red chilli pepper fingerprinting by photodiode array, qua- drupole-time-of-flight and ion mobility mass spectrometry (SFC×RP- UHPLC-PDA-QToF MS-IMS). Food Anal. Meth. 2018, 11, 3331-3341.
20. Bernal J.L., Martín M.T., Toribio L. Supercritical fluid chromatography in food analysis. J.Chromatogr. A 2013, 1313, 24–36.

21. Laboureur L., Ollero M., Touboul D. Lipidomics by supercritical fluid chromatography. Int. J. Mol. Sci. 2015, 16, 13868–13884.
22. Buchgraber M., Ulberth F., Emons H., Anklam E., Triacylglycerol profiling by using chromatographic techniques. Eur. J. Lipid Sci. Technol. 2004, 106, 621–648.
23. Lee M.L., Markides K.E., Chromatography with supercritical fluids. Science 1987, 235, 1342–1347.
24. Novotny M.V., Recent developments in analytical chromatography. *Science* 1989, 246, 51–57.
25. Manninen P., Laakso P., Kallio H. Method for characterization of triacylglycerols and fat-soluble vitamins in edible oils and fats by supercritical fluid chromatography. J. Am. Oil Chem. Soc. 1995, 72, 1001–1008.
26. Sandra P., Medvedovici A., Zhao Y., David F. Characterization of triglycerides in vegetable oils by silver-ion packed-column supercritical fluid chromatography coupled to mass spectroscopy with atmospheric pressure chemical ionization and coordination ion spray. J. Chromatogr. A 2002, 974, 231–241.
27. Lesellier E., West C., The many faces of packed column supercritical fluid chromatography-a critical review. J. Chromatogr. A 2015, 1382, 2–46.
28. Nováková L., Perrenoud A.G.G., François I., West C., Lesellier E., Guillarme D., Modern analytical supercritical fluid chromatography using columns packed with sub-2 particles: A tutorial. Anal. Chim. Acta 2014, 824, 18–35.
29. Bonaccorsi I., Cacciola F., Utczas M., Inferrera V., Giuffrida D., Donato P., Dugo P., Mondello L. Characterization of the pigment fraction in sweet bell peppers (*Capsicum annuum L.*) harvested at green and overripe yellow and red stages by offline multidimensional convergence chromatography/liquid chromatography-mass spectrometry. J. Sep. Sci. 2016, 39, 3281-3291.
30. Lesellier E. Overview of the retention in subcritical fluid chromatography with varied polarity stationary phases. J Sep Sci. 2008, 31, 1238-1251.
31. Donato P., Inferrera V., Sciarrone D., Mondello L., Supercritical fluid chromatography for lipid analysis in foodstuffs. J. Sep. Sci. 2017, 40, 361–382.
32. Funada Y., Hirata Y. Retention behavior of triglycerides in subcritical fluid chromatography with carbon dioxide mobile phase. J. Chromatogr. A 1997, 764, 301–307.
33. Lesellier E., Tchapla A. Retention behavior of triglycerides in octadecyl packed subcritical fluid chromatography with CO_2/modifier mobile phases. Anal. Chem. 1999, 71, 5372–5378.
34. Lísa M., Holčapek M., Triacylglycerols profiling in plant oils important in food industry, dietetics and cosmetics using high-performance liquid chromatography-atmospheric pressure chemical ionization mass spectrometry. J. Chromatogr. A 2008, 1198-1199, 115–130.
35. Holčapek M., Lísa M., Jandera P., Kabátová N., Quantitation of triacylglycerols in plant oils using HPLC with APCI-MS, evaporative light scattering, and UV detection. J. Sep. Sci. 2005, 28, 1315–1333.